DEVELOPMENT OF STRUCTURAL HEALTH MONITORING AND ARTIFICIAL INTELLIGENCE BASED DAMAGE DETECTION AND EARLY WARNING SYSTEM FOR TRUSS LIKE IN-WATER STRUCTURES

A THESIS SUBMITTED TO
THE GRADUATE SCHOOL OF NATURAL AND APPLIED SCIENCES
OF
MIDDLE EAST TECHNICAL UNIVERSITY

BY

SERAP KARA

IN PARTIAL FULFILLMENT OF THE REQUIREMENTS
FOR
THE DEGREE OF MASTER OF SCIENCE
IN
CIVIL ENGINEERING

SEPTEMBER 2019

Approval of the thesis:

DEVELOPMENT OF STRUCTURAL HEALTH MONITORING AND ARTIFICIAL INTELLIGENCE BASED DAMAGE DETECTION AND EARLY WARNING SYSTEM FOR TRUSS LIKE IN-WATER STRUCTURES

submitted by **SERAP KARA** in partial fulfillment of the requirements for the degree of **Master of Science in Civil Engineering Department, Middle East Technical University** by,

Prof. Dr. Halil Kalıpçılar
Dean, Graduate School of **Natural and Applied Sciences** _____

Prof. Dr. Ahmet Türer
Head of Department, **Civil Engineering** _____

Prof. Dr. Ahmet Türer
Supervisor, **Civil Engineering, METU** _____

Examining Committee Members:

Prof. Dr. Alp Caner
Civil Engineering, METU _____

Prof. Dr. Ahmet Türer
Civil Engineering, METU _____

Prof. Dr. Eray Baran
Civil Engineering, METU _____

Assoc. Prof. Dr. Ozan Cem Çelik
Civil Engineering, METU _____

Assist. Prof. Dr. Alper Aldemir
Civil Engineering, Hacettepe University _____

Date: 10.09.2019

I hereby declare that all information in this document has been obtained and presented in accordance with academic rules and ethical conduct. I also declare that, as required by these rules and conduct, I have fully cited and referenced all material and results that are not original to this work.

Name, Surname: Serap Kara

Signature:

ABSTRACT

DEVELOPMENT OF STRUCTURAL HEALTH MONITORING AND ARTIFICIAL INTELLIGENCE BASED DAMAGE DETECTION AND EARLY WARNING SYSTEM FOR TRUSS LIKE IN-WATER STRUCTURES

Kara, Serap
Master of Science, Civil Engineering
Supervisor: Prof. Dr. Ahmet Türer

September 2019, 129 pages

Continuously growing industry necessitates substantial amount of energy which is frequently harvested in-water regions. Electricity, gas, and oil collected offshore areas generally require platforms constructed in seas and oceans. Inspection of offshore platforms is hard and it is difficult to detect damage in early stages of these structures that perform in harsh salty water environments, which might cause catastrophic failures if unattended. Damage identification of these structures is a challenging issue. Structural damage detection at its earlier stage would prevent possible collapses, economic losses, and environmental disasters. Structural Health Monitoring (SHM) approach for early damage detection and warning for truss-like tower structures in water is investigated in this thesis study. This thesis targeted to set rules about damage detection and warning system using simple and sophisticated methods (Artificial Intelligence – AI) for tower like structures. Wave loading, stored mass changes, and damaged members are considered in the developed monitoring system, which is verified by tests on a small scale laboratory model. Finite Element Model (FEM) of the lab model is calibrated using static and dynamic test results. Damage scenarios are generated using a VBA based program through Application Programming Interface

(API) to generate analytical structural response of damage scenarios. An artificial intelligence (AI) based monitoring system is developed using a large number of analytically simulated damage and mass change scenarios. The trained ANN is tested using FEM generated structural response that are not used during training. Total of 22 damage scenarios are also implemented on the physical lab model and tests are conducted to obtain dynamic and static properties which are then fed into the trained ANNs to see if damage locations can be identified. A Graphical User Interface (GUI) is also developed to show the current health status of the structure including specific details such as natural vibration frequencies, current mass in the tank, displacements, etc. A damage level warning system is also implemented on the GUI to alarm for any detected damage.

Keywords: Artificial Neural Network, Damage Detection, Structural Health Monitoring, Tower, Truss

ÖZ

SU İÇİNDEKİ MAKAS TİPİ YAPILAR İÇİN YAPISAL SAĞLIK İZLEME VE YAPAY ZEKA TABANLI HASAR TESPİTİ VE ERKEN UYARI SİSTEMLERİNİN GELİŞTİRİLMESİ

Kara, Serap
Yüksek Lisans, İnşaat Mühendisliği
Tez Danışmanı: Prof. Dr. Ahmet Türer

Eylül 2019, 129 sayfa

Sürekli büyüyen endüstriyel aktiviteler için gerekli olan yüksek derecede enerji ihtiyacı, su altında kalan bölgelere de uzanılmasını gerekli kılmıştır. Açık deniz bölgelerinden elde edilecek elektrik, gaz ve petrol genellikle denizlerde ve okyanuslarda inşa edilecek platformların kullanılmasını gerektirir. Sert koşullar ve tuzlu ortamlarda bulunan bu tür yapıların denetimi ve bu yapılarda oluşabilecek hasarların erken tespiti zordur ve istenmeyen büyük felaketlere neden olabilir. Bu nedenlerden dolayı hasar tespiti bu yapılar için zorlu bir problemdir. Yapıda oluşacak herhangi bir hasarın erken tespiti olası kazaları, ekonomik kayıpları ve çevresel felaketleri önleyebilir. Bu tez çalışmasında, sudaki makas benzeri kule yapılarında oluşan hasarlar için erken hasar tespiti ve ikaz için Yapısal Sağlık İzleme (YSİ) yaklaşımı ele alınmıştır. Bu tez, kule benzeri yapılar için basit ve sofistike yöntemler (Yapay Zeka -YZ) kullanarak hasar tespit ve uyarı sistemi ile ilgili kurallar koymayı amaçlamaktadır. Dalga yükü, depolanan kütledeki değişiklikler ve hasarlı elemanlar geliştirilen izleme sisteminde düşünülmüş ve sistem küçük ölçekli bir laboratuvar modelinde test edilmiştir. Fiziksel laboratuvar modelinin sonlu elemanlar modeli statik ve dinamik deney sonuçlarına göre kalibre edilmiştir. Hasar senaryoları ve senaryoların analitik yapısal tepkisi Uygulama Programlama Ara Yüzü kullanan VBA

tabanlı bir program tarafından oluşturulmuştur. Yapay zekaya dayalı bir izleme sistemi analitik olarak simüle edilmiş çok sayıda hasar ve kütle değişim senaryosu kullanılarak geliştirilmiştir. Eğitilen YSA, eğitim sırasında kullanılmayan ve sonlu elemanlar metodu ile elde edilen hasar senaryoları kullanılarak test edilmiştir. 22 hasar senaryosu fiziksel laboratuvar modelinde de uygulanmış ve her senaryoya ait dinamik ve statik özellikleri elde etmek için testler tekrarlanmıştır. Elde edilen sonuçlar, eğitilen her bir YSA için girdi olarak kullanılmış ve fiziksel laboratuvar modelinde oluşan hasarların yerlerini tahmin etmek için kullanılmıştır. Yapının mevcut haldeki yapısal sağlık izlemeleri (doğal salınım frekansları, depolanan mevcut kütle ve deplasman vb.) için kullanıcı ara yüzü geliştirilmiştir. Tespit edilen hasar olduğunda uyarı vermesi için kullanıcı ara yüzünde hasar seviyesi alarm sistemi uygulanmıştır.

Anahtar Kelimeler: Hasar Tespiti, Kule, Makas, Yapay Sinir Ağı, Yapısal Sağlık İzleme

To My Family

ACKNOWLEDGEMENTS

This thesis was completed under the supervision of Prof. Dr. Ahmet Türer. First and foremost, I would like to express my gratefulness to him for invaluable guidance, assistance, support and patience. He encouraged me through this period.

I would like to thank to my family for their encouragements and supports.

This thesis has been made with the scope of the project titled “Structural Health Monitoring and Artificial Intelligence Based Damage Detection and Early Warning Systems for Truss Like In-Water Structures” with the scholarship of TÜBİTAK. Finally, I would like to thank to TÜBİTAK for valuable supports through this project 1002-214M349.

TABLE OF CONTENTS

LIST OF TABLES

TABLES

LIST OF FIGURES

FIGURES

CHAPTER 1

INTRODUCTION

1.1. Objective and Scope

The primary goal of this thesis is to develop a Structural Health Monitoring (SHM) approach for early damage detection and warning for truss-like tower structures in water. It is called as truss-like tower structures because the joints are rigid and it causes the behavior similar to both truss and frame structures. One of the most important types of these tower structures is the oil and natural gas extraction facilities located in seas, oceans, or lakes. Different than the ones on land, towers in-water are exposed to various challenges such as salty water, continuous and cyclic loads coming from waves, changing mass and natural vibration frequencies because of storage, etc. Collapse or damage to in-water oil platforms have multiple adverse economic and natural disasters. Preventive measures and damage detection at early stages have vital role for these important structures. This thesis targeted to set rules about damage detection and warning system using simple and sophisticated methods (Artificial Intelligence – AI) for tower like structures. The main objectives are listed below:

1) Investigate types of the offshore towers and forces acting on truss like tower structures especially the ones in water.
2) Develop a testing program for damage response and changes in static and dynamic properties of lab model.
3) Construct a realistic 3D finite element model (FEM) of the lab tower to simulate damage and compare against available experiment data.
4) Generate a VBA based program utilizing API to generate multiple scenarios to be used for the training and testing of artificial neural network (ANN) for damage detection.

5) Design a user friendly interface for early damage detection.

The stages of the thesis to reach these objectives are summarized below in the form of scope:

1) Conduct literature survey on types of in-water towers and review basic wave theory.
2) Design a 1/75 scale lab specimen and construct a realistic 3D-FEM.
3) Construct a lab specimen with the same characteristics as the analytical model.
4) Test lab specimen statically and dynamically to obtain natural vibration frequencies and stiffness.
5) Update nominal FEM to replicate the experimental properties as closely as possible by changing material, connectivity, mass, and support stiffness properties.
6) Write a VBA based API code to repeatedly run SAP2000 to generate 10,200 damage and mass change scenarios, which will be then used subsequently to calibrate ANN.
7) Test the trained ANN using FEM generated damage scenarios that were not used during training.
8) Conduct 22 damage scenarios on the physical lab model and repeat tests to obtain dynamic and static properties.
9) Use trained ANN to guess damage locations of the damage induced lab model using test data as input.
10) Generate simplistic damage detection methods using available experimental data and test their significance.

1.2. Truss Like Structures with Emphasis on In-Water Towers

In this chapter, firstly basic descriptions about offshore structures and types of offshore platforms are given. Then, main forces applied on the offshore structures and the method used are defined. Final section gives brief information about ANNs. Type of the ANNs and its use for damage detection will also be covered.

Oil was discovered in the mid-19th century by obtained from coal gas, and then crude oil was discovered from the first oil well in 1859. In the beginning, the demand for petroleum was met from land. However, the demand of oil has increased significantly day after day. To meet this growing need, studies were started to enable the use of petroleum in the shallow waters near the shore in the middle of the 20th century.

Today, the ever-increasing need for oil and gas exploration is met through platforms built into open and deep waters. There are various types of offshore structures depending on the characteristics of the regions they are built (depth of water and other environmental factors).

1.2.1. Types of Offshore Structures

According to the behaviors and geometries of offshore structures, they are divided into three groups (Figure 1.1).

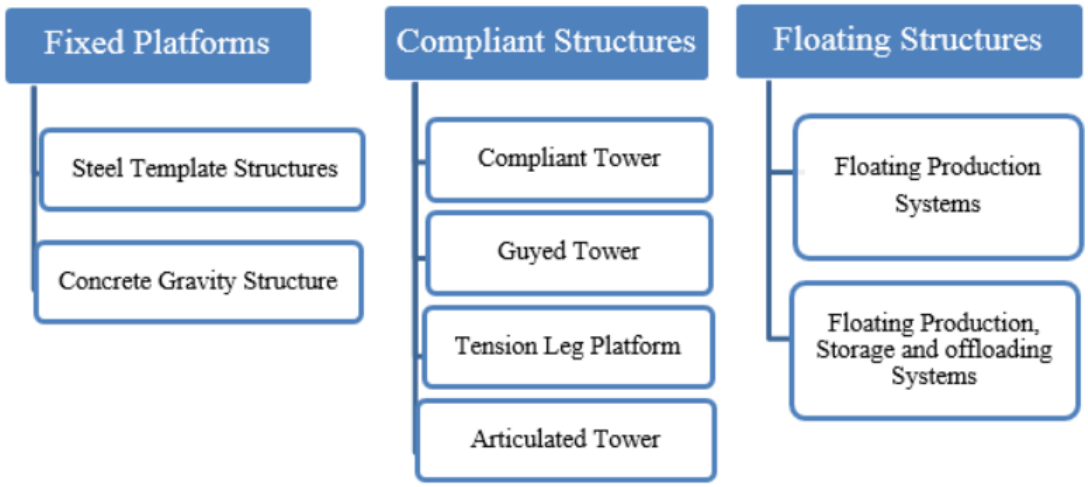

Figure 1.1. Classification of Offshore Structures

Steel Template Structures: They can be used in water depths up to 500 meters. They are fixed with tubular steel members supported by pipe piles to the sea bed.

Concrete Gravity Structures: They are generally preferred in the areas where no installation of piles is needed. They can be used in water depths up to 350 meters.

The typical examples mentioned above are given in Figure 1.2.

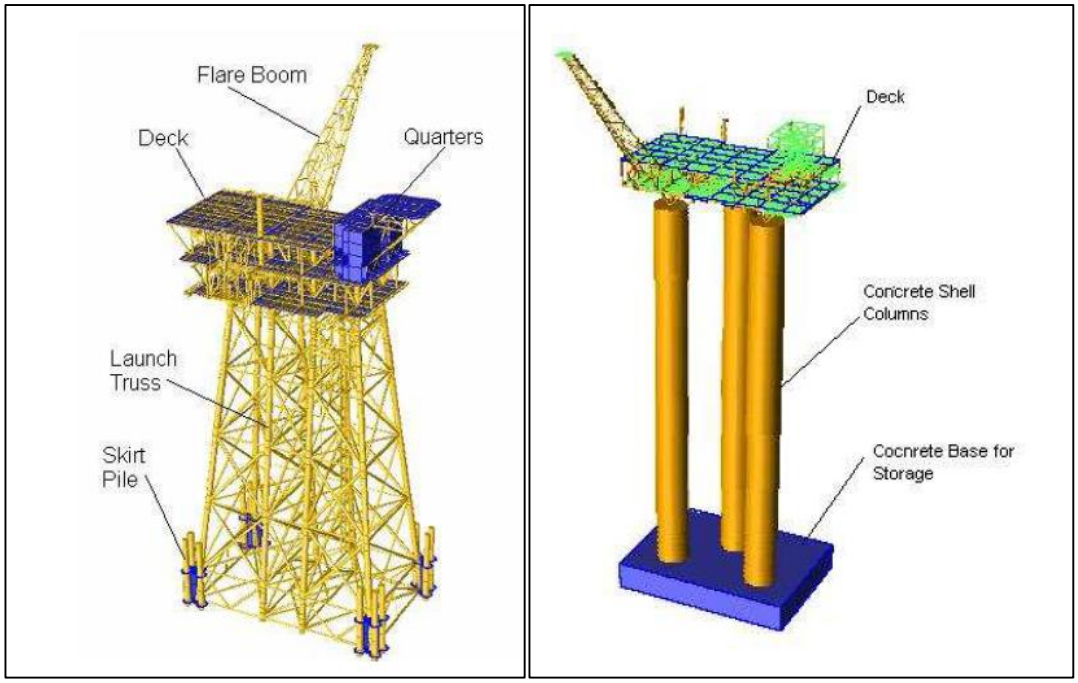

Figure 1.2. Examples of Steel Template Structure and Concrete Gravity Structure

Compliant Tower: They are used in deep waters. They resist strong lateral forces causing large deflections. They are used generally in water depths between 300 and 600 meters.

Guyed Tower: They are similar to the compliant towers. Differently from compliant towers, they are connected to the seabed with guy wires by means of piles or anchors. These wires prevent the lateral displacement of the top significantly and minimize.

The typical examples of compliant tower and guyed tower are given in Figure 1.3.

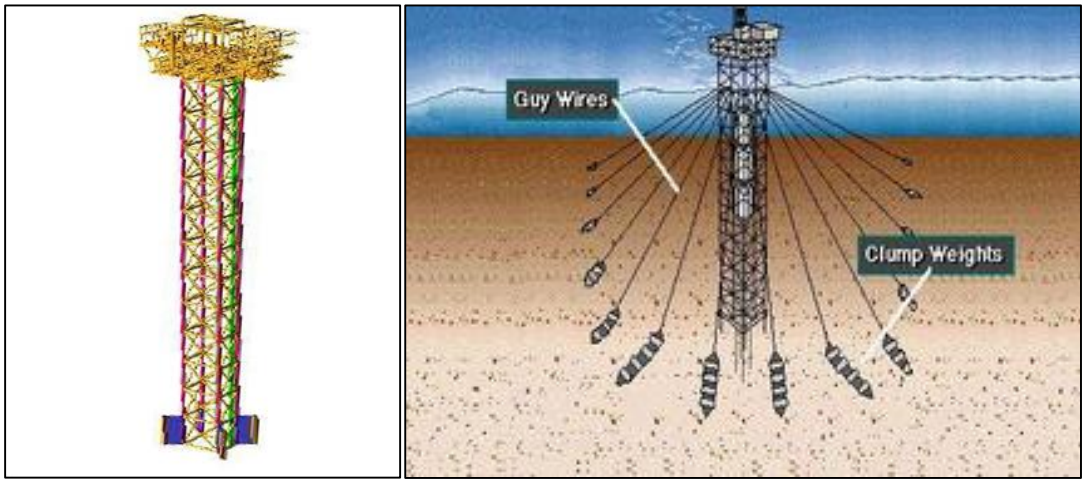

Figure 1.3. Examples of Compliant Tower and Guyed Tower

Tension Leg Platform: They are generally used in water depths between 1,000 and 1,200 meters. Mini Tension Leg Platform (Mini-TLP) and SPAR Platform are two main types of the tension leg platforms.

Articulated Tower: Instead of the wires of tension leg platforms, they have a concrete block or driven pile at the foundation. They are suitable for intermediate water depths between 150 m and 500 m. This type of structure is given in Figure 1.4.

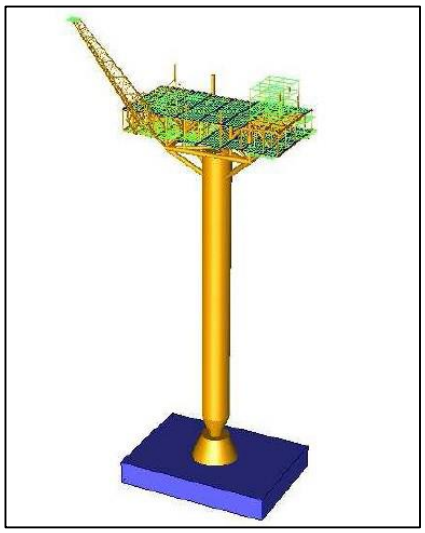

Figure 1.4. Articulated Tower Model

In addition to these models, other offshore platforms used for production, storage and discharge are available. Apart from the fixed types, they have also floating models. These types are shown in Figure 1.5.

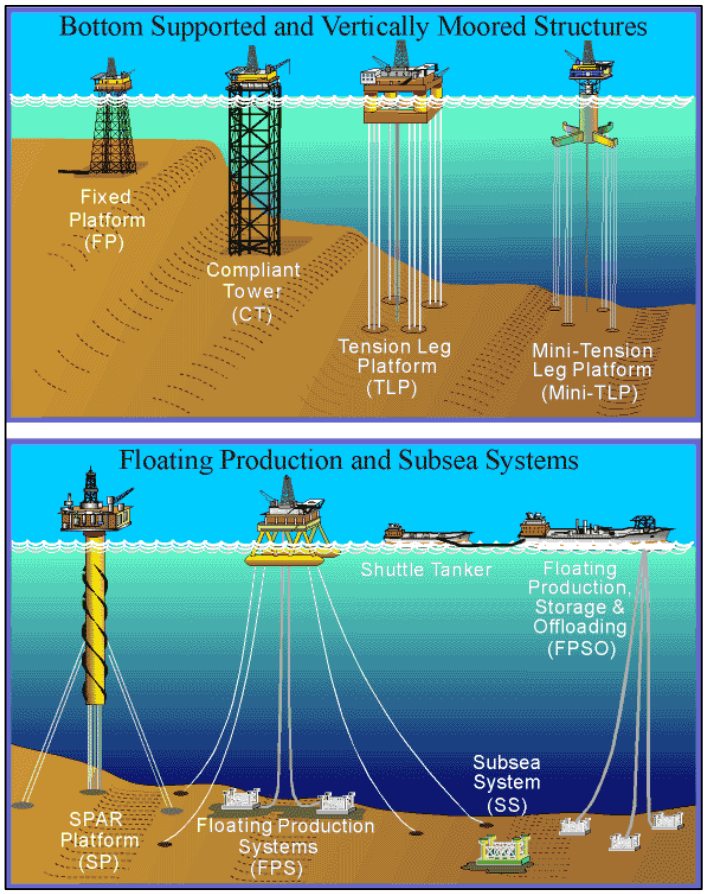

Figure 1.5. General Classification of Offshore Platforms

1.2.2. Loads Acting on Offshore Structures

The most important forces that affect offshore structures are the forces created by wind and waves.

In order to calculate the wave forces, it is firstly necessary to obtain the wave profile. Since the definition of a real wave profile is very complex and difficult, sinusoidal waves are usually used.

The basic parameters to define a wave profile are wave height, wave period and depth of water.

When the mentioned parameters are obtained, other parameters which are not available can be calculated by means of various relations. Wave type classification can be determined by using the ratio of the depth of the water (d) to the wave length (L) and multiplying with the wave number (k= 2π/L). The criteria used for this classification are shown in Table 1.1.

Table 1.1. *Wave Classification*

d/L	kd=(2π/L)d	Wave Type
0<d/L<0.05	0<kd<0.1π	Shallow Water Wave
0.05<d/L<0.50	0.1 π <kd< π	Intermediate Depth Wave
d/L>0.50	kd> π	Deep Water Wave

Waves are classified into three groups: shallow water waves, intermediate depth waves and deep water waves. For deep water waves, wave height and wave length are the main parameters to determine the type of wave. Water depth has no effect on the classification. After the decision of wave type, wave length, wave celerity and velocity equations of water particle in horizontal and vertical directions can be calculated using the formulas in Table 1.2.

Table 1.2. *Wave Equations*

		Deep Water $d/L_o \geq 0.5$	Intermediate Depth $0.0157 < d/L_o < 0.5$	Shallow Water $d/L_o \leq 0.0157$
Water Celerity	C	$\frac{g}{2\pi}T$	$\frac{g}{2\pi}T\tanh(\frac{2\pi d}{L})$	$(g\,d)^{0.5}$
Wave Length	L	$\frac{g}{2\pi}T^2$	$\frac{g}{2\pi}T^2\tanh(\frac{2\pi d}{L})$	$T\,(g\,d)^{0.5}$
Horizontal Particle Velocity	u	$a*\sigma*e^{k\,z}*\cos(kx-\sigma t)$	$a*\sigma*\frac{\cosh\,k(z+d)}{\sinh\,kd}*\cos(kx-\sigma t)$	$\frac{a\,\sigma}{k\,d}\cos(kx-\sigma t)$
Vertical Particle Velocity	w	$a*\sigma*e^{k\,z}*\sin(kx-\sigma t)$	$a*\sigma*\frac{\sinh\,k(z+d)}{\sinh\,kd}*\sin(kx-\sigma t)$	$a\,\sigma\,(1+\frac{z}{d})\sin(kx-\sigma t)$

The forces are calculated using the Morison approach after the wave profile is obtained. The Morison approach calculates the total force as the sum of the drag force that used acceleration parameter and the inertia force that used velocity parameter. After the determination of the wave theory that will be used (Linear Theory, Stoke's wave theory etc.), C_M and C_D coefficients are selected according to the theory and forces are calculated.

The Morison equation for forces on a unit length of thin cylindrical member is given below:

$F = F_I + F_D$

where

$F_D = 1/2\ C_D\ \rho_f\ D\ U^2$

$F_I = \pi/4\ C_M\ \rho_f\ D^2\ dU/dt$

F : Total wave force

F_I : Inertia force

F_D : Drag force

D : Diameter of cylindrical member

ρf : Density of fluid

U : Fluid velocity

dU/dt : Fluid acceleration

C_M, C_D : Inertia and drag coefficients respectively

Marine growth is an important problem for submerged members. Its main effect is to increase the wave forces on the members by increasing exposed areas and drag coefficient due to higher surface roughness. This effect is taken into consideration in

design through appropriate increases in the diameters and masses of the submerged members.

Standards of “API RP-2A-WSD” and “ISO 19902:2007 Petroleum and natural gas industries — Fixed steel offshore structures” also calculates the wave force with Morison equation.

1.3. Artificial Neural Networks

Artificial neural network is a programming technique that uses a large number of cells that mimic the functions of the human brain and functional connections between these cells. The functions on the created network (Figure 1.6) are optimized by changing the variables on the neurons that symbolize each cell. Using the input and output data obtained, ANN is trained and it is tried to reduce the error between the outputs of the ANN and the outputs that should have. When this error level goes down to the minimum level, ANN training is accepted as complete.

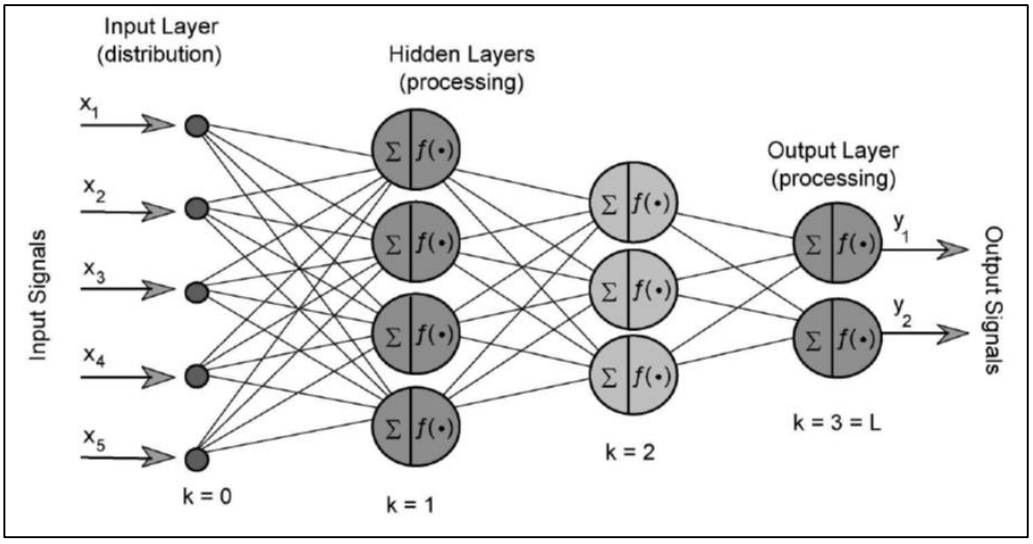

Figure 1.6. General View of ANN Structure (Priddy, K.L. and Keller P.E., 2005)

1.3.1. Types of ANN

Generally, ANNs are classified with respect to the mathematical operations and set of required parameters. Some of the most used types are listed below:

-Feedforward Neural Network: It is the simplest type. In this type, the data moves only from the input layers directly through any hidden layers to output layer without loops.

-Radial Basis Function (RBF): Radial basis functions consider the distance of a point with respect to the center. This network consists of two layers. In the first layer, the properties are combined with the Radial Basis Function in the inner layer and after that output of these properties are taken into consideration while computing the same output in the next time-step that is basically a memory.

There are also various artificial networks types. General regression neural networks (GRNN), recurrent neural networks, convolutional neural networks, Boltzmann machine networks, and Hopfield networks are some of the other artificial neural networks.

1.3.2. Usage of ANN for Early Damage Detection

ANNs are commonly used for complex systems that are difficult to classify using linear programming. Neural Networks have the capability to mimic human brain working mechanism and best at noisy and complex problems. Early damage detection requires continuous monitoring of a structural system and give a warning if a damage is detected so that the damage will not propagate to other members and cause a complete collapse. A monitoring system is not adequate for damage detection since a simple threshold check is not applicable to complex systems. Currently, instrumenting each and every member and connection on a complex tower like structure in water is assumed to be not feasible and unlikely to happen. Therefore, a more complicated monitoring and decision making system is deemed to be necessary to capture structural response and assess if any damage has occurred. This work planned to be a

good match for ANN and has been the main focus of this thesis. A series of ANN were formed and different transfer functions available in MATLAB (logsig, tansig, etc) were tested to give the best training performance. Usage of ANN for damage detection in the literature exists by 1) using statistical approach applying Rosenblueth's point estimate method, which was verified using Monte Carlo simulation and 2) using probabilistic approach of Bayes' Theorem to obtain operating characteristic curves to trade-off between true and false positives.

1.4. Literature Survey

1.4.1. Structural Health Monitoring

There are many different approaches for damage detection. Structural health monitoring is an important approach used in damage detection studies.

Nichols (2003) studied an empirical damage detection model that benefits from the advantages of the environmental excitations affecting offshore structures. The study shows that this technique is unsuitable with basic modal approach due to the ocean wave data based on predictions and low frequency nature of the waves. The main purposes of the study are to increase the system response of the band-limited predictable excitations, to show phase space modelling causing this result and to write an algorithm which shows the changes of the parameters. This study is also supported by a numerical example. However, the empirical formulas used to find damage location and damage type have some insufficiency and it is an ineffectual technique than the ANN damage detection method that is the main subject of this thesis.

Mangal et al. (1999) used neural networks to develop an automatic, on-line monitoring system for offshore structures. A scaled model has created with FEM. The data obtained from this analytical model are compared with the data measured. Responses in transient time domain are converted to the responses in frequency domain using discrete Fourier transform. The six impulse and relaxation tests have been conducted

for different masses to investigate the effect of mass change. These tests show that different masses cause very small changes in natural frequencies of the model and also it is observed that the change is very high in damaged cases compared to the less damaged condition. It is stated that the experimental results are consistent with the analytical model data obtained by FEM and these results can be used for neural network trainings. However, only dynamic effects were considered in this study. The dynamic properties of the structures are related to not only mass but also rigidity in offshore structures, and it is not always possible to distinguish dynamic readings due to the mass or rigidity effects because they can occur at the same time. In this thesis, by adding static loading and displacement measurements in addition to dynamic parameters, the effects of mass changes due to oil storage on the platform are taken into consideration by separating them from the damage effects.

Mei et al. (2014) investigated the parametric and nonparametric methods that use vibration data to solve the disadvantages (local insensitivity to local damage, failure to record signals at low frequencies, etc.) of vibration-based SHM methods. A non-parametric method was proposed by using time series analysis for damage detection. Auto-Regressive Moving Average model with Exogeneous Inputs (ARMAX) was used as the time series analysis model. The location and the severity of the damage were estimated by taking advantage of the changes in the physical parameters. The accuracy of this method has been studied on two different types of models. Apart from the location and amount of damage, the method also differentiates between mass and stiffness changes. Changes in mass and rigidity can be determined separately. Statistical methods for structural health monitoring have also been studied. However, it is stated that the theoretical approach should be confirmed by tests.

Vanik et al. (2000) used Bayes theorem for SHM. It is stated that the method should be tested for complex structures. It is considered that the structure model used in this thesis is chosen very complex compared to the other models in the literature.

1.4.2. Calibration / Model Updating

Hu et al. (2006) have developed a method that establishes a relationship between the finite element model and the measured data. Mass and stiffness matrices were updated with Cross-Model Cross-Mode (CMCM) method using the limited number of modal frequencies. The method has two important advantages compared to other methods: (1) iterations are not required, so it does not require many calculations. (2) measured modes and analytical modes do not require matching or scaling. The most important limitation of the method is that it needs all mode shapes of structure and it is necessary to obtain the missing mode shapes using the measured mode shapes (modal expansion). The accuracy of the method was investigated with two numerical samples. Only analytical data was used in this article. However, both analytical and experimental data are used in this thesis.

Wang et al. (2015) carried out experimental studies by using the CMCM method and the offshore platform as a model. It is stated that CMCM method is suitable for the use of structural monitoring of offshore structures.

Elshafey et al. (2009) examined the dynamic responses of scaled jacket type offshore structure both theoretically and experimentally and compared these results with each other. The experiments were conducted in both air and water. The reaction force in the foundation was calculated using unit deformation measurements and compared with analytical model. Acceleration and deformations were measured for different masses scenarios. Finally, it was observed that acceleration and unit deformations were affected by small changes in mass. Finite element model data and experimental results were found to be compatible with each other.

Elshafey et al. (2010) developed a simple method used random decrement method to estimate damping ratios and natural frequencies of offshore platforms. The method also calculates roughly the reaction forces and bending moment on the ground. In this study, ground reactions were calculated approximately with less than 5% error. Although it is thought to be useful in calculating the forces that the waves will form

on the structure, is not used for damage assessment. It is thought that it should be part of the structural analysis and it is planned to be integrated into this thesis study.

Sun et al. (2006) performed a shaking table test by scaling a real offshore model. They have determined the dynamic responses in this test using both unit deformation gauges and various FBG (Fiber Bragg Grating) sensors and investigated whether FBG sensors can be used for this purpose. At the end of the test, the results were consistent with each other.

1.4.3. Damage Detection

Abdo and Hori (2002) studied to develop a method of damage detection using rotation of the mode shapes as an indicator. A plate was used as an analytical model and the damages of plate were modeled by releasing some nodes. Then, the damage location and the extent of the damage were tried to be determined. Although this method has been shown to work, it has some weaknesses. For example, a simple model and analytically simulated data were used. Because of that, it may not work on real measured data and for more complex structures.

Similarly, Yan et al. (2006) proposed a damage detection method using simple grid and finite element model. A graphical method based on the prediction that damage locally causes a reduction in rigidity has been studied. In the study conducted on the analytical model of a composite structure, 2249 elements were used in the conventional system, 1212 elements were used and the location and size of the damage were determined, but again only limited to analytical modeling and simulation. In this thesis study, the method proposed is prepared using both analytical and experimental data.

Friswell and Penny (1997) reported that damage assessment studies should be performed on both the simulated analytical and actual data.

Salehi et al. (2010) proposed a method that uses both the actual and relative parts of the frequency response functions (FRF) measured for damage detection parallel to the

Friswell and Penny's suggestion. In the study using the Gapped Smoothing Method (GSM) method, they found that there were changes when compared to undamaged and damaged FRFs. In this study 900x6.5x25.5 mm size analytical and 800x25x50 mm dimensions of the actual ruler was used. In this thesis study, damage detection method was carried out on a complex laboratory model similar to the real structure because it is suitable to show the method in such a simple structure. It is estimated that the study on the simple ruler will not be very successful in the hyper static complex structures with multiple degrees of freedom.

Yoon et al. (2005) studied to determine the variability of structural rigidity. The one-dimensional (1D) gapped smoothing method was expanded into two-dimensional space (2D). Sudden changes in the amount of curvature were scanned and damage assessment studies was performed. Statistical methods were used in this study. Both analytical and experimental plate models were used. As a result, the local rigidity changes, which are small in size according to the size of the structure, can be found in all homogenous structures by this method. However, only damage on the edge regions can be detected with this method and a simple model has been used as in the previous studies. The model in this thesis will be close to the real structure.

Gawronski and Sawicki (2000) tried to determine damage on laboratory truss structure by using modal and sensor directions. However, an excessive number of sensors were used in their study and more sensors were put into the region of the damage. In this thesis, fewer sensors were used.

Yang (2009) has developed a method that uses the matrix disassembly technique to determine the damage location and the vectors were used to calculate the amount of the damage.

Yang and Liu (2007) developed an algorithm to detection of damage location used modal residual force as a criterion. The method assumes that the measured eigenvalue dimension and the analytical eigenvalue dimension are the same and that the damage only causes loss of rigidity.

Yang and Liu (2007) accepted the modal force error (bj) defined for each mode as a criterion. If bj is zero, it is assumed that there is no damage to the member otherwise, that is, bj is different from zero and the member is damaged. Yang (2009) developed a new algorithm using this criterion. The loss of rigidity was defined with the diagonal matrix (α) consisting of a stiffness connectivity matrix and element rigidity damage parameters previously defined by Yang and Liu (2007). At the end of the algorithm, an equation emerges that the product of the diagonal matrix consisting of element rigidity damage parameters and a vector (dj) function of the damaged state eigenvalue vector is equal to another vector (ej) function of the damaged state parameters and the finite element model (undamaged case). If ej is zero, it is understood that the element is not affected by damage, and if it is any value other than zero, it is damaged. In order to determine the damage extent, the element damage parameters (α) are calculated by the division of ej to dj. The method was studied on a truss model consisting of 23 members. Two scenarios have been tried: (1) damage condition of a single member (2) damage condition of the two members. The study showed that the method works in both cases (in single or multiple damage cases). The method is remarkable because it uses only the matrix-vector and matrix-scalar products for damage location detection and the division technique for the damage extent.

Shi et al. (1998) tried to determine the location of damage by benefitting from the change of the modal strain energy for both damaged and undamaged cases.

Another method using the change of the modal strain energy was studied by Hu et al. (2006). Cross-Modal Strain Energy (CMSE) method was used to determine the damage extent for multiple damaged members. In the method, the mass was assumed as the same for both damaged and undamaged conditions and a five-story frame model was used for research. The methods generally accept the same masses of damaged and undamaged situations, but the masses of offshore oil platforms change constantly, not fixed. In this thesis, this change is taken into consideration.

Wang (2011, 2013) worked on estimating the damage severity of single or multiple damaged members and developed the IMSE (Iterative Modal Strain Energy) method. After the damage location was determined by any method, the IMSE method estimated the severity of damage by using modal frequencies that can be measured reliably with a single sensor instead of the mode shapes of the damaged structure. The major advantages of the method are that a minimum number of modal frequencies are sufficient and using of modal frequency which is more reliable than the mode shape. It is assumed that the damage will only change in the stiffness matrix, while the mass will remain the same. The eigenvalue and the eigenvector of the undamaged structure and the eigenvalue of the damaged structure are taken as known, and the damaged stiffness matrix and eigenvector as the unknown. Based on the eigen-analysis of the undamaged structure, the deformation energy equation, then the damage magnitude equation and eigenvectors of damaged case are obtained. After this stage, eigenvectors of the damaged model are found by taking the damage severity is 0 for the first iteration. In subsequent iterations, new damage magnitude values and eigen-vector values are found and then iterations are continued until the difference between the two iterations is reached to the desired tolerance range. A numerical example was conducted on a cantilever beam model with dimensions of 2.8x5.0 cm with a 2 m span length. The first three frequencies were used and two different scenarios were tried in the example. In addition, results were obtained by 1000 Monte Carlo simulations and these results were compared with the other test results using a similar beam model and it was observed that they were consistent and accurate with each other. The IMSE method which was studied in 2010 was improved and in this case, it was used to determine not only severity of damage but also both the damage location of the offshore platforms different from the previous study. The IMSE method has been studied to find the location and amount of damage in three-dimensional frame structures with incomplete or limited modal data. It was aimed to calculate the location and amount of the damage by using single algorithm unlike from the other studies related the damage detection. The study has significant advantages: (1) the ability to use the incomplete mode shapes in the algorithm without the need to use

model reduction and modal expansion methods to complete the missing data. (2) no need for full mode shape. However, mode shapes are proposed to be used in the method while determining the location of the damage instead of frequencies which are less susceptible than mode shapes. Because of that, the full mode shapes are suggested in order to improve the accuracy of the results. The full-mode shape was obtained by using the SDUP (Slave Degree of Freedom Iterative Updating Procedure) method, instead of using conventional model reduction or modal expansion techniques. SDUP is a method for completing slave DoF mode shapes using measured degrees of freedoms (DoF). (3) The first few modal frequencies are sufficient and do not need to be matched to the mode shapes. The most important disadvantage is that the damage only results in loss of stiffness, assuming the mass remains constant. Therefore, it is stated that there may be practical problems for the structures whose mass is constantly changing. The amount of damage was calculated using the IMSE method, but unlike the previous one, the damage locations are re- obtained by using another new method. This new method is based on the idea that "only the actual damage scenario causes different combinations of frequency changes in the measurements of the damaged structure". The combination of two different frequency changes and the severity of damage for each scenario (i.e. each member) is calculated and the member is assumed to be damaged where the difference of the two severity of damage is minimum. The effectiveness of the method was investigated for different scenarios on a numerical sample. Damage detection methods have also been studied for offshore structures.

Li et al. (2008) studied the damage detection of offshore jacket-type platforms in the case of limited or incomplete modal data are available. They focused on detection of damage using the first few modal parameters. Cross-model cross-mode (CMCM) method was used. The main advantages of this method are that only a few modes in the damaged case are sufficient and no matching or scaling between the measured and analytical modes is required. However, full mode is required to use the method. The method creates a matrix of linear equations, including unknown correction factors necessary to correct the selected stiffness and mass sub-matrices. In this study,

matrices including damaged and undamaged mass and stiffness matrices were obtained from the free vibration damping dynamic equation. Masses in damaged and undamaged cases are accepted as the same and this is a significant disadvantage of the method. In order to use this method in case of missing data, model reduction or modal expansion techniques are used. Guyan or SEREP (System Equivalent Reduction Expansion Process) methods were used to obtain the transformation matrix (T) required to obtain full-order coordinates in the main model. It was investigated which method was more successful. A test model consisting of 36 steel elements was damaged by reducing rigidity at various ratios to any three elements and the method was studied on this model. It was ascertained that iterative (repetitive) Guyan model reduction method gives the best results in the studies. Artificial neural network method was used in another study on damage detection in offshore platforms.

Elshafey et al. (2010) used random decrement signature and neural network methods for damage detection in offshore oil platforms. Neural networks were used to calculate the damage state function. The change in bearing conditions in the 1:30 scale model, similar to real one, was noticed by using a limited number of vibration-reading sensors. However, the growth of marine organisms (mussels, algae, etc.) on the structure and the additional mass of oil, natural gas, etc. collected on the platform has not been evaluated in the study. This deficiency has been taken into consideration in this study proposed and more close to reality and holistic study was made. In addition to the support conditions, changes in structural elements were investigated in our study. Moreover, in the available studies, structural measurement information related to the first undamaged form of the structure is needed, while the preliminary measurements in our study will not be needed.

Kim and Stubbs (1995) previously studied a similar study. Only the analytical model for offshore platforms and ABAQUS were used. At the end of the study, some results were obtained but it was stated that this study should be tested on real structures. In this study, damage detection method was carried out on a realistic laboratory model. In parallel with this study and the support letter from TPAO, the accuracy and

feasibility of the method can be investigated using real offshore platform measurements in the next studies.

Viero and Roitman (1999) conducted damage assessment studies on two different small-scale hydro-elastic offshore platform models. Inside of the pipe elements were filled with mercury to keep their rigidity low while increasing the mass of the elements. The location and magnitude of the damage were attempted to be found using MAC (Modal Assurance Criterion), COMAC (Coordinate Modal Assurance Criterion), MSF (Modal Scale Factor), RD (Relative Difference) and modal vectors. In this study, the parameters related to the marine creatures did not participate in the evaluation and be ignored, but it is estimated that their effect on damping rate will be great. Ruotolo et al. using novelty detection and SVD (single value decomposition) based techniques to create NASTRAN models for steel offshore platforms. In some of the simulations performed for five working conditions and four different damage cases, damages were detected but for some of them were not. In the study, it was stated that the novelty method could give outputs that would provide inputs to artificial neural networks and also stated that there was a need for undamaged model knowledge for the SVD technique. There are also damage detection studies using statistical methods.

Arangio and Beck (2012) benefited from statistical methods for assessing damage to the bridge. A statistical method was developed using Bayesian statistics and neural networks method together. In the first step of the method consisting of two phases, the neural network model was trained for the undamaged structure and then the damage estimate was made using the prediction errors in the new data that obtained for different damage situations. In the second step, it was tried to determine which element was damaged and the amount of the damage. It is noted that the method can also be used in complex structures (long bridges, offshore structures, etc.). The other important advantage is that there is no need for information about the structural model.

Hills and Courtney (2010) developed a general damage assessment study using nonlinear effects of fatigue damage. The bicoherence function of measured structural acceleration for early damage detection of offshore structures was used. It was stated that bicoherence analysis was commonly used for the detection of non-linear components from the answers in the bilinear system. In this study, it was used to understand the effect of fatigue damage caused by environmental vibrations of an element in a simulated offshore platform model. A real offshore platform was modeled and worked with loads originating from the natural environment instead of any external stimulus. The studies indicated that damage detection is sensitive only to rigidity changes even if very small but it is not affected by load changes, system damping and sea conditions.

Brincker et al. also studied on a statistical method. The ARMA (self-regressing moving average) model was used to obtain damage in offshore structures. The change in the obtained modal parameters was accepted as a damage indicator.

To sum up, this thesis has some significant advantages when compared with the other studies:

1) The model used was chosen very complex compared to the other models in studies in the literature. The model is close to the real structures.
2) The methods generally accept the same masses of undamaged and damaged cases, but the masses of offshore platforms change constantly due to the storage oil in the tank. This was taken into consideration in this thesis.
3) Static loading and displacement measurements in addition to dynamic parameters (natural vibration frequencies) were used.
4) Support conditions were investigated.
5) Calculation of forces that the waves form on the structures was explained and it was integrated into the method.
6) The method was studied using both analytical and experimental data.

CHAPTER 2

ANALYTICAL MODEL

2.1. Development of a Realistic Finite Element Model

A steel template offshore structure which has 175 m height was used as a model when considering general types for offshore structures in shallow water. Preliminary dimensioning is done using AUTOCAD and a model is scaled by 1:75 and this model was used for both analytical analyses and laboratory studies. The model consists of 20 vertical members, 20 horizontal members and 16 diagonal members. In the middle part of the model, 2 horizontal diagonal members are fixed to prevent the stability problems. Model general and plan views are shown in Figure 2.1 and Figure 2.2 respectively.

The SAP2000 program (Computers and Structures, 2015) was used for the finite element analyses. An analytical model that is compatible with AUTOCAD drawings was created before the physical experiments were performed. Before this model was calibrated, analyses of 10,000 damage scenarios randomly generated, and damage detection method was investigated, which was intended to be developed using the obtained analyses data and trained artificial neural networks.

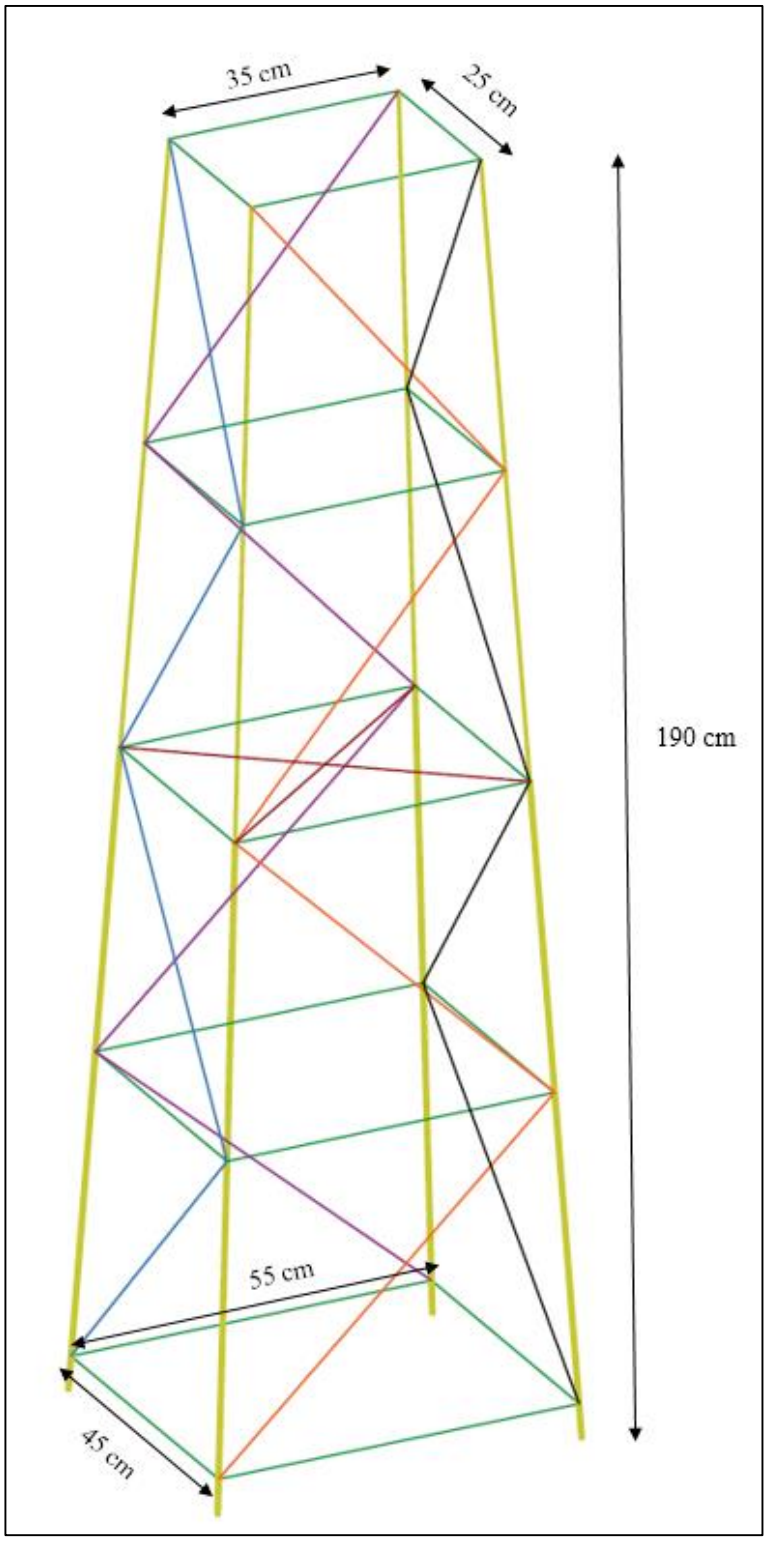

Figure 2.1. General View of the Model

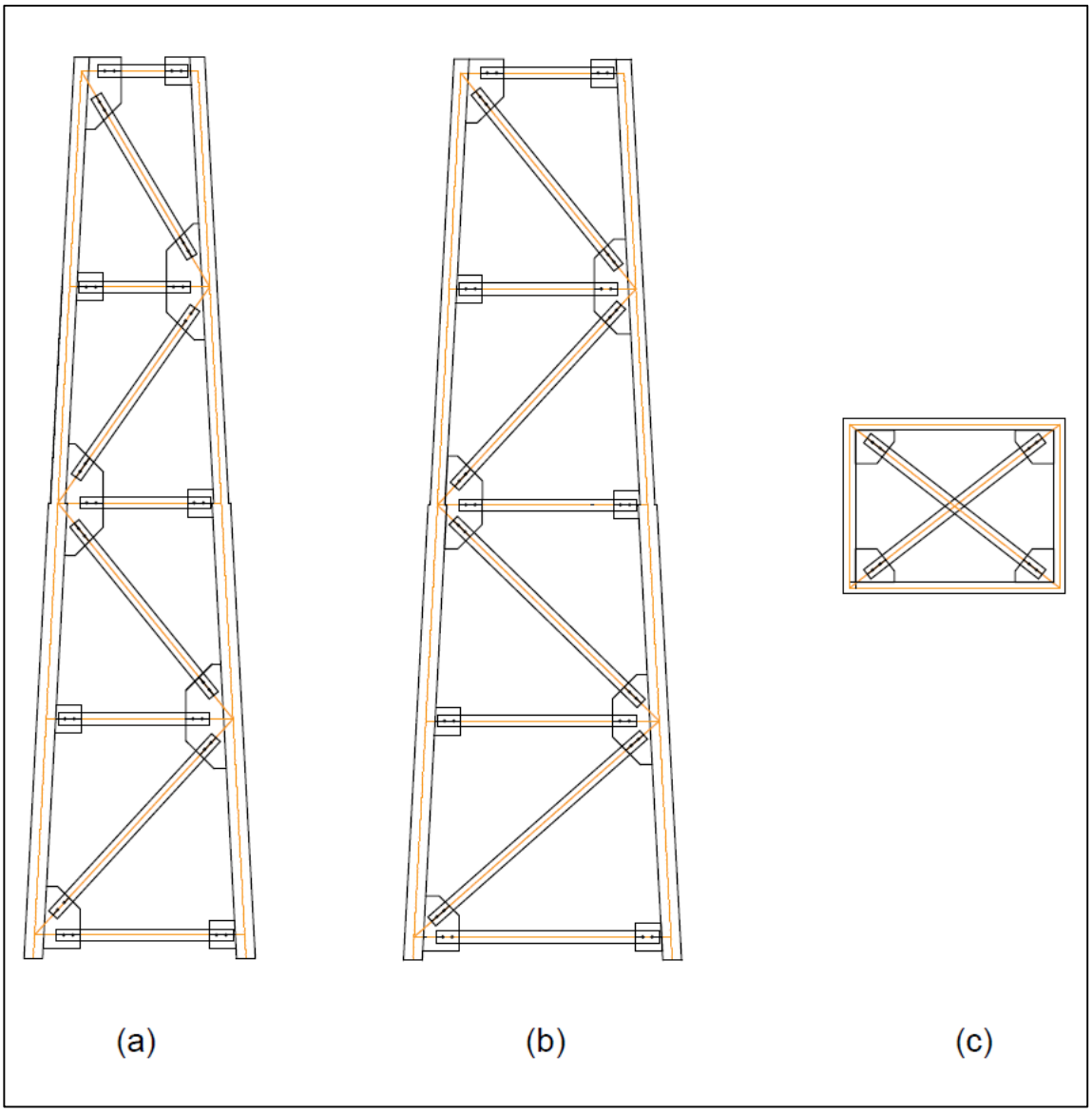

Figure 2.2. Planes View of the Model (a) in Y-Z, (b) in X-Z, and (c) mid-X-Y

2.2. Automated Generation of Random Damage States

Initial planning for damage considered possibility of rusting (section loss) and cracking (fatigue). Buckling failure is out of the scope of this study, but it can be taken into consideration for full-scale structures. Continuous and cyclic loading of waves might generate fatigue problem especially at connections where stresses might be

concentrated and salty sea water is a primary concern for rusting. The rusting of structural members is a slow progress and mostly concentrated at a region generating section loss. Hypothetically, section loss at a concentrated location is investigated using simple truss analogy. If a member of length L and area of A loses cross section by α amount, α being between 0 and 1, the remaining cross section is A(1- α). Assuming length of the rusted portion is β as a fraction of length L, then the remaining healthy length is L(1- β). The stiffness before section loss is EA/L while the reduced section would have stiffness of EA/(1- α)/(Lβ); the healthy part would have stiffness of EA/[L(1-β)]. The two members connected in series requires the same force acting on both of them. The total deformation is the sum of deformations of the damaged and undamaged members. Assuming a force of F acting on both of the members, the deformations are F/{EA/[L(1-β)]} and F/{EA(1- α)/(Lβ)}. The stiffness of the overall member composed of damaged and undamaged parts would be F divided by total deformation. The effective stiffness equation is obtained as

$$k_e=F/[\ F/\{EA/L(1-\beta)\} + F/\{\ EA(1-\alpha)/(L\beta)\}]$$

and simplified to be

$$k_e=(EA/L)/[1/(1-\beta)+\beta/(1-\alpha)]$$

The effective stiffness (k_e) as compared to the undamaged stiffness shows minimal changes as seen from Table 2.1. The rusted length up to 5% of the length and section loss up to 50% of the original area changes stiffness by only 5% to 10% of the original stiffness. Considering that one of the member's stiffness change will have minimal impact on the global stiffness and vibration frequencies of the tested structure, it was deemed to be ineffective to model rusting damage. Similarly, cracking of a section would also have negligible effect on the overall stiffness of a member and the tested structure; because, damaged section area (cracked section area to the total area ratio) α would have no effect if damaged section length to total length ratio (β) is zero, which is the actual case when a crack is formed. Therefore, generation of a crack cannot be theoretically detected unless the crack propagates to the total cross section causing a

totally cracked (detached) member. The member might transfer compressive force and zero tensile force after a total crack is formed; however, this nonlinear condition has been left out of the scope of this thesis. The simulations are based on either a member is fully functional or totally lost. Furthermore, the damage scenarios considered removal of a single member rather than two or more members at the same time. The reason for such an assumption is due to the fact that monitoring will be continuously done and the very first damage will be promptly detected and alarm will be sent out.

Table 2.1. *Effective Stiffness of a Member (k_e) With Respect to α and β*

	α																					
β	0.00%	2.50%	5.00%	7.50%	10.00%	12.50%	15.00%	17.50%	20.00%	22.50%	25.00%	27.50%	30.00%	32.50%	35.00%	37.50%	40.00%	42.50%	45.00%	47.50%	50.00%
0.00%	1.000	1.000	1.000	1.000	1.000	1.000	1.000	1.000	1.000	1.000	1.000	1.000	1.000	1.000	1.000	1.000	1.000	1.000	1.000	1.000	1.000
0.20%	0.996	0.996	0.996	0.996	0.996	0.996	0.996	0.996	0.996	0.995	0.995	0.995	0.995	0.995	0.995	0.995	0.995	0.995	0.994	0.994	0.994
0.40%	0.992	0.992	0.992	0.992	0.992	0.991	0.991	0.991	0.991	0.991	0.991	0.991	0.990	0.990	0.990	0.990	0.989	0.989	0.989	0.988	0.988
0.60%	0.988	0.988	0.988	0.988	0.987	0.987	0.987	0.987	0.987	0.986	0.986	0.986	0.986	0.985	0.985	0.985	0.984	0.984	0.983	0.983	0.982
0.80%	0.984	0.984	0.984	0.984	0.983	0.983	0.983	0.983	0.982	0.982	0.982	0.981	0.981	0.980	0.980	0.980	0.979	0.978	0.978	0.977	0.977
1.00%	0.980	0.980	0.980	0.980	0.979	0.979	0.979	0.978	0.978	0.978	0.977	0.977	0.976	0.976	0.975	0.975	0.974	0.973	0.972	0.972	0.971
1.20%	0.976	0.976	0.976	0.975	0.975	0.975	0.974	0.974	0.974	0.973	0.973	0.972	0.972	0.971	0.970	0.970	0.969	0.968	0.967	0.966	0.965
1.40%	0.973	0.972	0.972	0.972	0.971	0.971	0.970	0.970	0.969	0.969	0.968	0.968	0.967	0.966	0.965	0.965	0.964	0.963	0.962	0.961	0.960
1.60%	0.969	0.968	0.968	0.968	0.967	0.967	0.966	0.966	0.965	0.964	0.964	0.963	0.962	0.962	0.961	0.960	0.959	0.958	0.957	0.955	0.954
1.80%	0.965	0.965	0.964	0.964	0.963	0.963	0.962	0.961	0.961	0.960	0.959	0.959	0.958	0.957	0.956	0.955	0.954	0.953	0.951	0.950	0.948
2.00%	0.961	0.961	0.960	0.960	0.959	0.959	0.958	0.957	0.957	0.956	0.955	0.954	0.953	0.952	0.951	0.950	0.949	0.948	0.946	0.945	0.943
2.20%	0.957	0.957	0.956	0.956	0.955	0.955	0.954	0.953	0.952	0.952	0.951	0.950	0.949	0.948	0.947	0.945	0.944	0.943	0.941	0.939	0.938
2.40%	0.954	0.953	0.953	0.952	0.951	0.951	0.950	0.949	0.948	0.947	0.946	0.945	0.944	0.943	0.942	0.941	0.939	0.938	0.936	0.934	0.932
2.60%	0.950	0.949	0.949	0.948	0.947	0.947	0.946	0.945	0.944	0.943	0.942	0.941	0.940	0.939	0.937	0.936	0.935	0.933	0.931	0.929	0.927
2.80%	0.946	0.946	0.945	0.944	0.943	0.943	0.942	0.941	0.940	0.939	0.938	0.937	0.936	0.934	0.933	0.931	0.930	0.928	0.926	0.924	0.922
3.00%	0.943	0.942	0.941	0.940	0.940	0.939	0.938	0.937	0.936	0.935	0.934	0.933	0.931	0.930	0.928	0.927	0.925	0.923	0.921	0.919	0.917
3.20%	0.939	0.938	0.937	0.937	0.936	0.935	0.934	0.933	0.932	0.931	0.930	0.928	0.927	0.926	0.924	0.922	0.920	0.919	0.916	0.914	0.912
3.40%	0.935	0.935	0.934	0.933	0.932	0.931	0.930	0.929	0.928	0.927	0.925	0.924	0.923	0.921	0.920	0.918	0.916	0.914	0.912	0.909	0.906
3.60%	0.932	0.931	0.930	0.929	0.928	0.927	0.926	0.925	0.924	0.923	0.921	0.920	0.918	0.917	0.915	0.913	0.911	0.909	0.907	0.904	0.901
3.80%	0.928	0.927	0.926	0.925	0.924	0.923	0.922	0.921	0.920	0.919	0.917	0.916	0.914	0.913	0.911	0.909	0.907	0.904	0.902	0.899	0.896
4.00%	0.924	0.924	0.923	0.922	0.921	0.920	0.919	0.917	0.916	0.915	0.913	0.912	0.910	0.908	0.906	0.904	0.902	0.900	0.897	0.895	0.892
4.20%	0.921	0.920	0.919	0.918	0.917	0.916	0.915	0.913	0.912	0.911	0.909	0.908	0.906	0.904	0.902	0.900	0.898	0.895	0.893	0.890	0.887
4.40%	0.917	0.916	0.915	0.914	0.913	0.912	0.911	0.910	0.908	0.907	0.905	0.904	0.902	0.900	0.898	0.896	0.893	0.891	0.888	0.885	0.882
4.60%	0.914	0.913	0.912	0.911	0.910	0.908	0.907	0.906	0.904	0.903	0.901	0.900	0.898	0.896	0.894	0.891	0.889	0.886	0.884	0.880	0.877
4.80%	0.910	0.909	0.908	0.907	0.906	0.905	0.903	0.902	0.901	0.899	0.897	0.896	0.894	0.892	0.889	0.887	0.885	0.882	0.879	0.876	0.872
5.00%	0.907	0.906	0.905	0.904	0.902	0.901	0.900	0.898	0.897	0.895	0.893	0.892	0.890	0.888	0.885	0.883	0.880	0.878	0.874	0.871	0.868

A code was written to automatically create 10,000 damage scenarios using Excel VBA and SAP2000 API (Application Program Interface). The code does the following steps in the given order:

1) The code first automatically runs the SAP2000 program and relevant model file containing the original model through Excel VBA.
2) It randomly selects one of the elements previously labeled out 58 members in the model and assigns the coefficient of section area, torsional, and moment of inertia values of this element to 0 and assumes that the element is completely damaged.
3) Modal analysis performed for the generated damaged condition and the calculated modal frequencies are printed in a data table for the first six modes.

Furthermore, total of 500 Newton load is applied on two upper corner nodes and in each horizontal direction separately (Figure 2.3). Displacements and rotations at the corner joints of the platform above the structure due to these loads are also added to the data table for each direction. These displacements and rotation are used for damage detection as well.

4) The damaged member is restored and the code repeats the steps described above by assigning another randomly damaged member again.

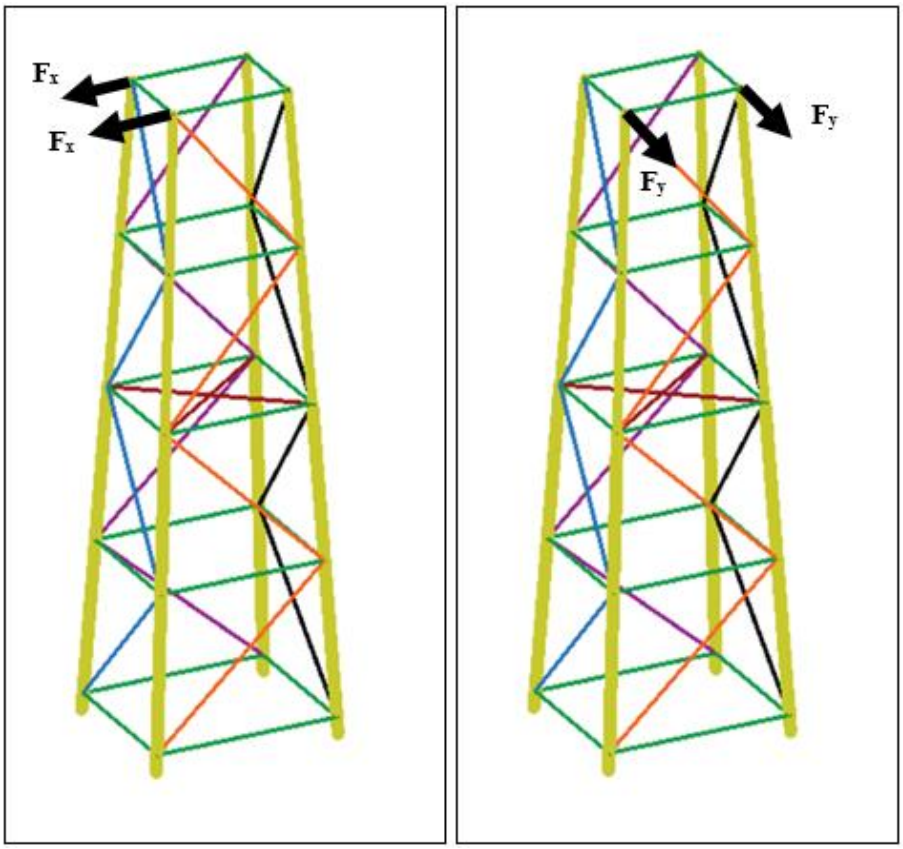

Figure 2.3. Configuration of Applied Forces in x and y Directions

Thus, the frequencies of the first six modes, the displacement and rotation values due to the force applied separately in both directions for the 10,000 damage scenarios are obtained by repeating steps 2 to 4 and used as input data for the Artificial Neural Network (ANN) based damage detection method developed in this study.

In the second stage of the studies, a new series of analytical models were created by considering the mass changes in the oil platform above the structure and using this model, 10,000 different damage scenarios were created which had random damaged members together with random mass assignments. Furthermore, additional 200 cases were generated where there are no damaged members but the platform mass is randomly changing.

2.3. ANN Training

Various ANN training sets were tested and success rates were all very high for the analytical data. Validation check that is overtraining has been controlled for all ANNs. Minimum success rate for all ANNs using FEM data was accepted as 90%. These sets are summarized below under headings and further details are given in the following section.

Input data must be normalized in order to be used in ANN technique. Since only analytical model data were used, differences were obtained by subtracting the frequencies, displacements, and rotations obtained from the analysis of each damaged scenario from the frequency, displacement, and rotation values of the undamaged condition. These differences were normalized and made ready to enter the artificial neural network as a parameter between 0 and 1.

$$\text{Normalization formula} \longrightarrow x' = (x - x_{min}) / x_{max} - x_{min}$$

An encoding of 0 and 1 was used for the groups, 0 indicating damaged member does not belong to a group and 1 indicates the damaged member belongs to that group.

A) 10,000 damage scenarios without platform mass. This set is repetitive damage scenarios of 58 members and ANN gave 100% success probably by memorizing the data. The output of this primitive network was not showing which member has the damage but rather categorizing the damaged member

being in one of the groups: 1) vertical, 2) horizontal, and 3) diagonal (Table 2.2). Figure 2.4 shows the Type-A ANN. Validation check that is overtraining has been controlled for all ANNs.

Type A and B based ANNs used the output damaged members of the model in three groups as shown in Table 2.2. The grouping was made as:

1) Vertical members
2) Horizontal members
3) Diagonal members

Table 2.2 *First Grouping of Member IDs as Used for Output in ANN Training*

Vertical Members ID	**Horizontal Members ID**	**Diagonal Members ID**
1	21	41
2	22	42
3	23	43
4	24	44
5	25	45
6	26	46
7	27	47
8	28	48
9	29	49
10	30	50
11	31	51
12	32	52
13	33	53
14	34	54
15	35	55
16	36	56
17	37	57
18	38	58
19	39	
20	40	

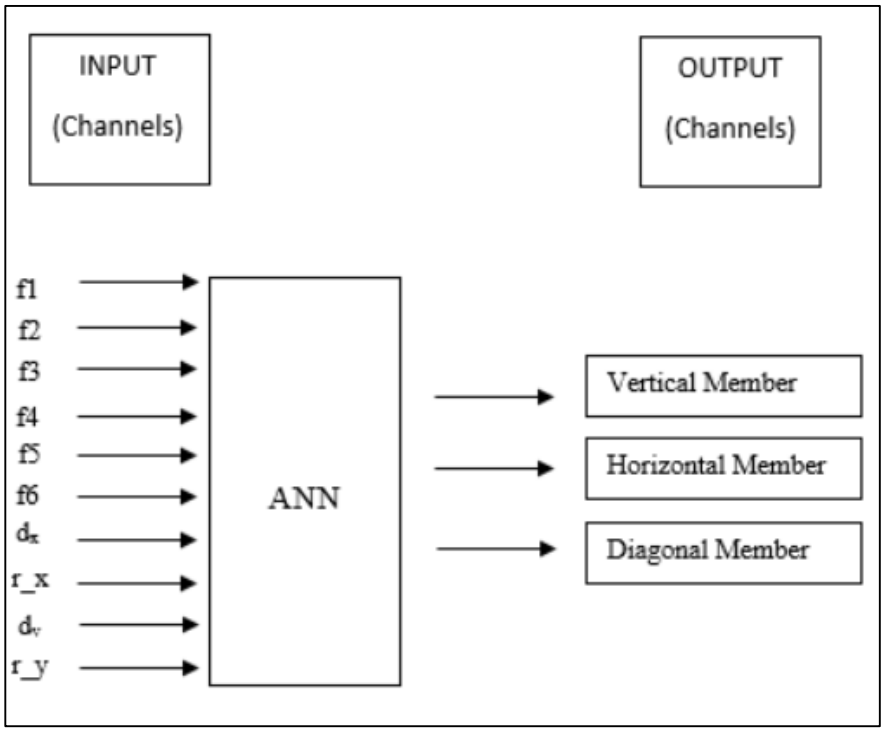

Figure 2.4. First Used ANN System (Type-A)

f1: first mode frequency

f2: second mode frequency

f3: third mode frequency

f4: fourth mode frequency

f5: fifth mode frequency

f6: sixth mode frequency

dx: Displacement due to 500 N force applied in X direction

r_x: Rotation due to 500 N force applied in X direction

dy: Displacement due to 500 N force applied in Y direction

r_y: Rotation due to 500 N force applied in Y direction

Example data set of Type-A input and outputs are given below (Table 2.3).

Table 2.3. *Example Input and Output Data Set for ANN Type-A Training*

Scenario No.		1	2	3	4	5	6	7	8	9	10
Damaged Member ID		22	6	36	34	6	31	58	41	11	27
Input	norm f1	0.55371	0.01876	0.66115	0.46504	0.055	0.56667	0.52355	0.83238	0.33314	0.90558
	norm f2	0.33988	0.09542	0.49469	0.20582	0.18267	0.36041	0.29545	0.96579	0.5741	0.86049
	norm f3	0.85233	0.61537	0.84112	0.78034	0.64463	0.84476	0.84494	0.22967	0.71059	0.94234
	norm f4	0.67227	0.59484	0.38499	0.32481	0.62204	0.56246	0.65753	0.3874	0.5467	0.44803
	norm f5	0.4907	0.42074	0.13488	0.02093	0.46379	0.51542	0.47737	0.9662	0.31523	0.65886
	norm f6	0.49544	0.10221	0.15967	0.09189	0.17638	0.51427	0.4515	0.7807	0.51687	0.2269
	norm dx	0.00056	0.71353	0.00068	0.00071	0.71353	0.00019	0.00011	0.00122	0.47973	0.00206
	norm r_x	0.49475	0.8161	0.49667	0.49414	0.8161	0.49522	0.49544	0.51187	0.15588	0.49502
	norm dy	0.00010	1	0.00041	0.00064	1	0.00014	1.8E-06	0.04393	0.81088	0.00057
	norm r_y	0.49406	0.06836	0.49411	0.49291	0.06836	0.4931	0.49363	0.61612	5.28E-15	0.49304
Output	Vetical Member	0	1	0	0	1	0	0	0	1	0
	Horizontal Member	1	0	1	1	0	1	0	0	0	1
	Diagonal Member	0	0	0	0	0	0	0	1	0	0

By adding the varying mass effect to the scenarios, 10,000 scenarios were renewed after Type-A and the analyses were repeated with an additional 200 scenarios for different masses without damage. Damage detection studies were repeated according to the output groups previously formed and successful results were obtained.

In this way, the network was able to find these output values correctly in trainings using feed-forward and log-sigmoid threshold function (which values between 0 and 1 for layer outputs). Upon the successful results of this training, the changes in the mass were also used in the determination study and ANN trainings were repeated. In the Type-A ANN model, the mass change was added as an additional input parameter and the Type-B ANN system was generated.

B) 10,200 damage scenarios with randomly changing platform mass. ANN based damage grouping network could successfully identify the damaged member's group (vertical, diagonal, horizontal) (Table 2.2) even though the mass is changing. Figure 2.5 shows the Type-B ANN.

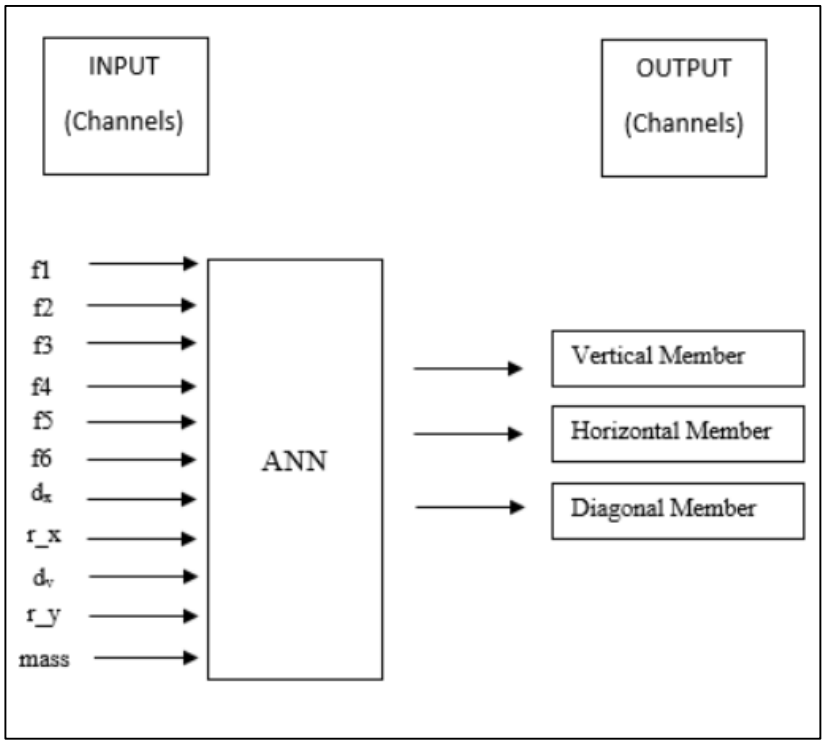

Figure 2.5. ANN System Including Mass Change (Type-B)

f1: first mode frequency

f2: second mode frequency

f3: third mode frequency

f4: fourth mode frequency

f5: fifth mode frequency

f6: sixth mode frequency

dx: Displacement due to 500 N force applied in X direction

r_x: Rotation due to 500 N force applied in X direction

dy: Displacement due to 500 N force applied in Y direction

r_y: Rotation due to 500 N force applied in Y direction

mass: Mass of oil platform when filled with various percentages

The Type-B ANN based on 11 input parameters have also been successful in the damage detection studies to identify one of the three groups (vertical, horizontal, diagonal) finding the type of damaged member.

Type-B based ANNs also used the output damaged members of the model in three groups similar as Type-A shown in Table 2.2.

C) The new generation ANN has been improved to have three stages, which are 1) type (vertical, horizontal, vertical diagonal, and horizontal diagonal) (Table 2.4, Figure 2.6), 2) layer indicating each floor (1, 2, 3, 4 from bottom towards top) (Table 2.5, Figure 2.7, and Figure 2.8), and 3) plane of damage (North, West, South, East, and middle horizontal plane) (Table 2.6, Figure 2.9, and Figure 2.10). The ANN generations after Type-A have all used 10,200 data points with changing mass including this one. The outputs of these three independent ANN were combined to pinpoint the location of damaged member. Success rate for this system is 100%.

The first group (Type-C1) was formed to indicate the type of the element:

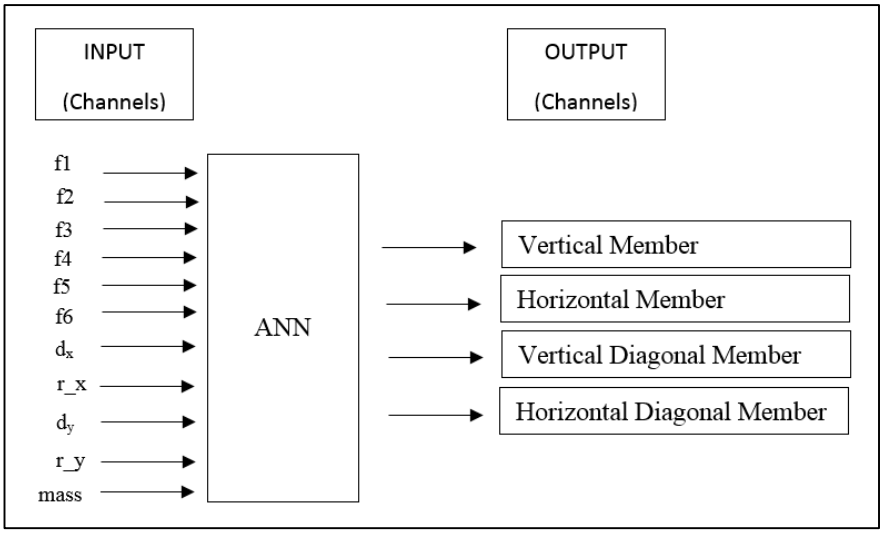

Figure 2.6. Type-C1 ANN

These groups mentioned above are shown in Table 2.4.

Table 2.4. *Type-C1 ANN for System with 3 Network Training*

Vertical Member ID	Horizontal Member ID	Vertical Diagonal Member ID	Horizontal Diagonal Member ID
1	21	41	57
2	22	42	58
3	23	43	
4	24	44	
5	25	45	
6	26	46	
7	27	47	
8	28	48	
9	29	49	
10	30	50	
11	31	51	
12	32	52	
13	33	53	
14	34	54	
15	35	55	
16	36	56	
17	37		
18	38		
19	39		
20	40		

The second group (Type-C2) was formed to show which floor the element belongs to:

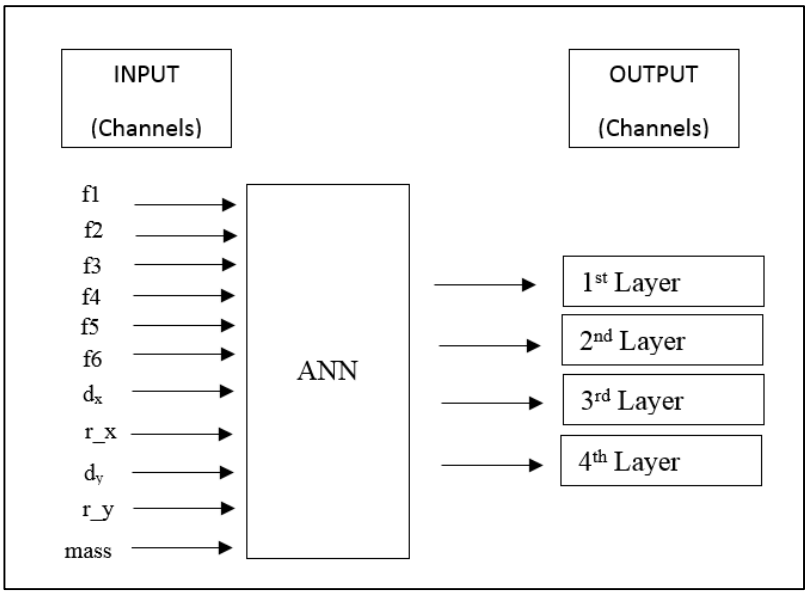

Figure 2.7. Type-C2 ANN

Table 2.5. *Type-C2 ANN for System with 3 Network Training*

1st Layer	2nd Layer	3rd Layer	4th Layer
1	9	13	17
2	10	14	18
3	11	15	19
4	12	16	20
5	25	29	33
6	26	30	34
7	27	31	35
8	28	32	36
21	42	43	37
22	46	47	38
23	50	51	39
24	54	55	40
41		57	44
45		58	48
49			52
53			56

Layer groupings of members are also available on the model plan (Figure 2.8).

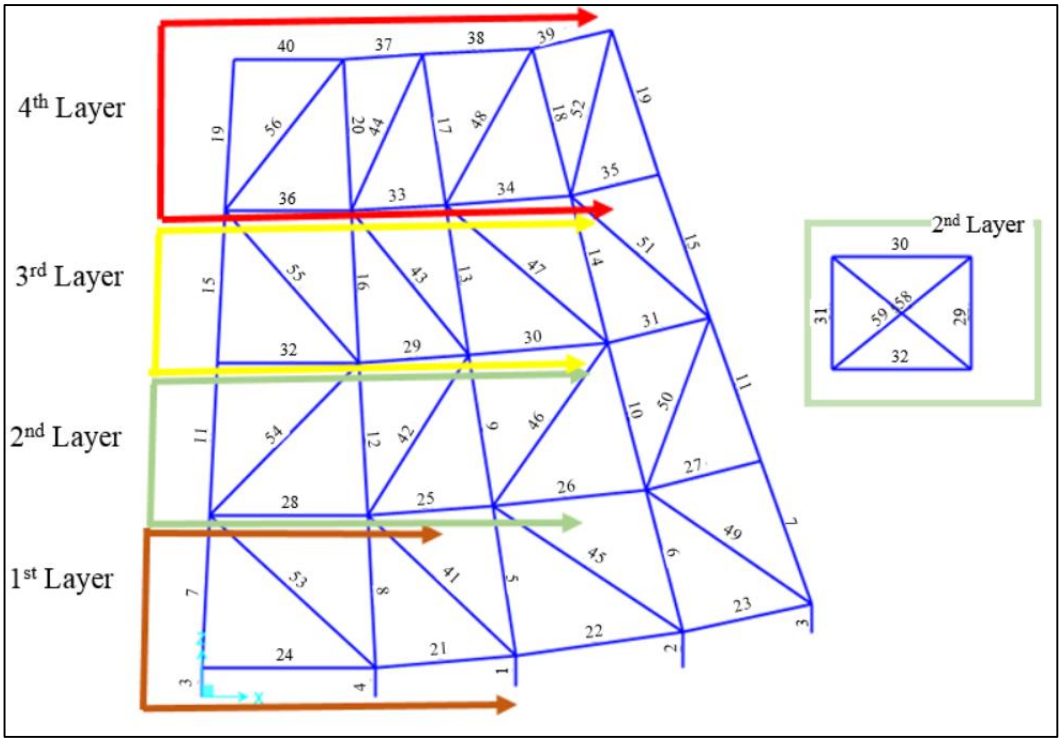

Figure 2.8. Layer Plan of the Model Used Type-C2

The third group (Type-C3) was formed to determine which plane of the structure the element is located:

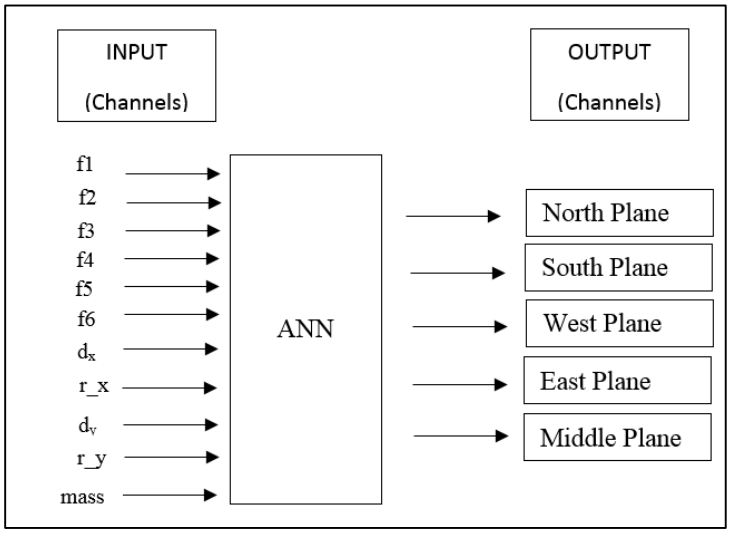

Figure 2.9. Type-C3 ANN

Table 2.6. *Type-C3 ANN for System with 3 Network Training*

North Plane	South Plane	West Plane	East Plane	Middle Plane
3	1	4	2	57
7	5	8	6	58
11	9	12	10	
15	13	16	14	
19	17	20	18	
24	22	21	23	
28	26	25	27	
32	30	29	31	
54	46	42	50	
53	45	41	49	
55	47	43	51	
36	34	33	35	
56	48	44	52	
40	38	37	39	

Plane groupings of members are also available on the model plan (Figure 2.10).

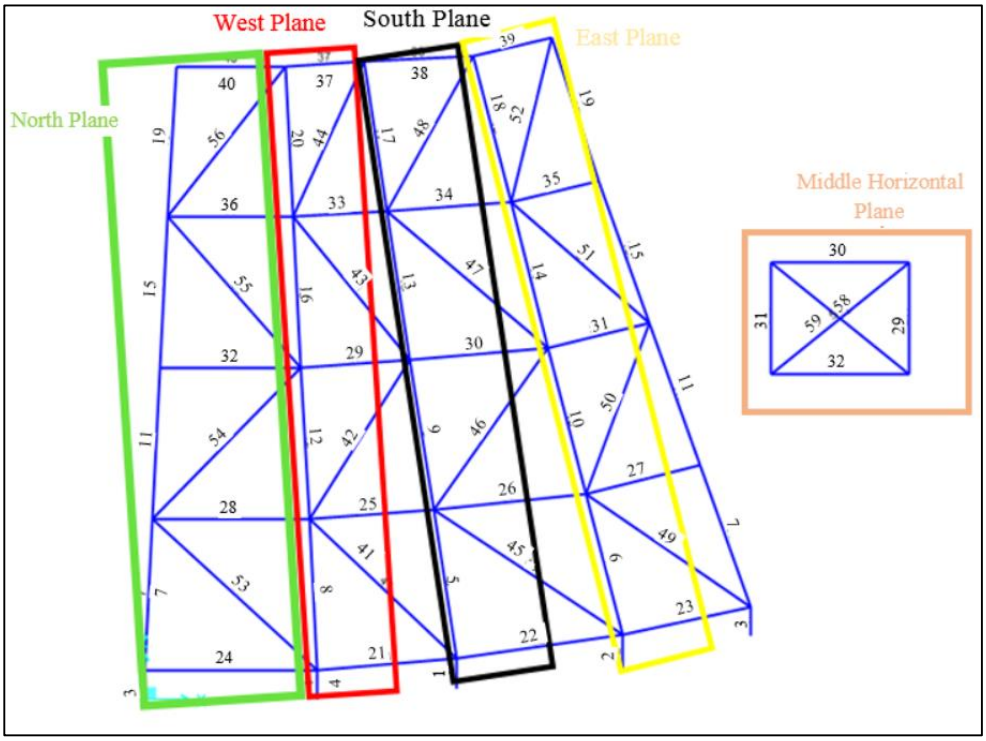

Figure 2.10. Plane Plan of the Model Used Type-C3

Example data set of Type-C input and outputs are given below (Table *2.7*).

Table 2.7. *Input and Output Sample Containing 3 Staged ANN Trainings (Type-C)*

Scenario No.		1	2	3	4	5	6	7	8	9	10
Damaged Member ID		20	40	14	22	32	50	30	42	36	35
Input	norm f1	0.73328	0.52128	0.38436	0.79823	0.82779	0.44296	0.49394	0.63833	0.60006	0.97062
	norm f2	0.53687	0.29069	0.33545	0.70205	0.74455	0.27895	0.25080	0.71121	0.40515	0.96919
	norm f3	0.80119	0.84236	0.63361	0.93453	0.94372	0.16405	0.82825	0.39389	0.82259	0.87721
	norm f4	0.52698	0.65638	0.08116	0.82218	0.84476	0.45822	0.64259	0.45629	0.36573	0.48113
	norm f5	0.20418	0.46453	0.41512	0.72962	0.58025	0.46824	0.28405	0.75121	0.09031	0.50613
	norm f6	0.47386	0.44797	0.41940	0.81376	0.84447	0.43601	0.40326	0.80845	0.14112	0.27359
	norm dx	0.14097	0.00349	0.16163	0.00056	0.00027	0.00160	0.00014	0.00129	0.00068	0.00219
	norm r_x	0.74728	0.50224	0.73354	0.49475	0.49570	0.51929	0.49503	0.47312	0.49667	0.49664
	norm dy	0.00351	0.00013	0.47682	0.00010	0.00079	0.08511	0.00017	0.10575	0.00041	0.00116
	norm r_y	0.45972	0.49280	0.03426	0.49406	0.49318	0.29307	0.49395	0.72738	0.49411	0.49056
	norm mass	0.37039	0.82333	0.67803	0.26529	0.22028	0.84492	0.89703	0.25565	0.63234	0.02280
Output	Vertical	1	0	1	0	0	0	0	0	0	0
	Horizontal	0	1	0	1	1	0	1	0	1	1
	Diagonal	0	0	0	0	0	1	0	1	0	0
	Middle Diagonal	0	0	0	0	0	0	0	0	0	0
	1. Layer	0	0	0	1	0	0	0	0	0	0
	2. Layer	0	0	0	0	0	1	0	1	0	0
	3. Layer	0	0	1	0	1	0	1	0	0	0
	4. Layer	1	1	0	0	0	0	0	0	1	1
	North Plane	0	1	0	0	1	0	0	0	1	0
	South Plane	0	0	0	1	0	0	1	0	0	0
	West Plane	1	0	0	0	0	0	0	1	0	0
	East Plane	0	0	1	0	0	1	0	0	0	1
	Middle Plane	0	0	0	0	0	0	0	0	0	0

Type C based Artificial Neural Network model was slightly improved to have four groups (Type-C1) instead of three by separating the horizontal diagonal member as shown in Figure 2.6. Furthermore, second (Type-C2) and third level (Type-C3) ANNs were added to actually pinpoint the damaged member. Similar to previous networks, damaged member groups from each level (C1, C2, and C3) are identified by outputs of either 0 or 1.

D) Staged independent ANNs were planned to be combined into ANN by changing the output channels to member IDs (Figure 2.11). If a member is damaged the output of corresponding channel would give 1 while all the others were zero. There are 58 members and 58 output channels; if all of the channels give zero output, this network is assumed to indicate that there are no damaged members.

One of the last two new ANNs were Type-D with 58 member outputs. In this grouping, it was studied directly on the detection of the damaged element. In Type-D, an output channel was created for each one of the 58 elements. The damaged member is determined by an output of 1 from its dedicated channel while all the other channels were zeros indicating no damage.

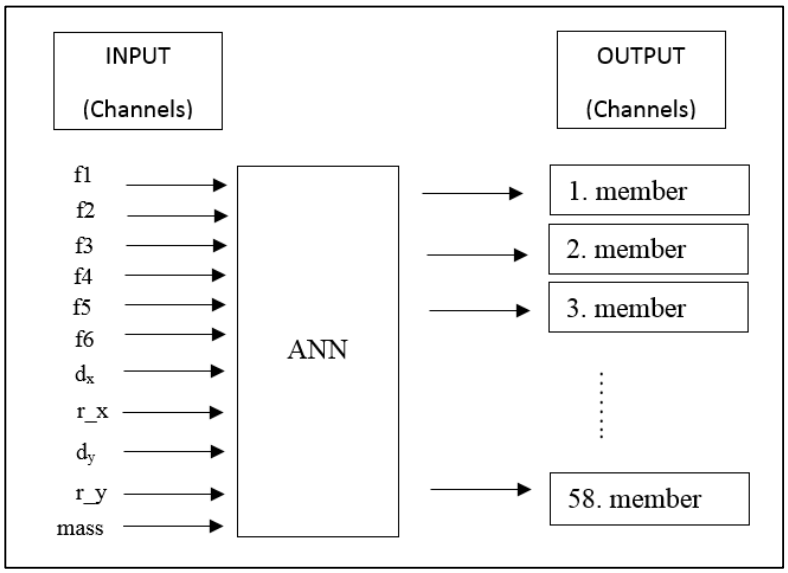

Figure 2.11. Type-D ANN with 58 Output Channels

E) Single ANN defined in (D) above was found to be indirect to identify the undamaged case and another set was tried by giving a dedicated output channel for the undamaged scenario. In this way, ANN would indicate from a channel that the system is healthy. There are 58 members and 59 output channels in Type-E (Figure 2.12). In this way, if all of the members are healthy, the ANN is supposed to give 1 for the undamaged channel #59.

The last ANN model, in addition to the 58-group system, a separate channel #59 was created for the undamaged state of all members. When channel 59 gives an output of 1, this indicates that all members are undamaged. On the contrary, channel 59 giving a zero output indicates a damaged state. When channel 59 is 0, one of the other 58 channels must be 1. This criterion is not defined within ANN but is a simple external self-check of the ANN Type-E and superior to other types. Thus, a new element identification method with self-checking was obtained that consists of 59 channels. This grouping system has also been very successful with 97% success rate. Therefore, it was decided to use the ANN system with 59 groups.

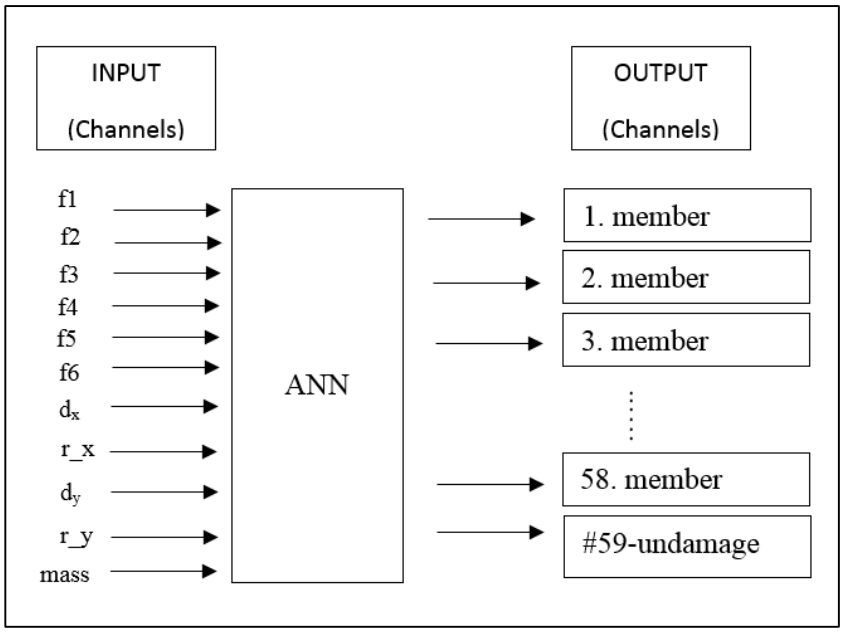

Figure 2.12. Type-E ANN with 59 Output Channels

2.4. Results

The studies conducted using different ANN types (A to E) were made to decide which type to be used for damage detection. Once Type-E was selected as the best option, a physical lab model with 1:75 scale was constructed in the structures laboratory and nominal analytical model was calibrated to closely mimic the actual physical model. The ANN data generation is repeated for 10,200 cases using the calibrated FEM and the network Type-E was trained using that data. Damage detection success rate of 97% was obtained using the calibrated analytical model damage simulation results by correctly identifying 970 of the 1000 damaged and undamaged damage case data (with changing platform mass) that was not used during the ANN training process.

CHAPTER 3

EXPERIMENTAL MODEL AND TESTING STUDIES

3.1. Lab Model Construction

The analytical model created in the 1:75 scale was built in the laboratory with the same scale. PVC pipes were used for the physical model of the structure instead of steel which is commonly used in full size applications. The plastic material has lower elastic modulus and would yield higher deformations as well as larger vibration frequencies. Since the tower model will be submerged in water at later stages of the study, plastic was also thought to be better against rusting.

The material properties of PVC pipe were obtained using simple bending tests and verified against available generic data about the material. These results are also used for the nominal FEM. The calibration was conducted after static and dynamic tests were conducted on the physical model because of the uncertainties coming from the connections. Metal plates, bolts, and clamps were used during the construction.

For the connection of PVC pipes, it was initially considered that the pipes are melted and bonded to each other or using a special adhesive / epoxy glue as an alternative; however, all of these methods were tested and found to be not a robust approach. The pipes were later decided to be connected using steel plates, bolts, and clamps. This established stronger bond than the other methods. Plates with 2 mm thick stainless steel were cut by CNC laser cutting method in accordance with the plan designed to be specific to each connection point shown in Figure 2.2. The plates were welded to the clamps and used to connect the horizontal and diagonal members. Figure 3.1 shows the connection plates in detail. The final state of connection plates is available in Figure 3.2.

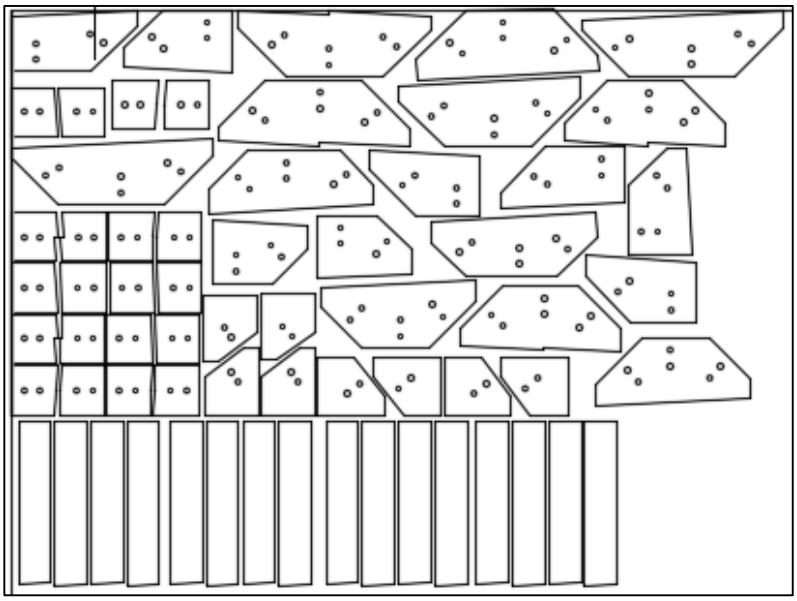

Figure 3.1. Cutting Plan of Connection Plates

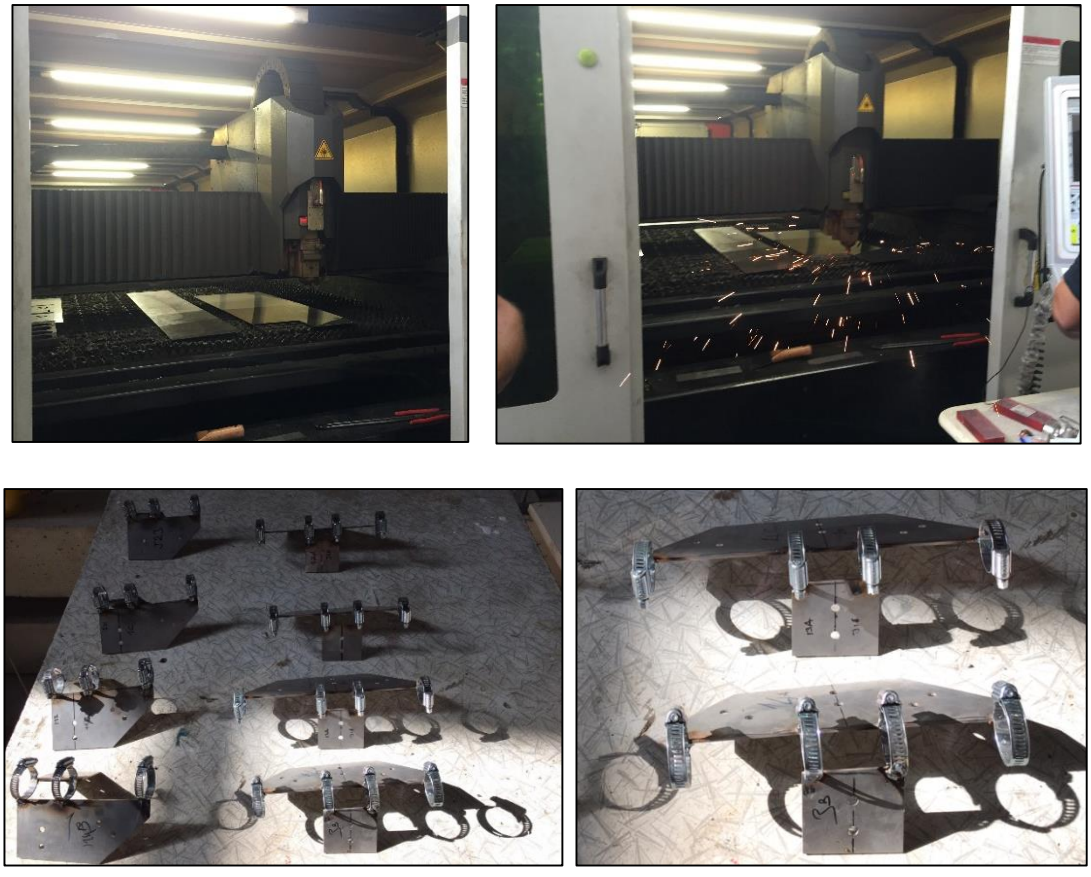

Figure 3.2. Ready to Use Connection Plates after Cutting and Welding

Two ϕ5mm diameter bolts were used at each joint to mount the horizontal and diagonal members. Holes of ϕ6 mm diameter were formed for the bolts. The fasteners are combined with clamps that are welded to the plates (Figure 3.3).

Figure 3.3. Joining of Connection Plates to the Members

Vertical members were formed by using PVC pipes with a diameter of ϕ40 mm for the lower two layers and PVC pipes with a diameter of ϕ32 mm for the upper two layers. PVC pipes with a diameter of ϕ25 mm were used for horizontal and diagonal members. The upper deck (platform) of the physical model was designed with 11 mm thick steel plate for rigidity and extra mass. The variable mass on the top of the tower is established using a 10 lt tank at the top of the platform rigidly connected to the platform. The tank is filled up with varying levels of water to simulate the extra mass and slushing effect. Construction steps of the model can be seen in Figure 3.4, Figure 3.5, and Figure 3.6.

Figure 3.4 Vertical Members and PVC Pipes Used as Horizontal and Diagonal Members

Figure 3.5. Welding Process of Connection Plates

Figure 3.6. Stages of Physical Model Construction

The model supports were fixed with three steel plates weighing approximately 16 kg each for a total of 48 kg/support for improved stability. However, it was seen that these weights were insufficient in static tensile tests, and heavier masses were placed in order to prevent the support from lifting up (Figure 3.7).

Figure 3.7. Lifting of the Feet and Fixing with Additional Weight

Calibration studies have begun after the completion of the physical model. It was aimed to develop the most appropriate analytical model. First step in the calibration stage was conducting the material tests.

A simple experiment was carried out to determine the elasticity modulus by fixing the PVC pipe with a diameter of 25 mm to the table in the form of cantilever beam. The load - displacement graph was obtained by measuring the displacement caused by the sandbag of various weights attached to the end of the cantilever beam and the elasticity module was calculated using the deflection formula. The frequency for the first mode of the beam was also determined and the modulus of elasticity was calculated by the formula used to find the frequency of the cantilever beams.

Displacements were different from linear analysis calculations because the test apparatus permitted the large displacements (Figure 3.8) and the fixed end of the beam was not as rigid as desired (permitted some rotation). Also read errors that may be

made in the measurements. These can change the results. However, these effects cause the elastic modulus lower than the expected value so this study helped to find the minimum limit of the modulus of elasticity. Because this information was later used during the calibration phase. In the event of the possibility of visco-elastic movement of the plastic material under a constant hanged load, dynamic measurements have been made and it was found that the modulus of elasticity was obtained relatively larger with the dynamic data.

Figure 3.8. Test Apparatus for Calculating the Modulus of Elasticity

In the experiment, displacements caused by the load created by hanging various weight bags at the end of the cantilever beam were measured. The test results were tabulated (Table 3.1) and deflection-load graph was obtained using these data. Beam properties, the outer diameter and inner diameter of the PVC pipe used, the unit mass of and the first mode frequency obtained by vibrating, calculated moment of inertia were tabulated to be used in the dynamic formula (Table 3.2).

Table 3.1. *Applied Loads in the Experiment and Displacement Values*

Load Applied (N)	Deflection (mm)
0.59	18
0.79	21
1.91	45
2.26	49
3.14	70
2.94	70
3.92	89
4.12	90
5.45	118
8.09	170

Table 3.2. *Properties of the Beam Used in the Experiment*

Inner diameter of the beam	15.4	mm
Outer diameter of the beam	25.5	mm
Length of the beam	1	m
Unit mass of the beam	0.28	kg/m
The first mode frequency	1.205	1/s
Moment of inertia	17994.46	mm^4

The graph in Figure 3.9 were drawn by using the values given in Table 3.1. The relationship between load and displacement was obtained as y = 0.0488 * x-0.289. As a result of this study, modulus of elasticity, calculated with displacement formulas, was obtained as 904 MPa based on the measurement.

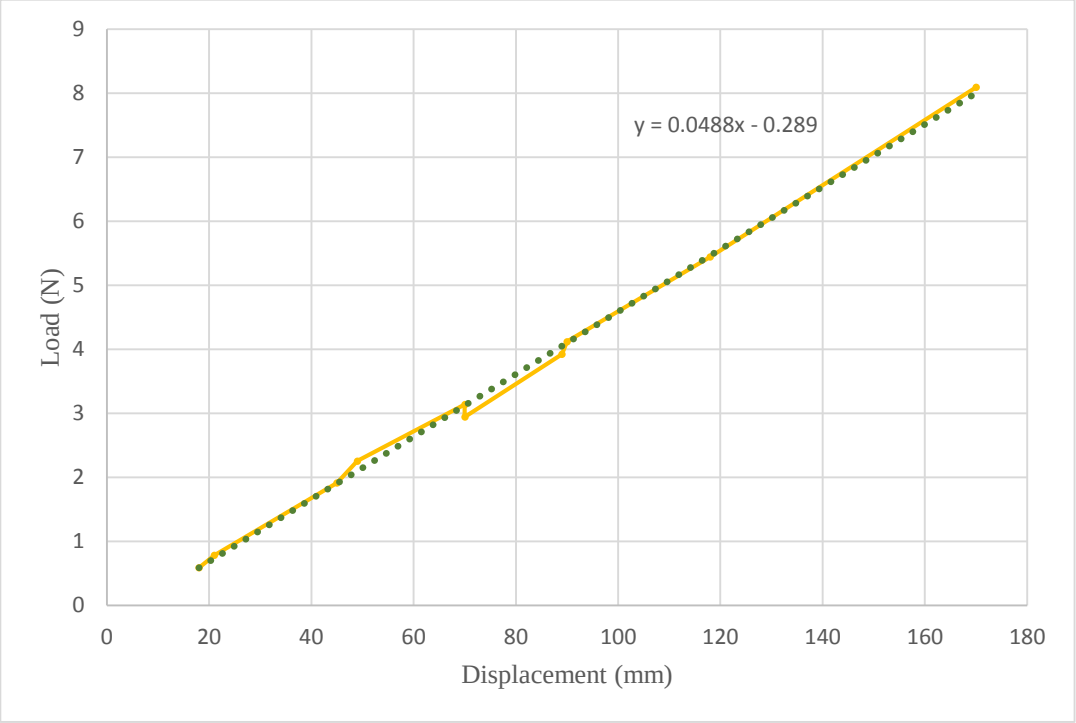

Figure 3.9. Load-Displacement Graph

Displacement formula for cantilever beam:

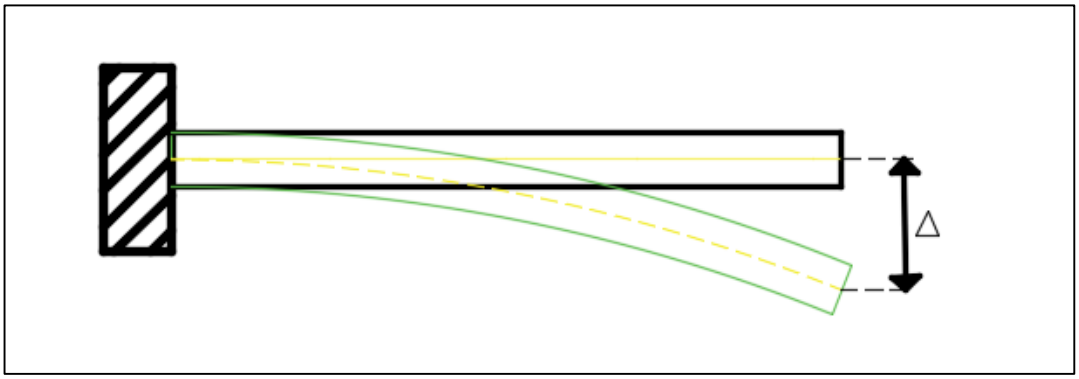

Figure 3.10. Cantilever Beam

$\Delta = PL^3/3EI \longrightarrow E = PL^3/3I\Delta$

P/Δ is the slope of the graph in Figure 3.9.

$$\omega_{1=} 3.52 \sqrt{\frac{EI}{ml^4}}$$

$f1 = \omega_1/2\pi$

Δ: displacement (mm)

P: load (N)

L, *l*: length of beam

E: modulus of elasticity (N/mm^2)

m: mass/length (kg/m)

I: moment of inertia (m^4)

ω: angular frequency (rad/s)

f: natural vibration frequency (1/s)

$E = (0.0488*1000^3)/(3*17994.46)$ = **904 N/mm²**

For the modulus of elasticity, additional calculations were made based not only on the measurement of the deflection, but also on the measurement of the vibration frequency of the pipe. In this way, the average value of E value was calculated as 994 MPa from the displacement and vibration measurements.

$\omega_1 = 2\pi*1.205 = 7.57$ rad/s

$E = (\omega_1/3.52)^2*(ml^4/I)$

$E = (7.57/3.52)^2*(0.28*1.97^4/1.799*10^{-8})$ = **1084 N/mm²**

$E_{mean} = (1084+904)/2$ = **994 N/mm²**

One of the steps to create a realistic nominal model is to define relatively more rigid parts at the connections. Vertical members are stiffer by the connection plates at locations where members are joined together. Rigid zone factor was defined in the regions where the connection plate was located in each vertical member in the analytical model. The moments of inertia of the horizontal and diagonal members were 10 times increased for the region in contact with the connection plates during calibration. In addition, the weight and mass of the connection plates, bolts, and clamps were defined in the analytical model in accordance with the reality. The upper deck (platform) of the model is defined as a single shell at the beginning but it was changed to fine meshed member composed of many small shells to better model the rotational inertia of the FEM. Support restraints were also improved by modeling spring coefficients at the ends to better simulate semi-rigid support conditions. The difference between the initial appearance of the analytical model and the final version obtained after the modifications to calibrate can be seen in Figure 3.11.

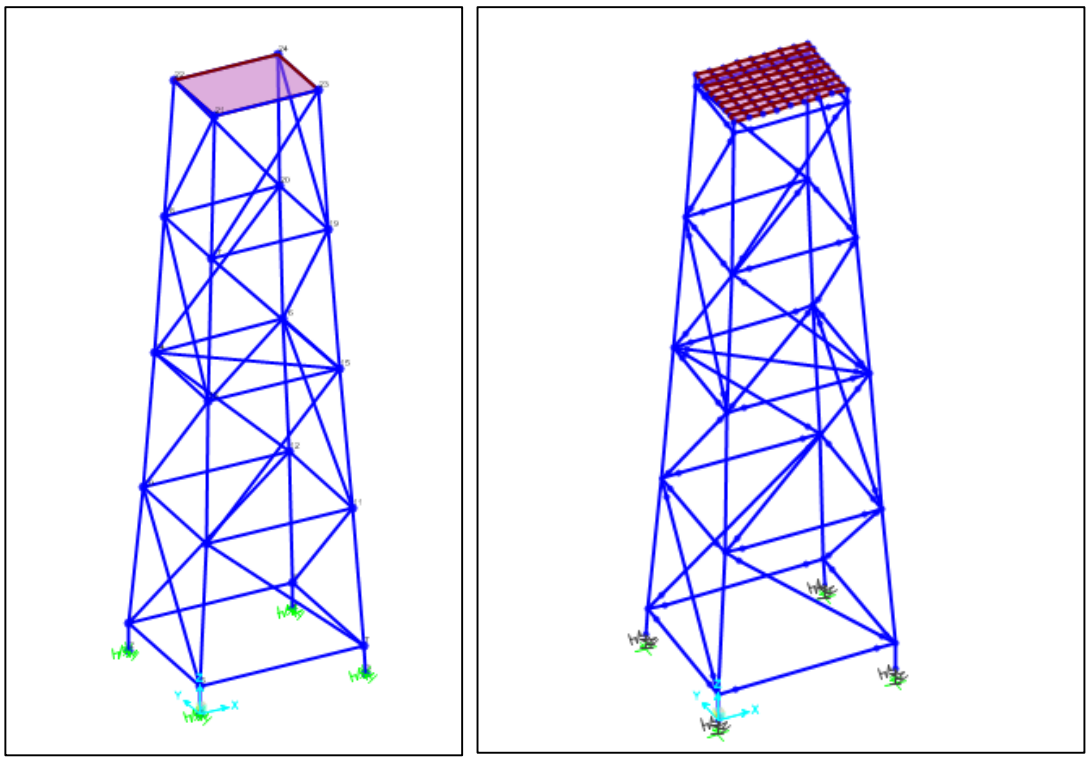

Figure 3.11. Initial and Calibrated Version of the Analytical Model

Natural vibration frequencies of the model before calibration and after calibration are given in Table 3.3.

Table 3.3. *Natural Vibration Frequencies of Uncalibrated, Calibrated, and Lab Model*

	Natural Vibration Frequencies (cyc/sec)		
	Uncalibrated Model	**Calibration Model**	**Physical Model**
f1	17.69	10.49	10.36
f2	20.23	12.29	12.13
f3	29.41	25.30	25.32
f4	46.09	35.63	-
f5	49.98	39.76	-
f6	65.01	51.20	-

3.2. Similitude of the Model

Reduced-scale models are generally used as experimental laboratory models because experiments conducted on full-scale models may not give economical end practical solutions. Similitude is a concept used in engineering models to build the relationships between the full-scale and reduced-scale model properties. In this study, reduced-scale with 1/75 model was used as a test model. Material properties are shown in Table 3.4.

P_{PVC} = unit mass of pipe obtained by weighing / section area of pipe with Ø25 mm

$$\rho_{PVC} = \frac{0.28\ kg/m}{0.25*\pi*(25.5^2-15.4^2)*10^{-6}\ m^2}$$

ρ_{PVC} = 863 kg/m^3

Table 3.4. *Material Properties*

Material	Steel (Full-Scale Model)	PVC pipe (Reduce-Scale Lab Model)
Density, ρ	7850 kg/m^3	863 kg/m^3
Modulus of Elasticity, E	200 GPa	1 GPa

$$f = 2\pi\sqrt{\frac{k}{m}} = 2\pi\sqrt{\frac{EA/L}{\rho V}}$$

where

f: frequency (cyc/sec)

k: stiffness (N/m)

m: mass (kg)

E: modulus of elasticity (GPa)

A: section area (m^2)

ρ: density (kg/m^3)

V: volume (m^3)

$$f_{reduce\text{-}scale} = \sqrt{\frac{\frac{1}{200}*\frac{1}{75^2}}{\frac{\frac{1}{75}}{\frac{863}{7850}*\frac{1}{75^3}}}}\, f_{full\text{-}scale}$$

$f_{reduce\text{-}scale}$ = 16 $f_{full\text{-}scale}$

If same material were used in the lab model:

$$f_{reduce\text{-}scale} = \sqrt{\frac{\frac{1}{75^2}}{\frac{\frac{1}{75}}{\frac{1}{75^3}}}}\, f_{full\text{-}scale}$$

$f_{reduce\text{-}scale}$ = 75 $f_{full\text{-}scale}$

Therefore, PVC pipe was selected as lab model material to reduce the difference between the lab model and real large structural model dynamic properties.

3.3. Conducted Tests on the Lab Model for 22 Damage States

In order to investigate the success and applicability of the ANN which was trained using calibrated FEM results, similar input parameters were obtained from the lab model. The lab model was modified by removing members to simulate damage conditions and mass on the platform was changed by adding water up to 10 liters. Dynamic and static tests were carried out on the calibrated physical model for a total of 22 different scenarios. Static experiments were made for the original (undamaged) model and used for all undamaged scenarios even with varying masses since mass change would not affect the static test results. Two 50 kN load cells were used for static testing together with a total of 4 linear variable differential transformers (LVDTs); two of them placed in the x-direction and other two placed in the y-direction, A data acquisition system with a total of three triaxial accelerometers were used, two in the upper deck and one in the middle layer, to obtain dynamic data (Figure 3.12).

Figure 3.12. Static and Dynamic Testing Equipment

Static experiments were carried out in both directions. Since the tests were carried out with a small scale physical model, it was sufficient to apply force by pulling the rope connected to the load cells for static loading tests. The experiments were repeated three times as loading and unloading in both directions, and load–displacement graphs were created. With these experiments, the displacement and rotation data, which are used as input in ANN damage detection method, were obtained. Experimental rotation results were greatly different when compared with the analytical model data possibly because of eccentrically applied loading, property of PVC material, uneven voids at bolt connections, etc.). Therefore, only displacements were taken as inputs.

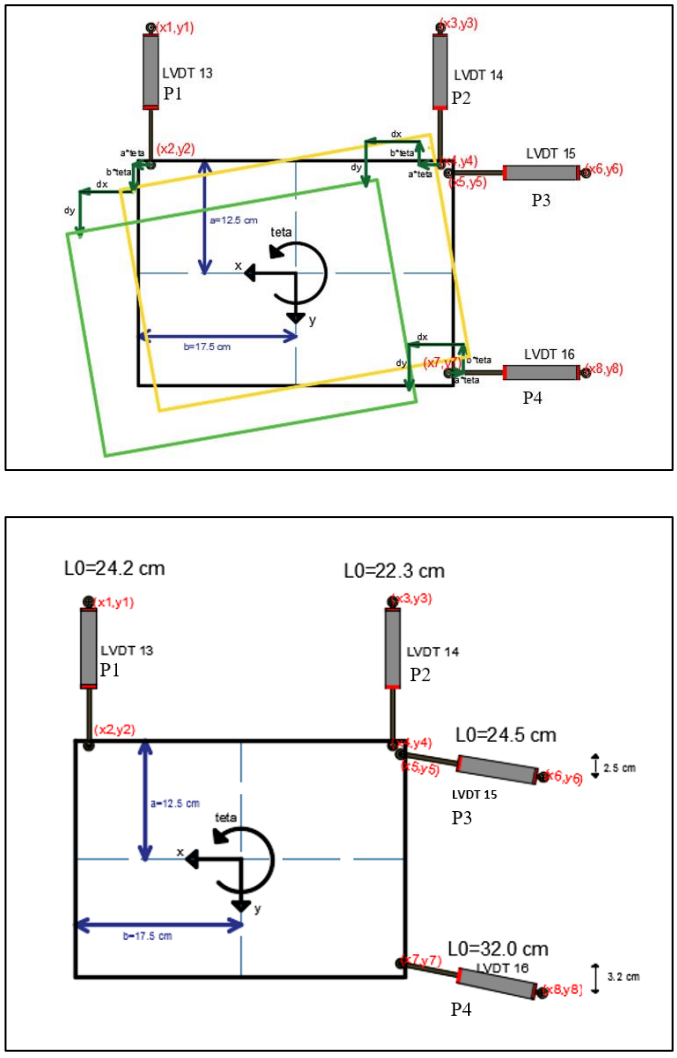

Figure 3.13. LVDT Layout Plan at the Deck

The load-displacements graphs were drawn using static experiment readings for each undamaged and damaged case scenarios. These were given in Figure 3.14 – Figure 3.25 below:

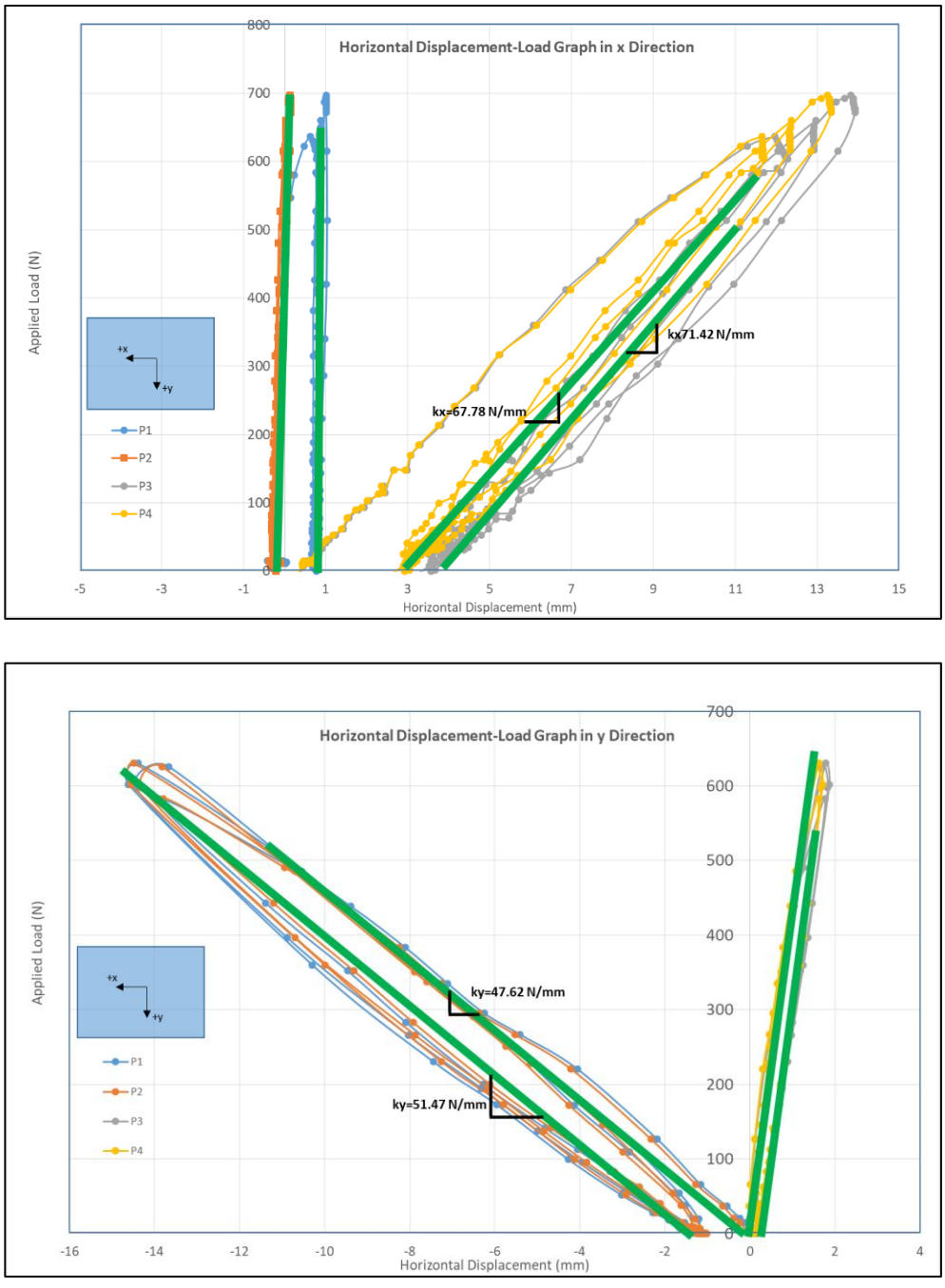

Figure 3.14. Horizontal Displacement - Applied Load Graphs in x and y Directions Respectively for No Mass - No Damage Case

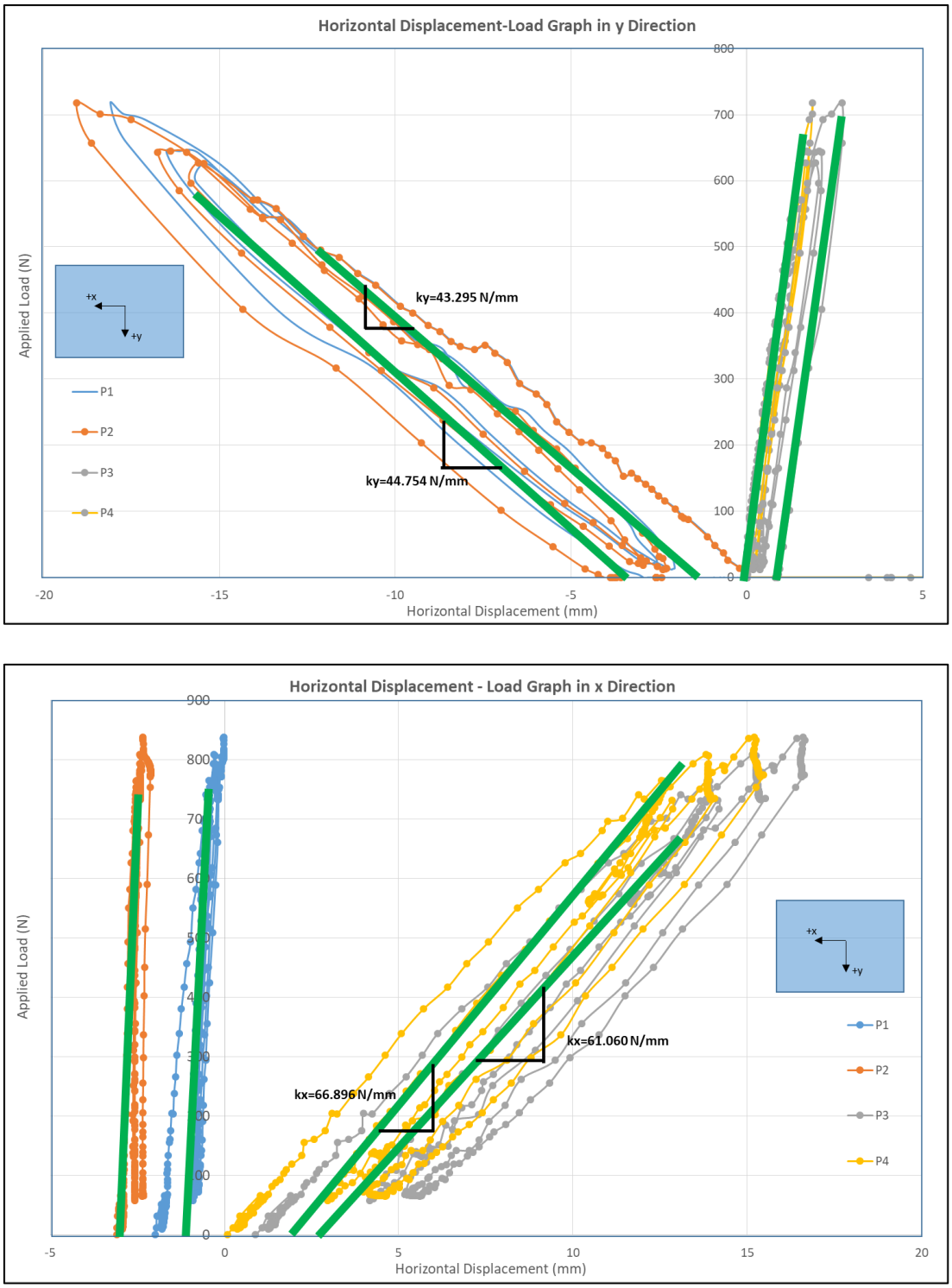

Figure 3.15. Horizontal Displacement - Applied Load Graphs in x and y Directions Respectively for 3 kg Deck Mass and 32nd Member Has Damaged

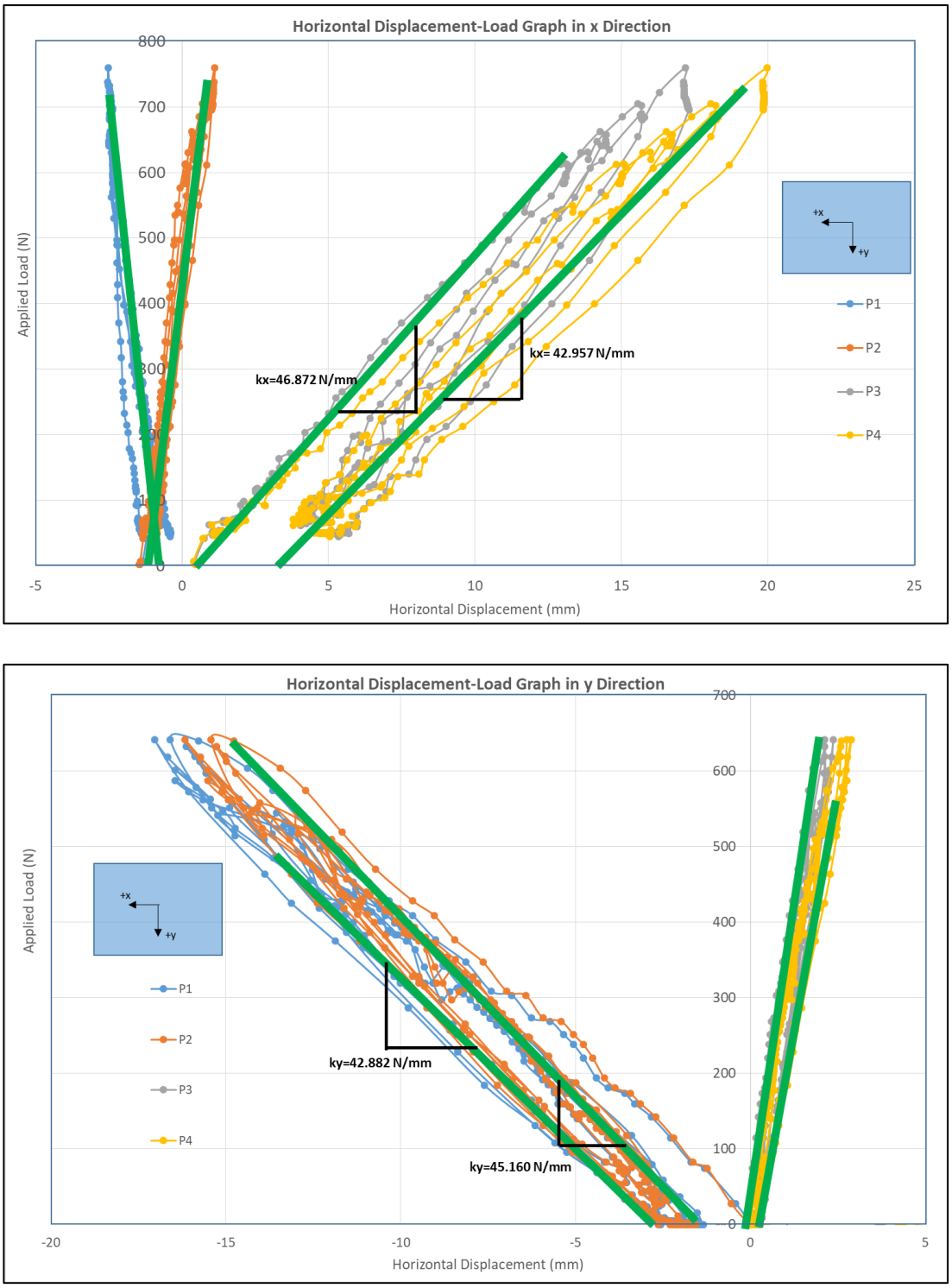

Figure 3.16. Horizontal Displacement - Applied Load Graphs in x and y Directions Respectively for 3 kg Deck Mass and 55th Member Has Damaged

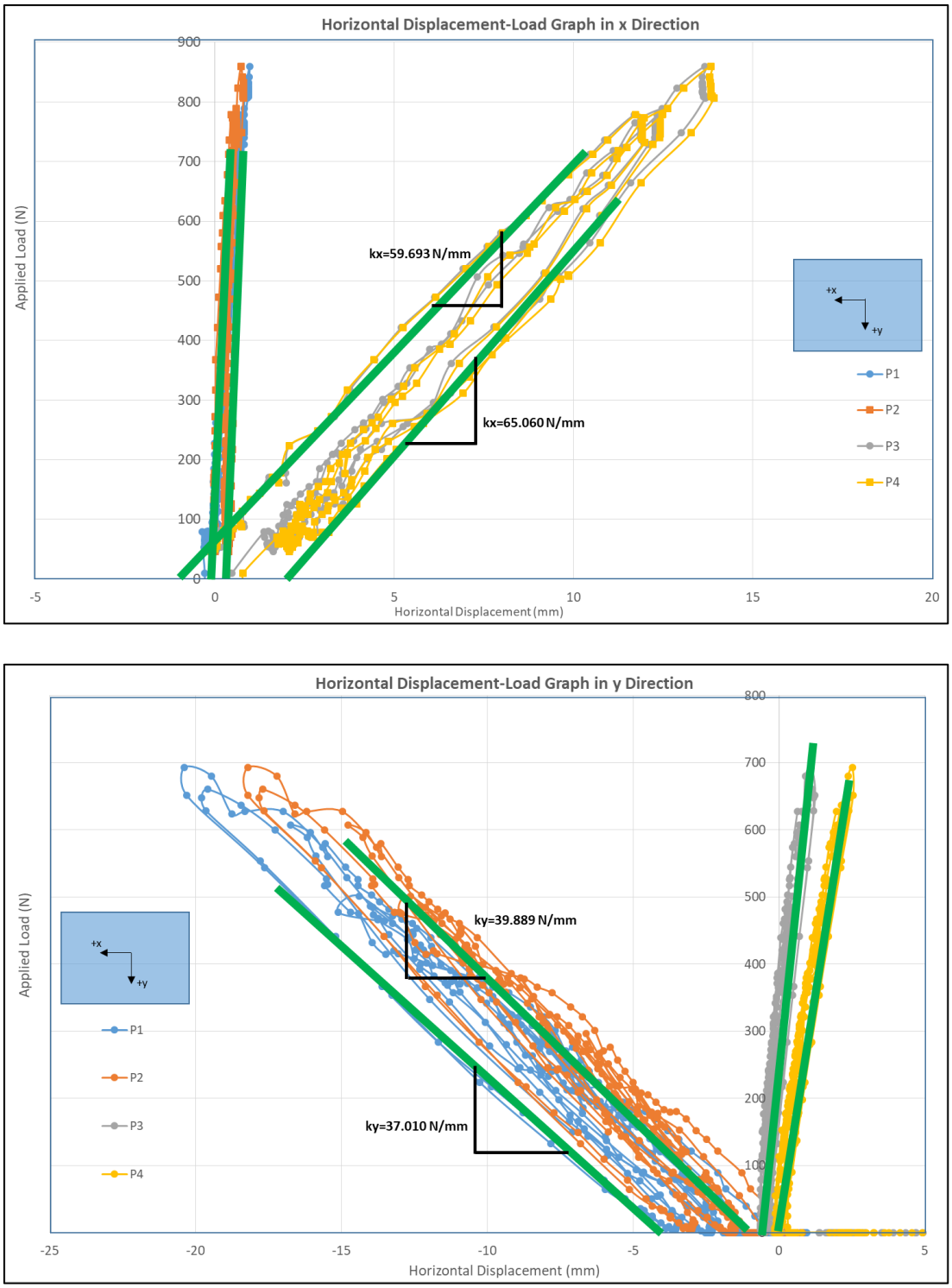

Figure 3.17. Horizontal Displacement - Applied Load Graphs in x and y Directions Respectively for 3 kg Deck Mass and 49th Member Has Damaged

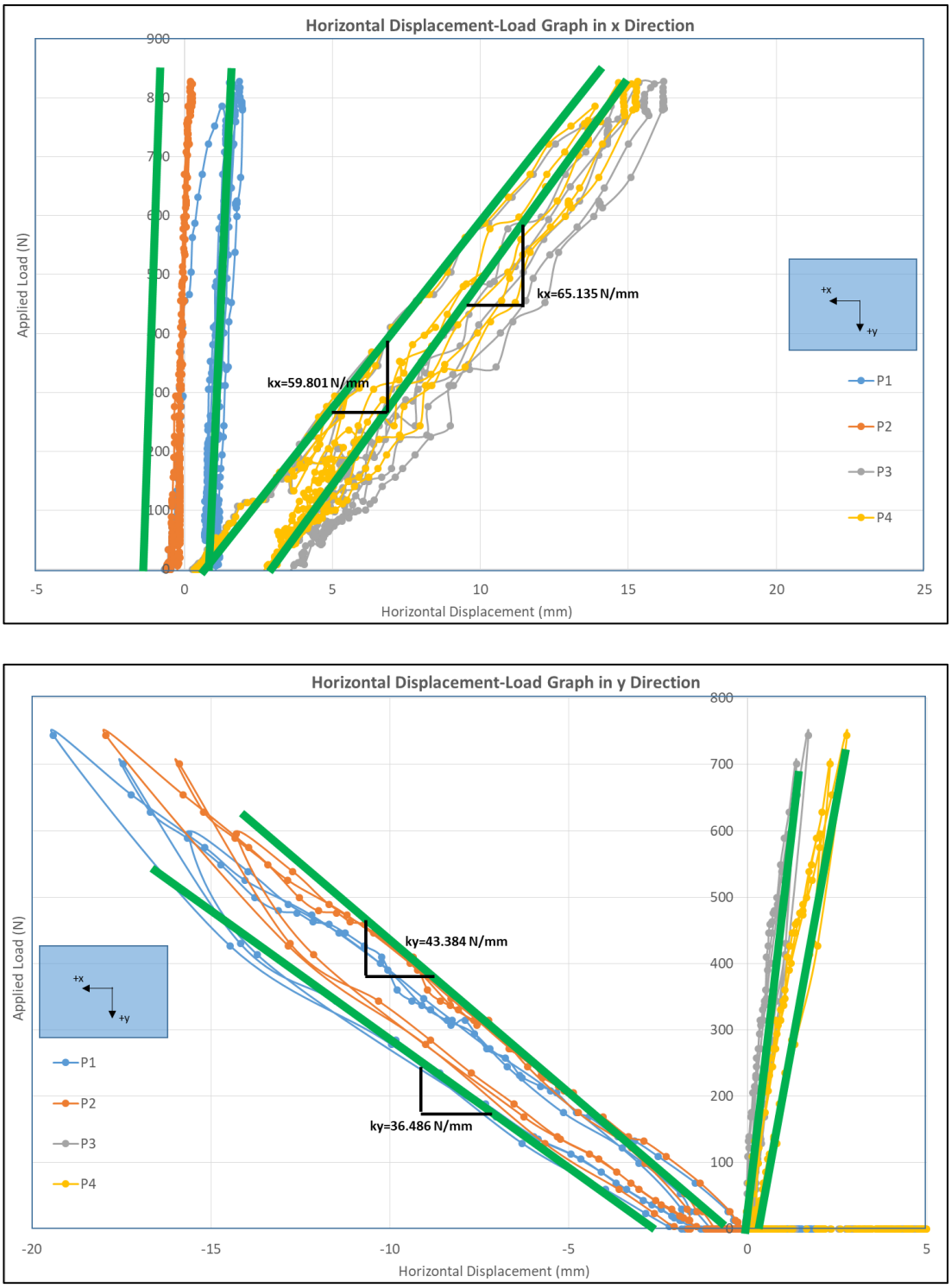

Figure 3.18. Horizontal Displacement - Applied Load Graphs in x and y Directions Respectively for 4 kg Deck Mass and 49th Member Has Damaged

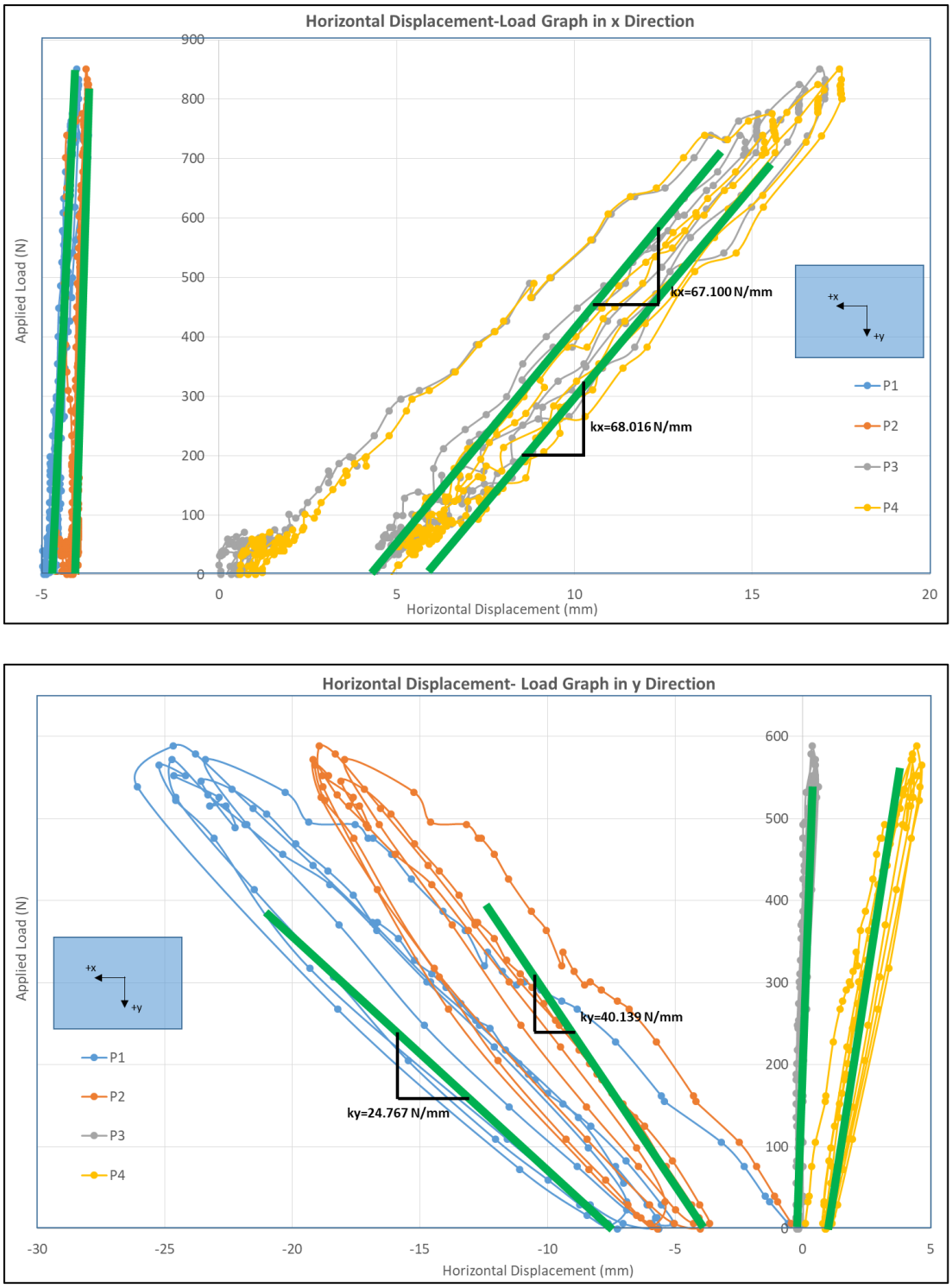

Figure 3.19. Horizontal Displacement - Applied Load Graphs in x and y Directions Respectively for 4 kg Deck Mass and 52nd Member Has Damaged

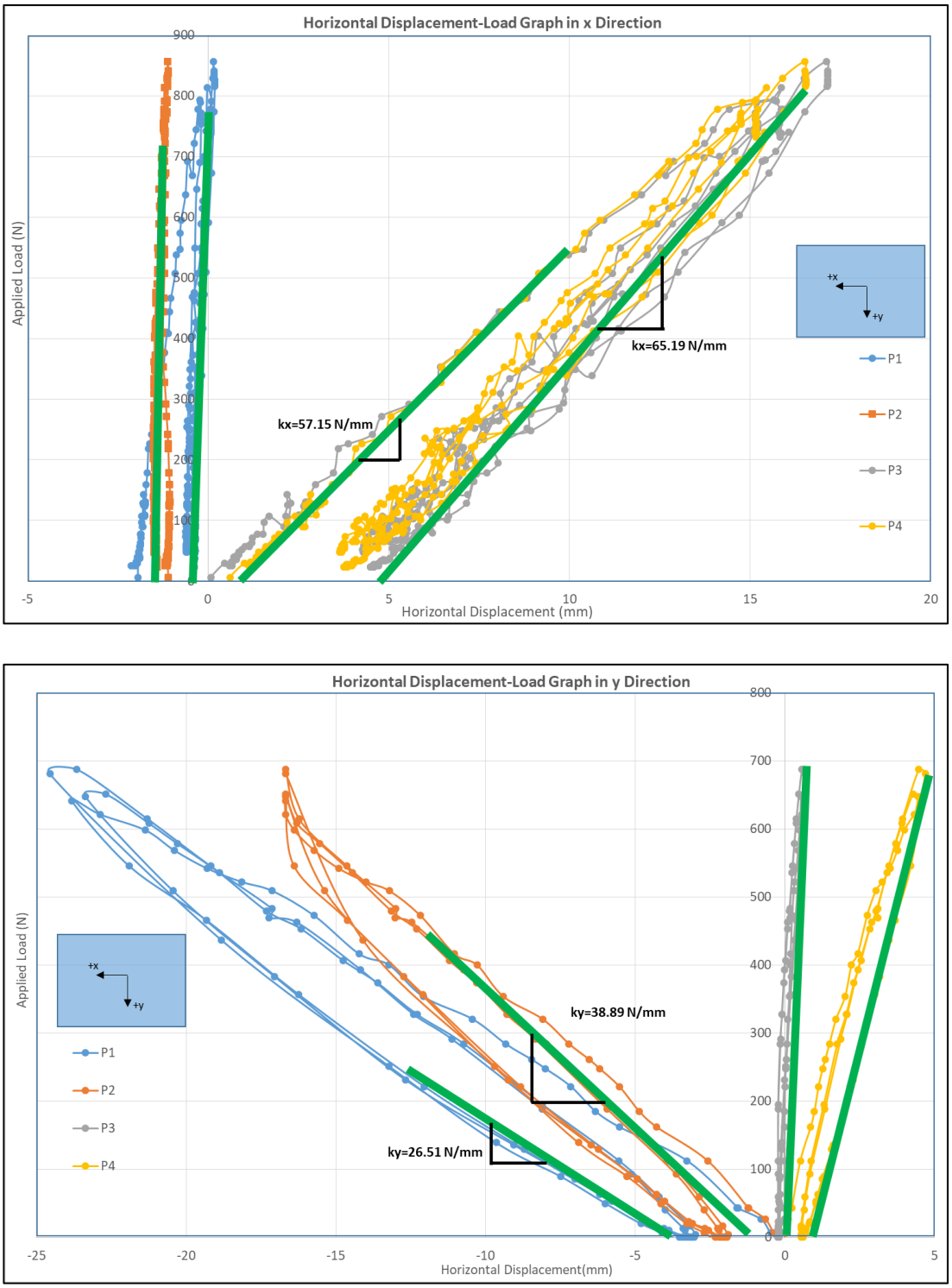

Figure 3.20. Horizontal Displacement - Applied Load Graphs in x and y Directions Respectively for 5 kg Deck Mass and 52nd Member Has Damaged

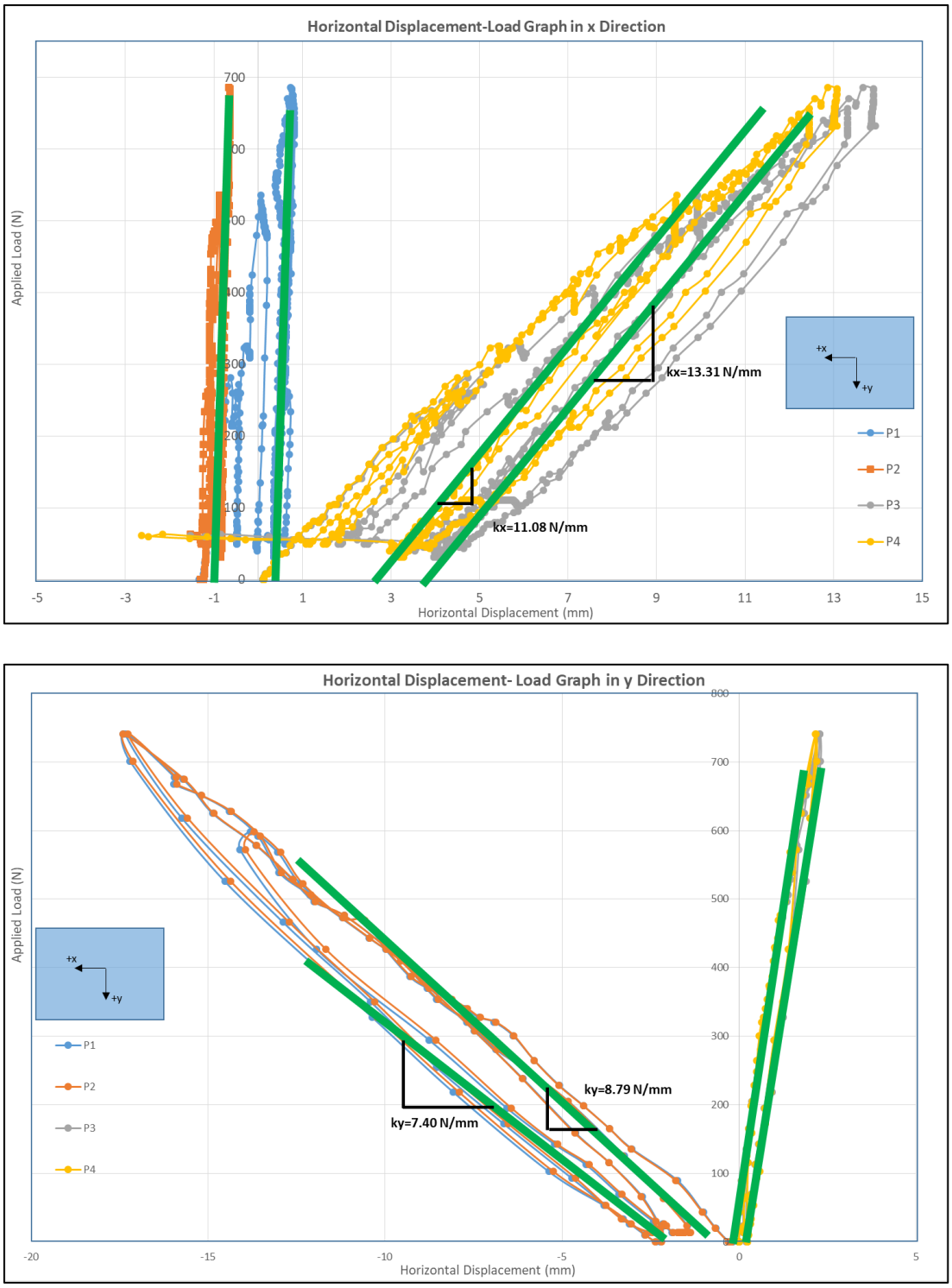

Figure 3.21. Horizontal Displacement - Applied Load Graphs in x and y Directions Respectively for 5 kg Deck Mass and 31st Member Has Damaged

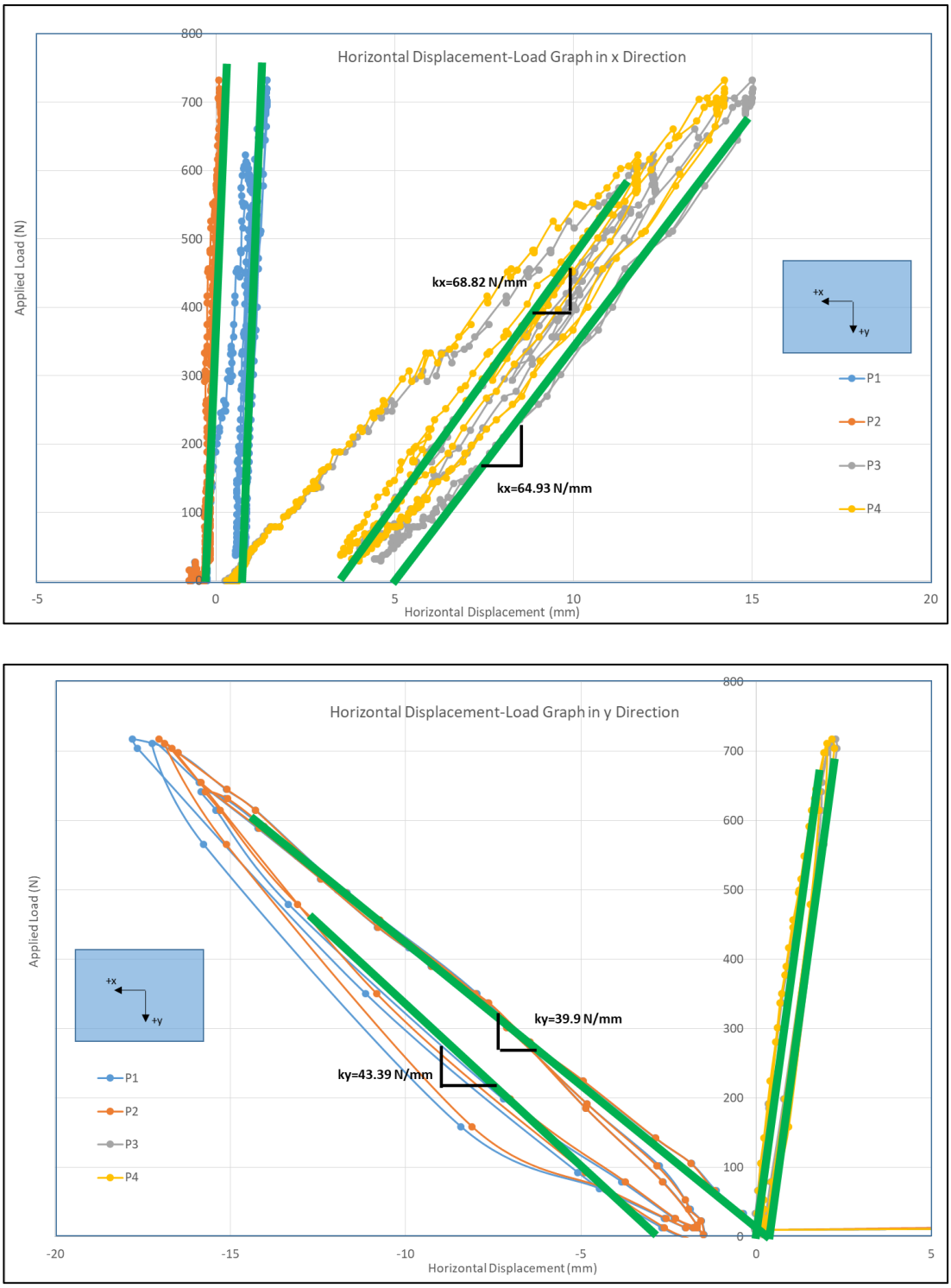

Figure 3.22. Horizontal Displacement - Applied Load Graphs in x and y Directions Respectively for 6 kg Deck Mass and 27th Member Has Damaged

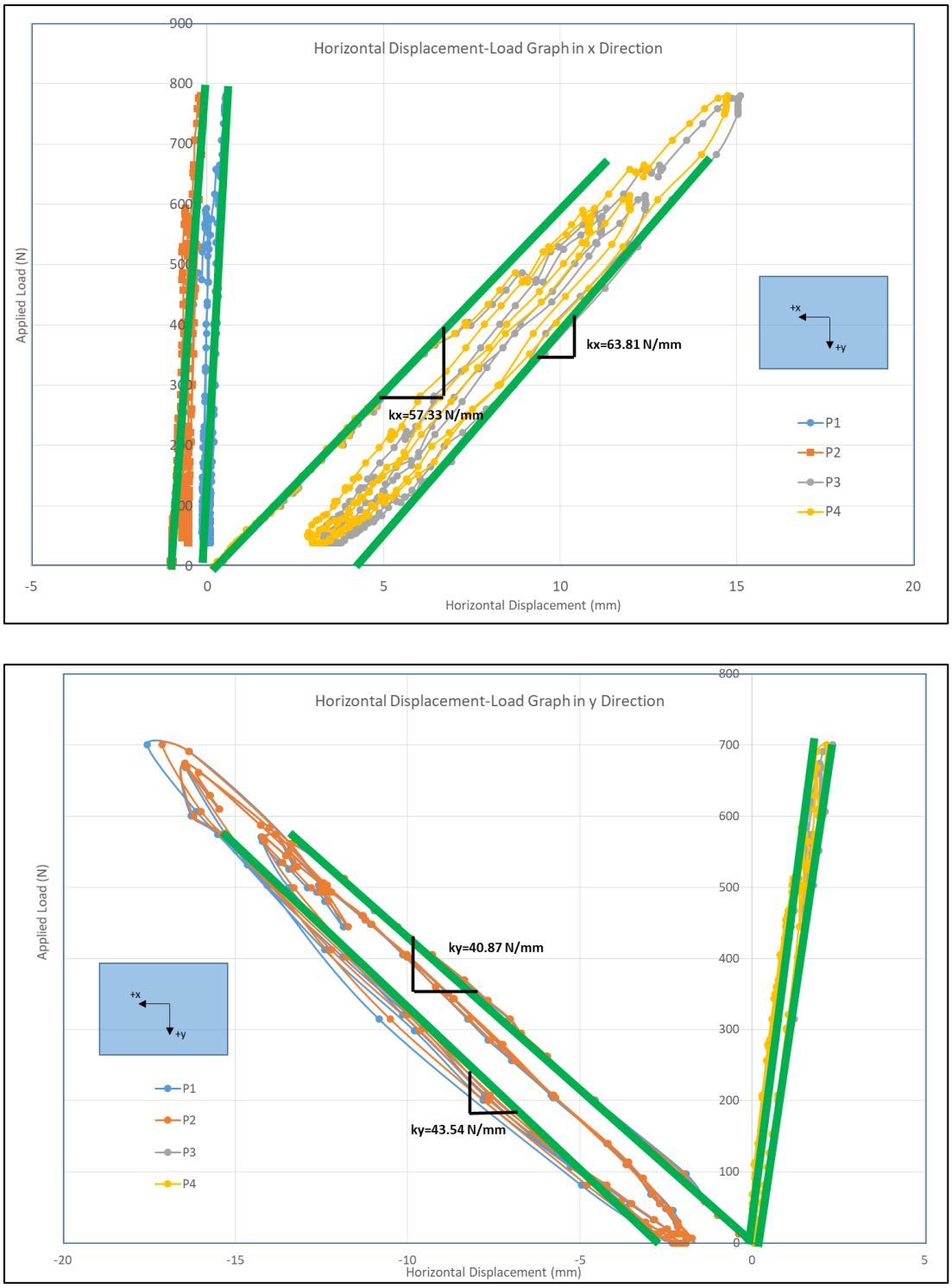

Figure 3.23. Horizontal Displacement - Applied Load Graphs in x and y Directions Respectively for 6 kg Deck Mass and 26th Member Has Damaged

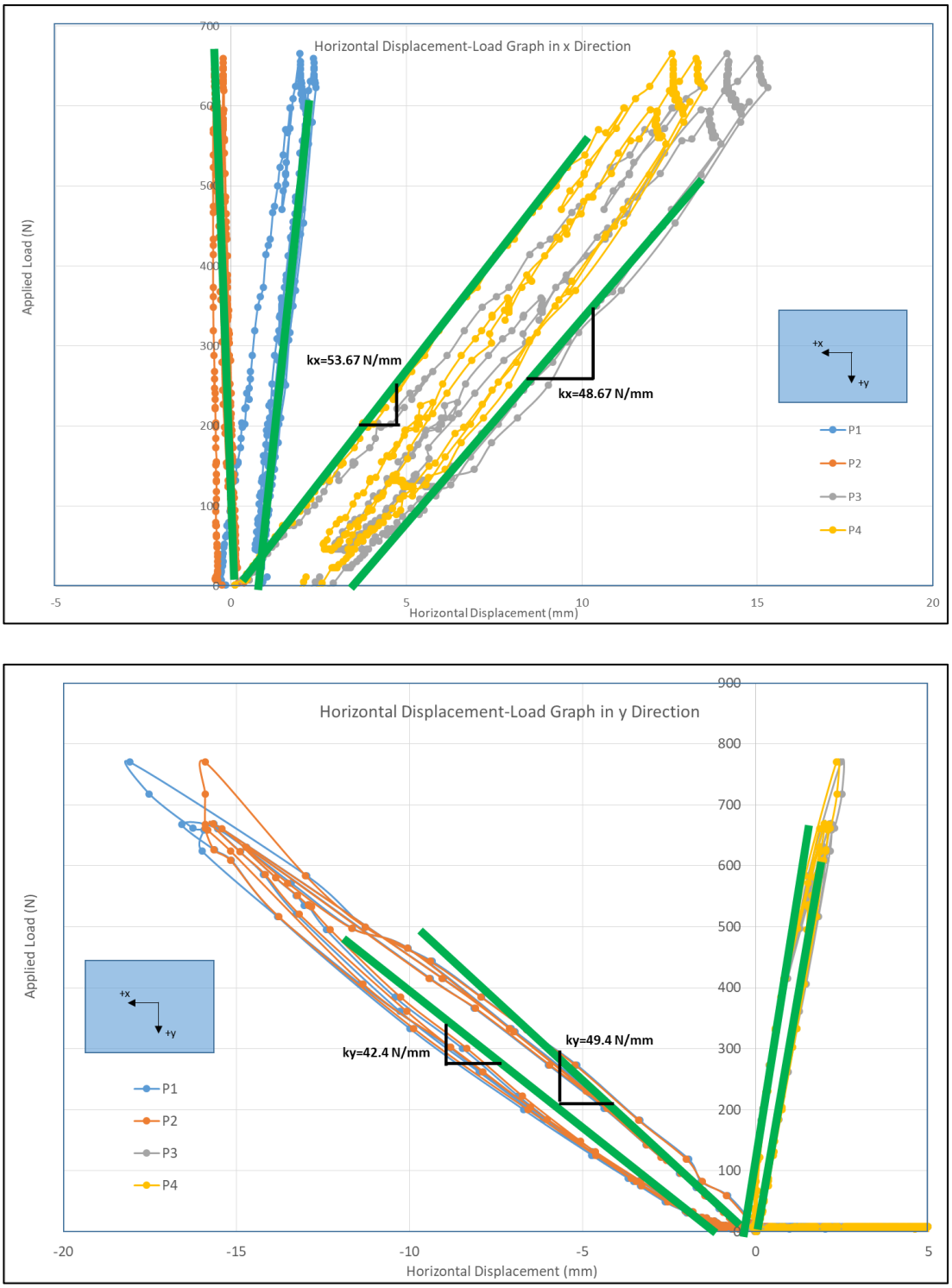

Figure 3.24. Horizontal Displacement - Applied Load Graphs in x and y Directions Respectively for 7 kg Deck Mass and 46th Member Has Damaged

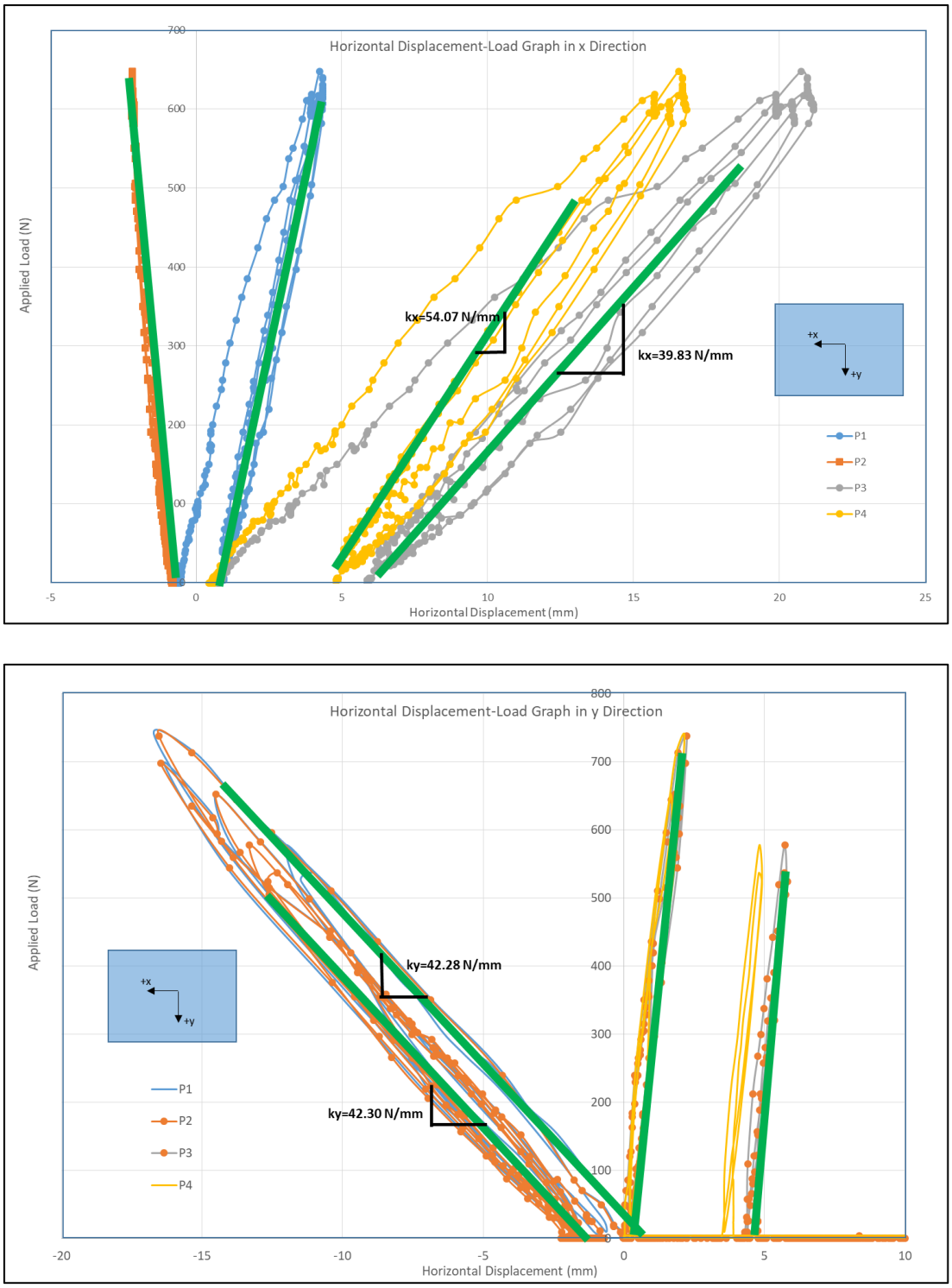

Figure 3.25. Horizontal Displacement - Applied Load Graphs in x and y Directions Respectively for 7 kg Deck Mass and 48th Member Has Damaged

The experimental loading test results for the FEM analyses and static loading tests in x and y directions are given in Table 3.5.

Table 3.5. *Displacement and Rotation Values Obtained from FEM Analysis and Experiments for 500N Loading*

Damage Member ID	Mass (kg)	FEM				IN X DIRECTION		IN Y DIRECTION	
		dX (mm)	Rx (°)	dY (mm)	Ry (°)	DX (mm)	Rotation (°)	DY (mm)	Rotation (°)
nodamage	**1**	6.4187	0.0017	9.0068	-0.0001	7.3447	-0.0261	10.6920	-0.0069
nodamage	**2**	6.4187	0.0017	9.0068	-0.0001	7.3447	-0.0261	10.6920	-0.0069
nodamage	**3**	6.4187	0.0017	9.0068	-0.0001	7.3447	-0.0261	10.6920	-0.0069
nodamage	**4**	6.4187	0.0017	9.0068	-0.0001	7.3447	-0.0261	10.6920	-0.0069
nodamage	**5**	6.4187	0.0017	9.0068	-0.0001	7.3447	-0.0261	10.6920	-0.0069
nodamage	**6**	6.4187	0.0017	9.0068	-0.0001	7.3447	-0.0261	10.6920	-0.0069
nodamage	**7**	6.4187	0.0017	9.0068	-0.0001	7.3447	-0.0261	10.6920	-0.0069
nodamage	**8**	6.4187	0.0017	9.0068	-0.0001	7.3447	-0.0261	10.6920	-0.0069
nodamage	**9**	6.4187	0.0017	9.0068	-0.0001	7.3447	-0.0261	10.6920	-0.0069
nodamage	**10**	6.4187	0.0017	9.0068	-0.0001	7.3447	-0.0261	10.6920	-0.0069
nodamage	**0**	6.4187	0.0017	9.0068	-0.0001	7.3447	-0.0261	10.6920	-0.0069
32	**3**	6.4214	0.0021	9.0130	-0.0005	7.7398	-0.0235	11.5436	-0.1388
55	**3**	7.9492	0.3211	9.0237	-0.0327	10.3062	-0.4664	11.7181	-0.0160
49	**3**	6.4318	-0.0142	9.5049	-0.1006	8.7397	0.0177	12.6801	-0.0099
49	**4**	6.4318	-0.0142	9.5049	-0.1006	8.7232	-0.1365	12.9896	-0.0102
52	**4**	6.4268	0.0213	10.7307	-0.2996	8.3804	0.0363	16.6980	-1.1972
52	**5**	6.4268	0.0213	10.7307	-0.2996	8.3805	0.1100	15.4792	-0.8532
31	**5**	6.4196	0.0015	9.0100	-0.0009	7.7256	0.0102	11.5421	-0.3039
27	**6**	6.4293	0.0015	9.0116	-0.0009	8.3836	-0.0028	11.3729	-0.0375
26	**6**	6.4280	0.0012	9.0073	-0.0002	8.3600	-0.0218	11.0115	-0.0218
46	**7**	7.2743	-0.1669	9.0083	-0.0063	9.3235	0.2684	11.3707	-0.1542
48	**7**	8.1965	-0.3588	9.0154	-0.0239	10.4697	0.6823	11.6442	-0.0123

Dynamic experiments were made by impact at the four points of the model, which were expected to vibrate all modes, and data were recorded to be used to obtain the mode frequencies of the model. The impact locations were at top and mid height locations and in both orthogonal horizontal directions to excite horizontal modes. These data were converted from time domain to frequency domain using Fast Fourier Transform (FFT) and natural vibration frequencies were found.

Total of 22 experiment scenarios were implemented and tests were repeated for each one of them. The first 11 of them were created without damage only by changing the platform mass, while the other remaining 11 cases were created for cases where the member were removed to simulate damage also with changing platform mass. After the FFT graphs of the experiments were obtained, the natural vibration frequencies of

each mode were obtained by selecting the spikes of the resonant frequencies belonging to each mode. The experiments were conducted for 90 seconds and the sampling frequency was taken as 256 Hz.

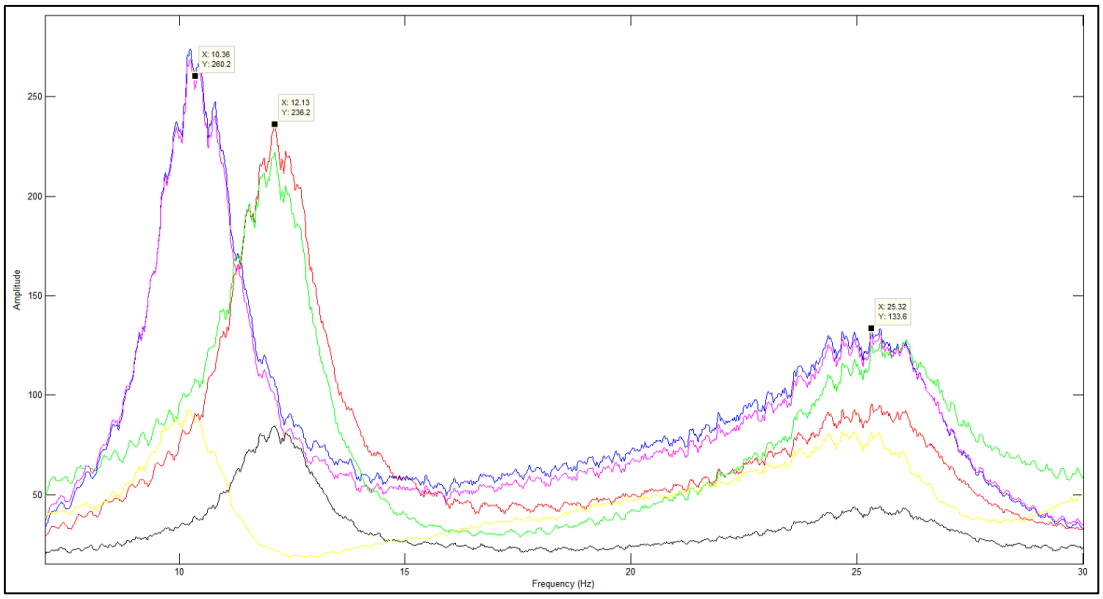

Figure 3.26. FFT Graph for No Damage and No Mass Case

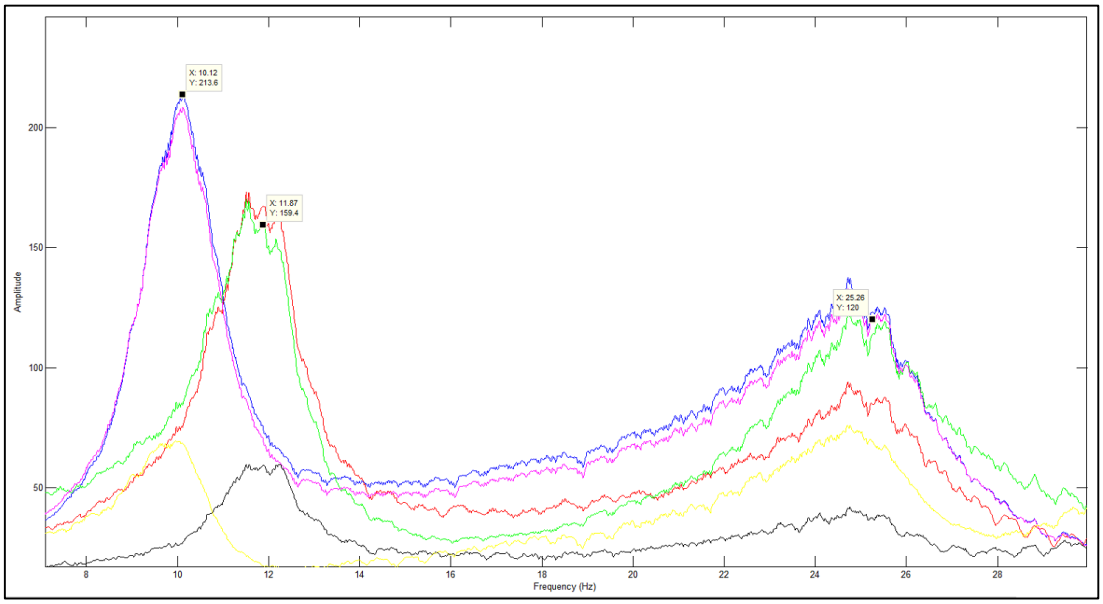

Figure 3.27. FFT Graph for No Damage and 1 kg Deck Mass Case

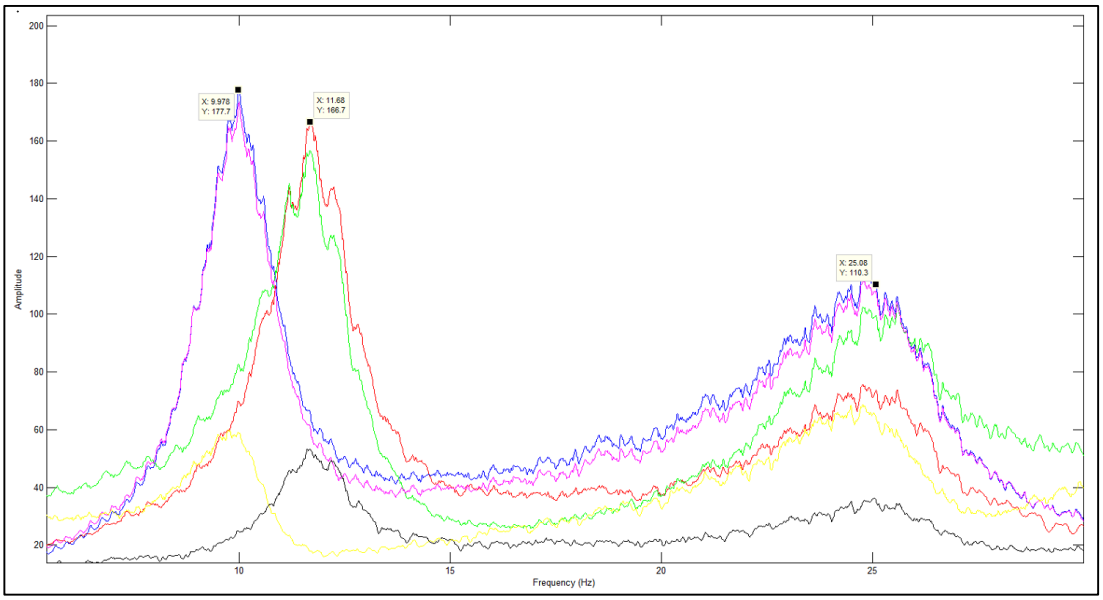

Figure 3.28. FFT Graph for No Damage and 2 kg Deck Mass Case

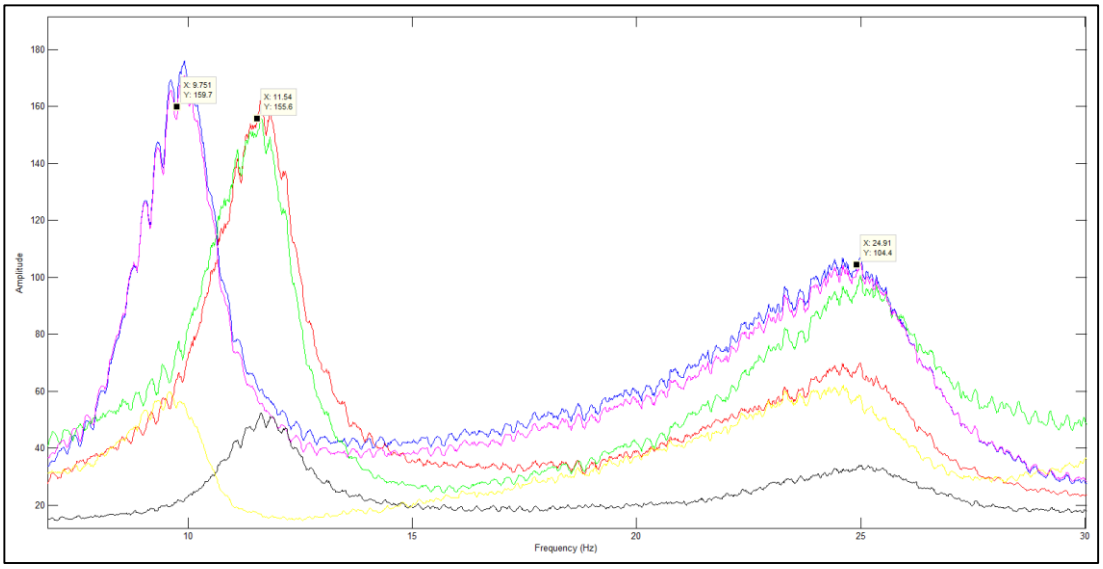

Figure 3.29. FFT Graph for No Damage and 3 kg Deck Mass Case

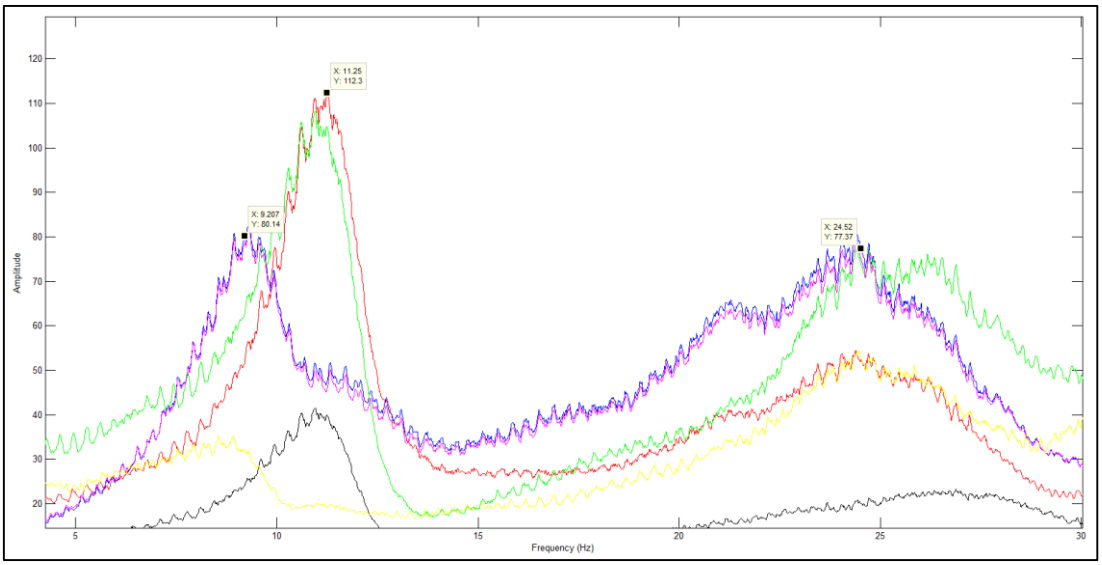

Figure 3.30. FFT Graph for No Damage and 4 kg Deck Mass Case

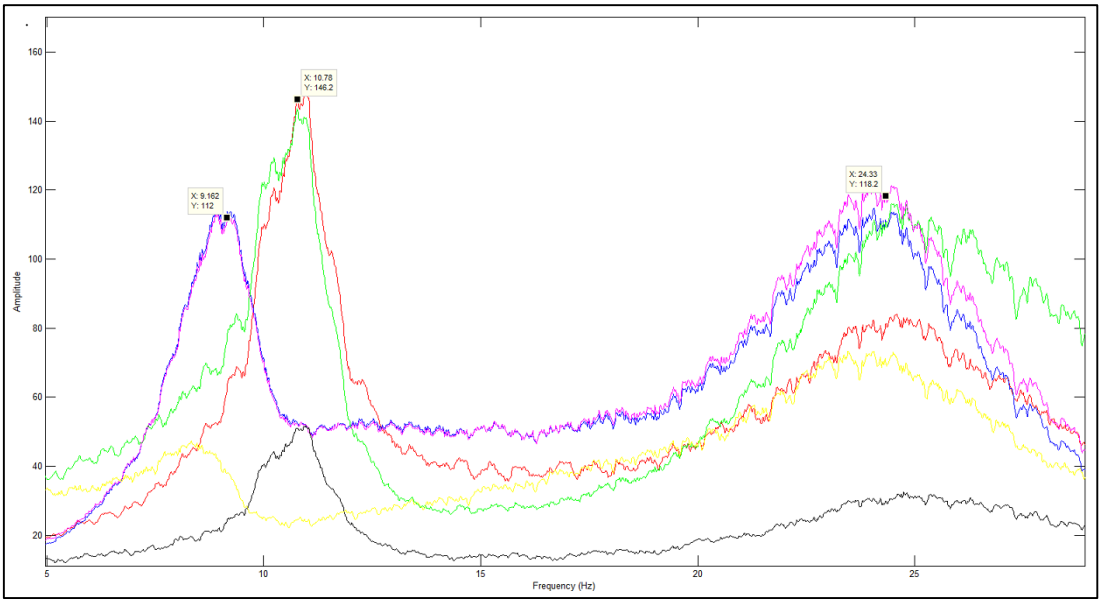

Figure 3.31. FFT Graph for No Damage and 5 kg Deck Mass Case

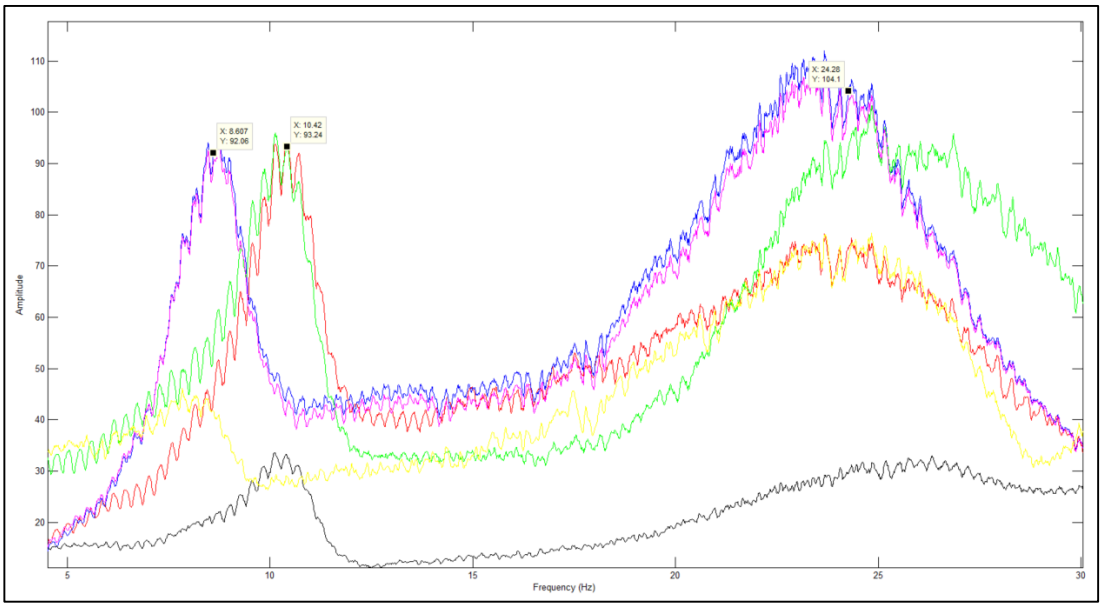

Figure 3.32. FFT Graph for No Damage and 6 kg Deck Mass Case

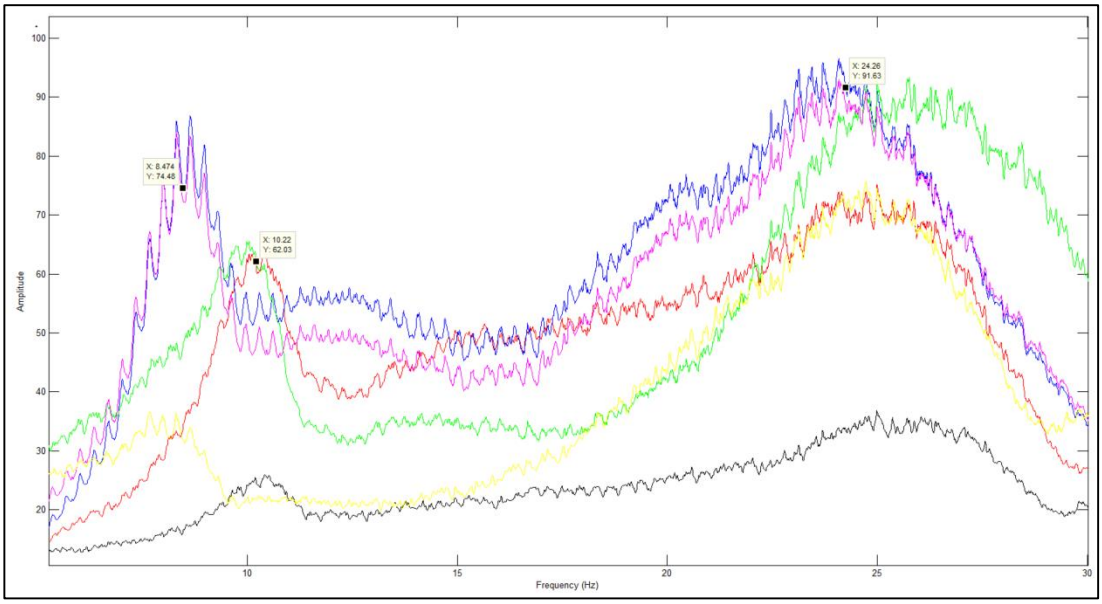

Figure 3.33. FFT Graph for No Damage and 7 kg Deck Mass Case

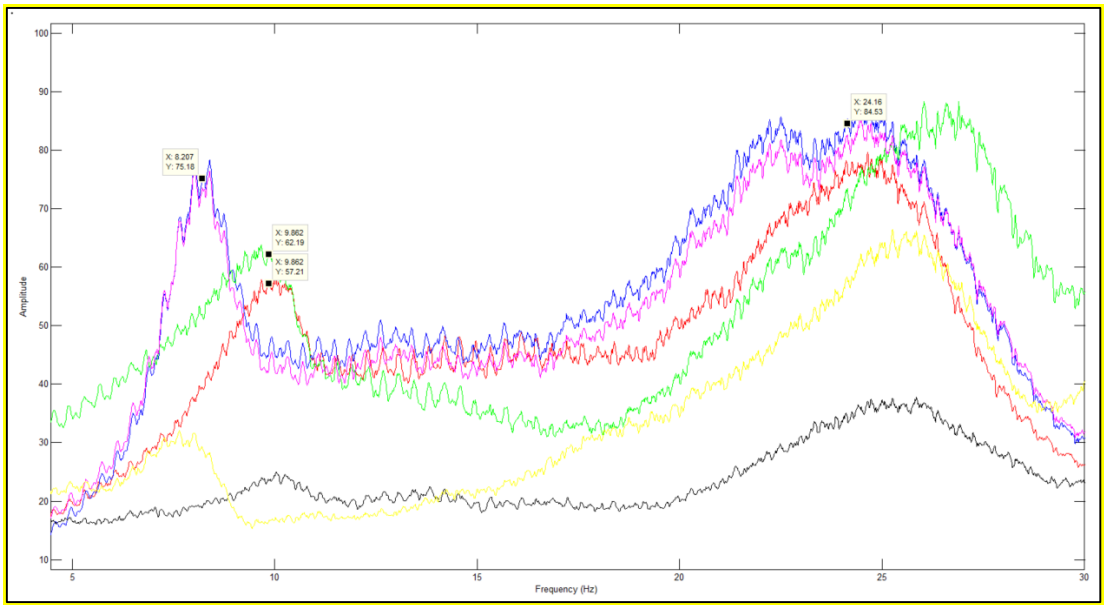

Figure 3.34. FFT Graph for No Damage and 8 kg Deck Mass Case

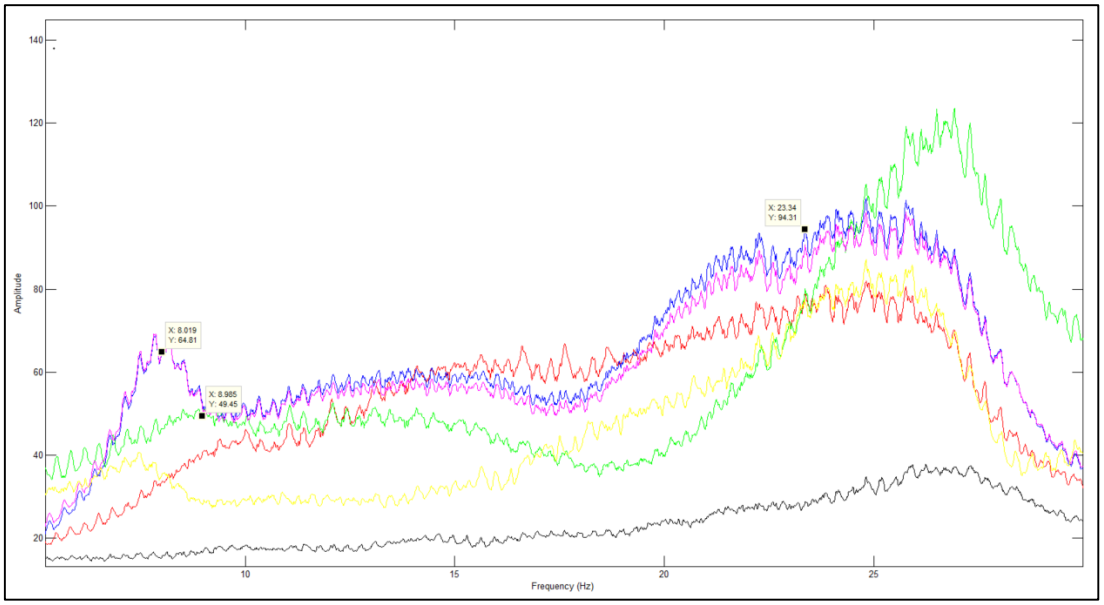

Figure 3.35. FFT Graph for No Damage and 9 kg Deck Mass Case

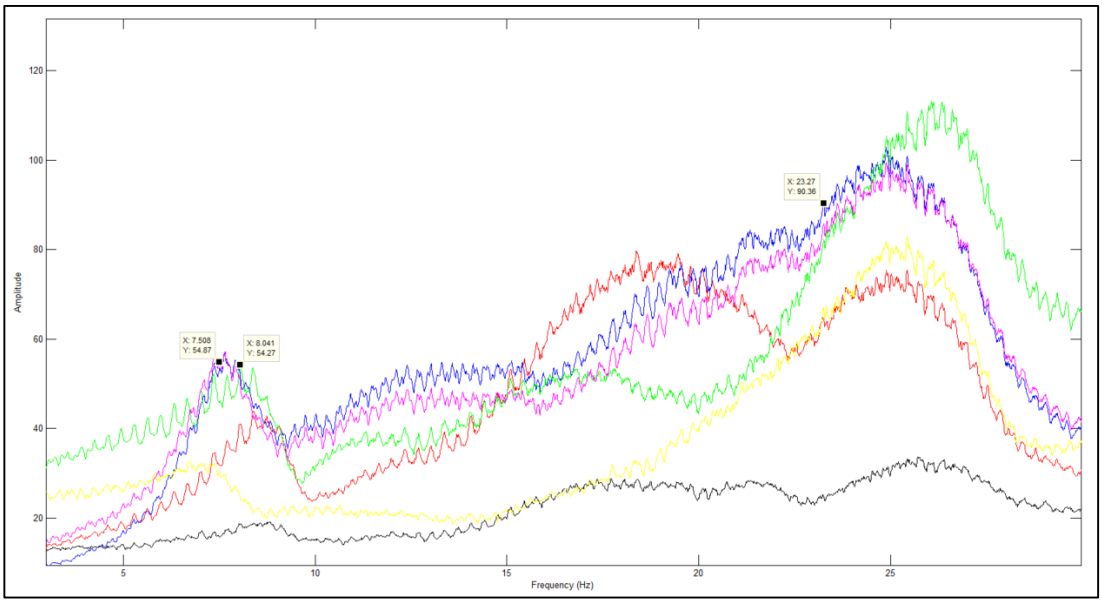

Figure 3.36. FFT Graph for No Damage and 10 kg Deck Mass Case

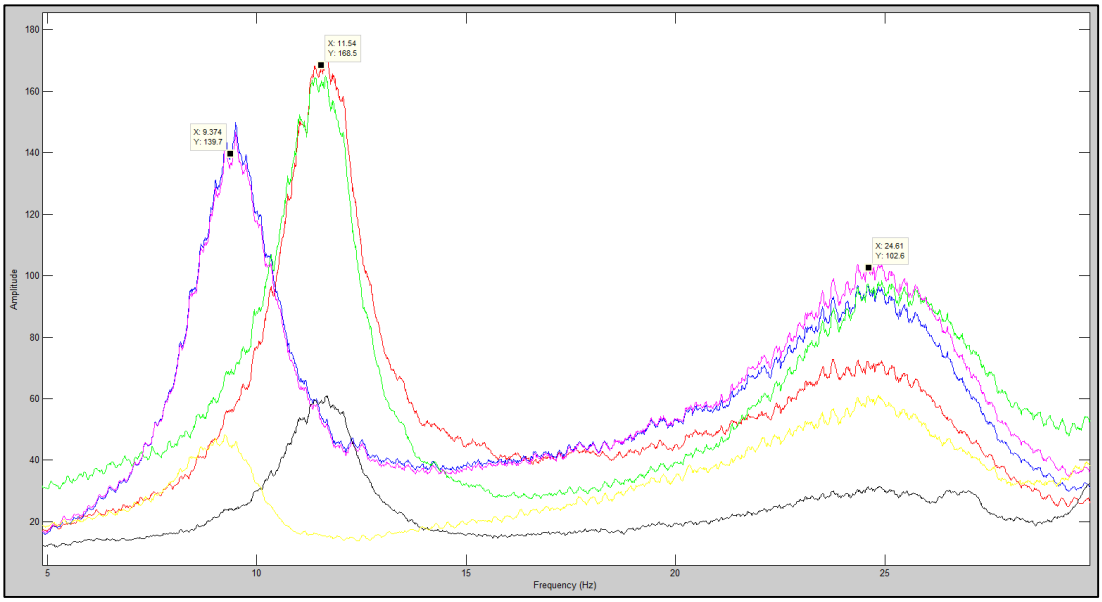

Figure 3.37. FFT Graph for 3 kg Deck Mass and 32nd Member Has Damaged Case

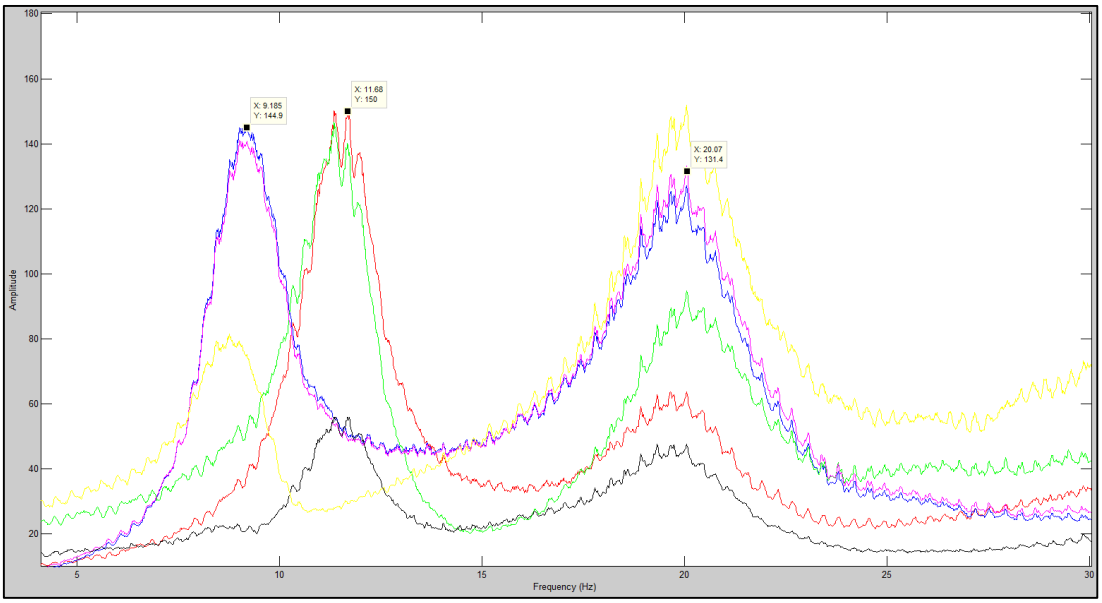

Figure 3.38. FFT Graph for 3 kg Deck Mass and 49th Member Has Damaged Case

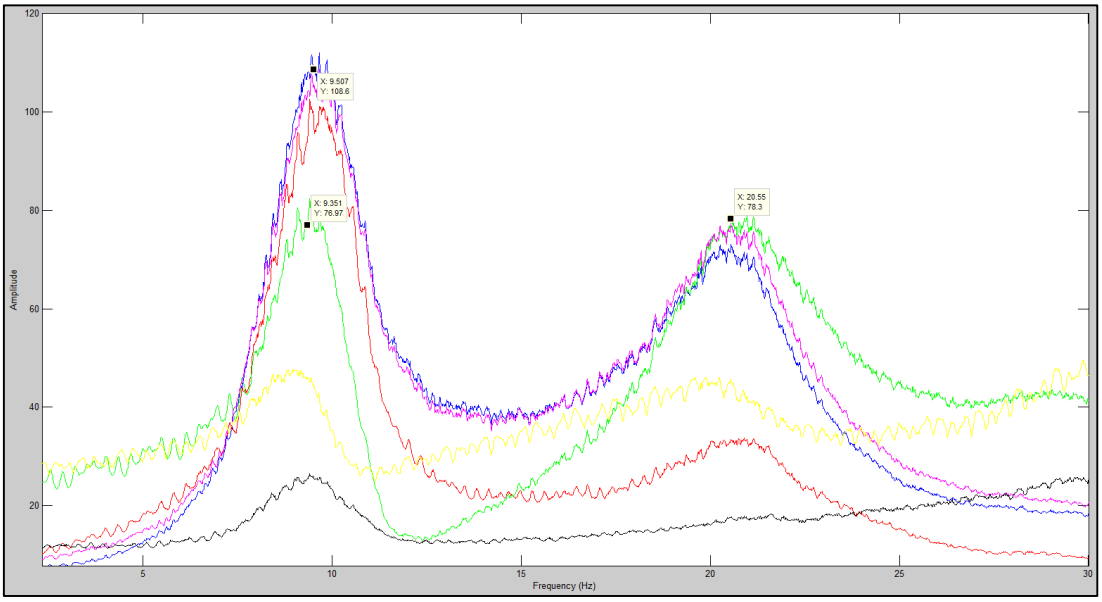

Figure 3.39. FFT Graph for 3 kg Deck Mass and 55th Member Has Damaged Case

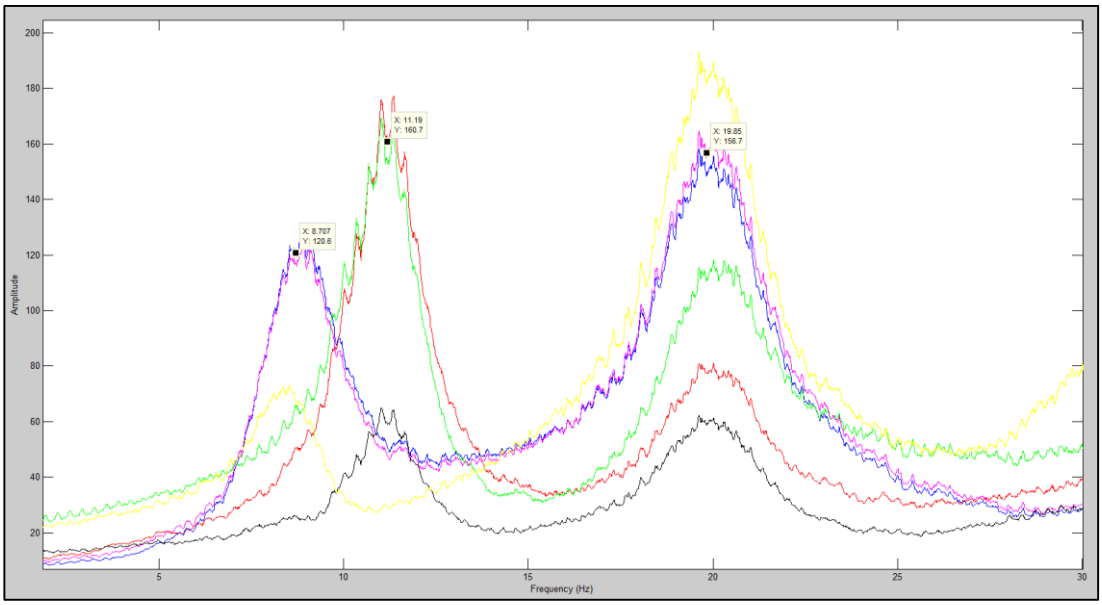

Figure 3.40. FFT Graph for 4 kg Deck Mass and 49th Member Has Damaged Case

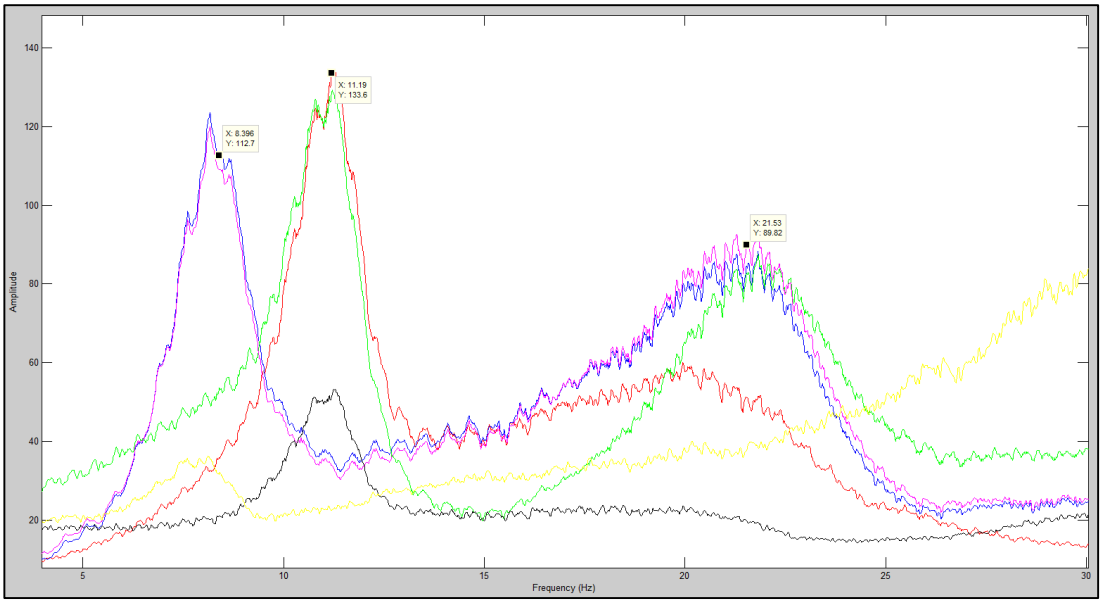

Figure 3.41. FFT Graph for 4 kg Deck Mass and 52nd Member Has Damaged Case

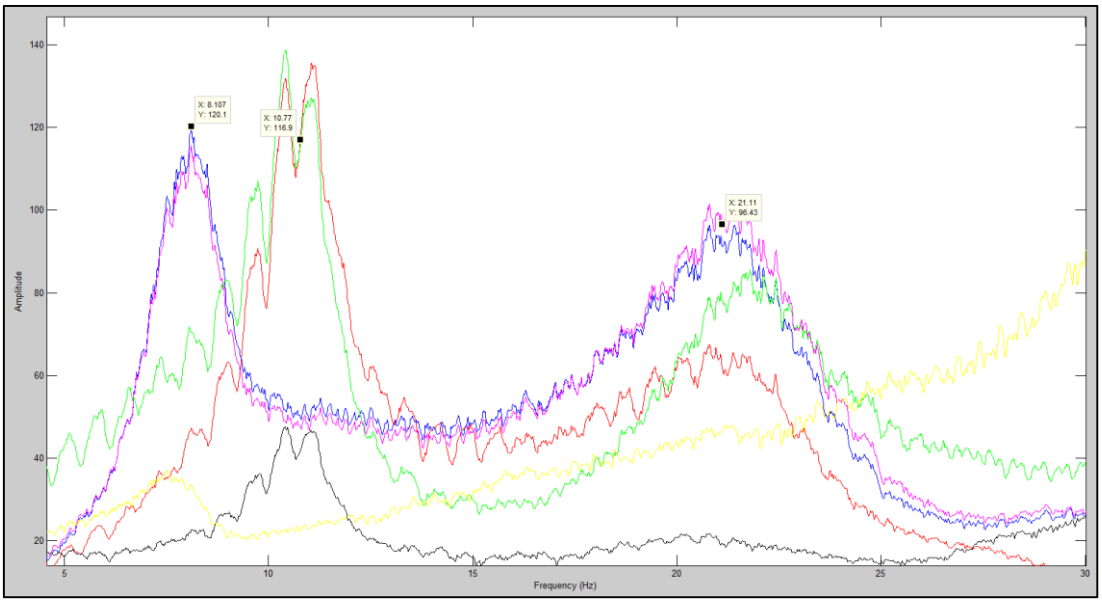

Figure 3.42. FFT Graph for 5 kg Deck Mass and 52nd Member Has Damaged Case

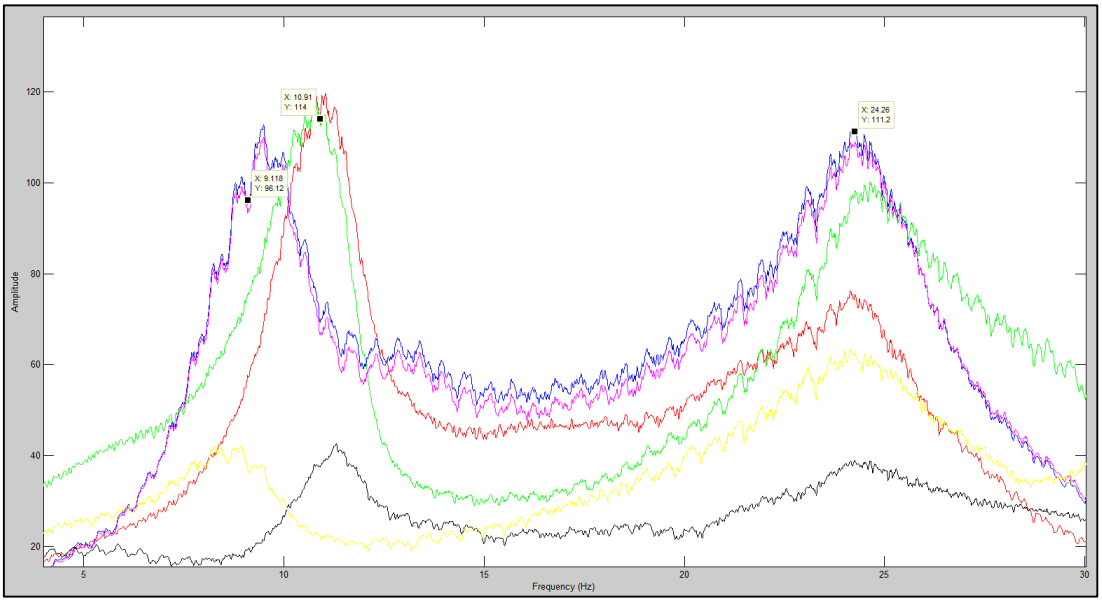

Figure 3.43. FFT Graph for 5 kg Deck Mass and 31st Member Has Damaged Case

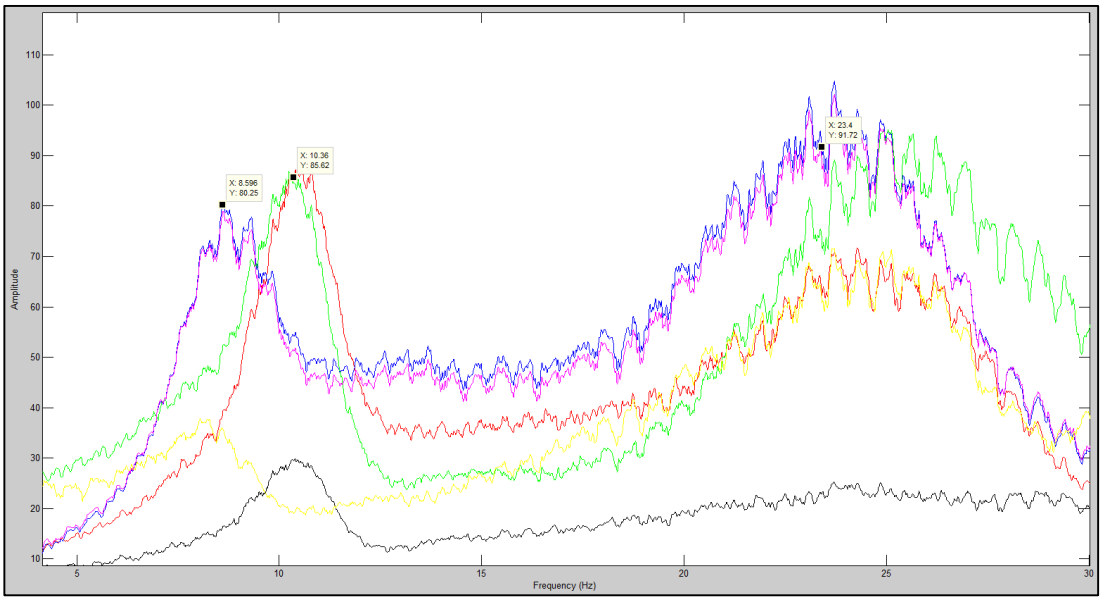

Figure 3.44. FFT Graph for 6 kg Deck Mass and 27th Member Has Damaged Case

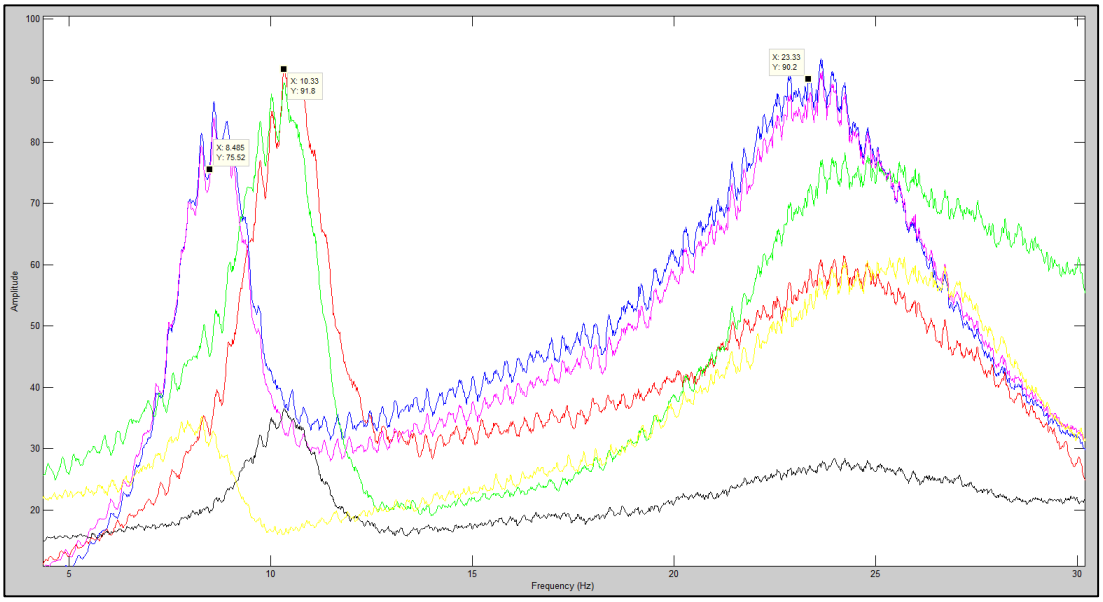

Figure 3.45. FFT Graph for 6 kg Deck Mass and 26th Member Has Damaged Case

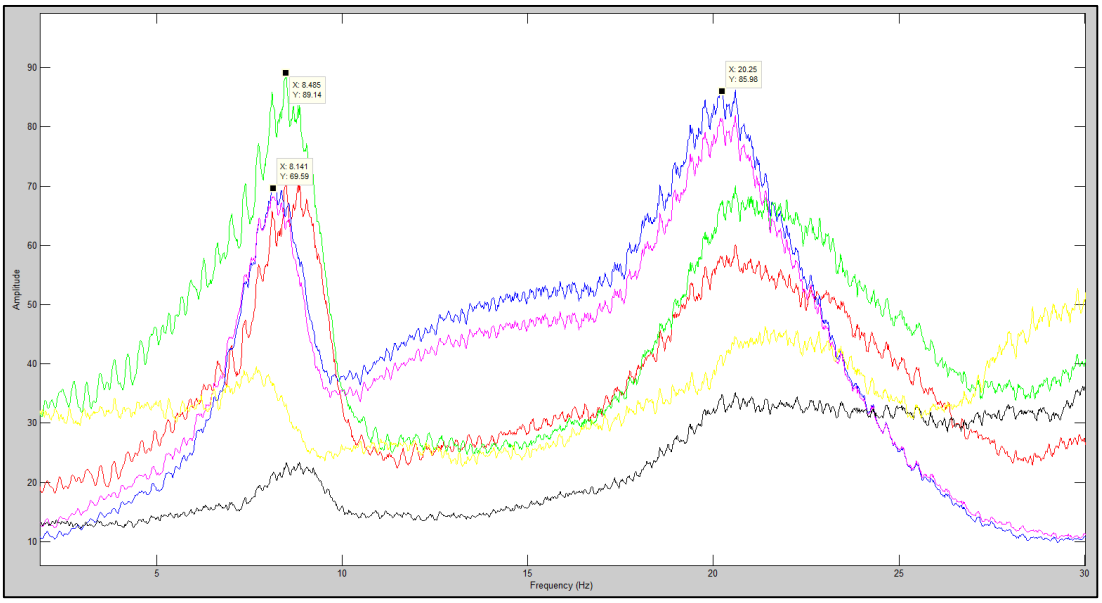

Figure 3.46. FFT Graph for 7 kg Deck Mass and 48th Member Has Damaged Case

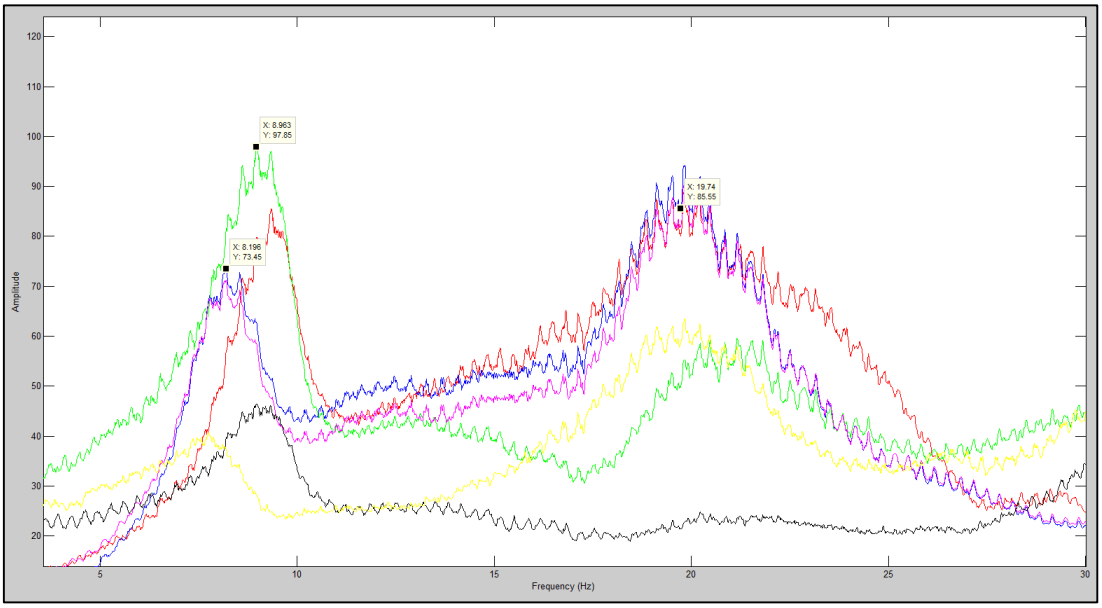

Figure 3.47. FFT Graph for 7 kg Deck Mass and 46th Member Has Damaged Case

After the physical lab experiments were completed, the analytical model was recalibrated according to these data. The program for the calibration of the analytical model is given in the appendix and the flowchart is given below. (Figure 3.48).

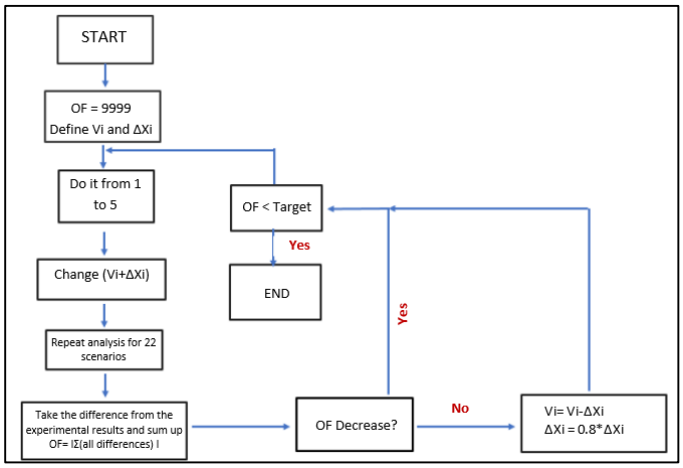

Figure 3.48. Analytical Model Automatic Calibration Code Flow Chart

The results obtained from all dynamic experiments are compared against corresponding FEM results and listed in Table 3.6.

Table 3.6. *Frequencies Obtained from FEM Analysis and Experiments*

Damaged Member ID	Mass (kg)	FEM			EXPERIMENTAL		
		Mod 1 (cyc/sec)	Mod 2 (cyc/sec)	Mod 3 (cyc/sec)	Mod 1 (cyc/sec)	Mod 2 (cyc/sec)	Mod 3 (cyc/sec)
No damage	0	10.49	12.29	25.29	10.36	12.13	25.32
	1	10.11	11.86	25.02	10.12	11.87	25.26
	2	9.76	11.46	24.77	9.98	11.68	25.08
	3	9.44	11.10	24.55	9.75	11.54	24.91
	4	9.16	10.77	24.34	9.21	11.25	24.52
	5	8.89	10.47	24.15	9.16	10.78	24.33
	6	8.65	10.20	23.97	8.61	10.42	24.28
	7	8.42	9.94	23.80	8.47	10.22	24.26
	8	8.22	9.70	23.64	8.21	9.86	24.16
	9	8.02	9.48	23.49	8.02	8.99	23.34
	10	7.84	9.27	23.34	7.51	8.04	23.27
32	3	9.44	11.09	24.52	9.37	11.54	24.61
49	3	8.92	11.09	20.27	9.09	11.51	19.87
55	3	9.38	9.89	21.58	9.35	9.51	20.55
49	4	8.65	10.77	20.21	8.71	11.19	19.85
52	4	8.46	10.77	22.94	8.40	11.19	21.53
52	5	8.19	10.47	22.72	8.11	10.77	21.11
31	5	8.89	10.47	24.10	9.12	10.91	24.26
27	6	8.65	10.19	23.91	8.60	10.36	23.40
26	6	8.65	10.19	23.91	8.49	10.33	23.33
48	7	8.36	9.02	21.74	8.14	8.49	20.25
46	7	8.40	9.09	20.38	8.20	8.96	19.74

3.4. Identification of Damaged Members Using Trained ANN and Discussion of Results

Two different approach was fallowed to generate and train ANN. The first system was only targeted to identify if there is any damage and if the damage is located on a certain type of member (i.e., diagonal, horizontal, vertical). This ANN was trained using randomly generated 10,000 damage scenarios with damage to only one of the members. However, this approach caused generation of the same damage multiple times. Furthermore, storage mass was always assumed to be zero. However, ANN primary rule is variability in the input to prevent network to memorize data. Furthermore, mass is always changing during operation and changed mass would directly affect the natural vibration frequencies of the tower. Therefore, the ANN is modified to include input mass and trained using a set of damage data to include randomly generated mass content on the tower to simulate different levels of oil or gas storage. Both of the ANN worked successfully with the analytical data. A portion of 10,000 data was reserved for testing. The training has been carried out using 9,000 (validation as well) data points and 1,000 analytically generated test data were all correctly identified.

However, only 3 out of the 21 damage and mass change scenarios of experimental test results were identified correctly by selected as the trained ANN (Type-E). The ANN is highly successful in identification of the analytical damage simulations with greater than 97% success rate while experimental damage scenarios could only be identified with 14% success rate.

Other ANNs (Type-A, Type-B, Type-C and Type-D) success rates were also investigated. They have also low success rates. Table 3.7 shows the results.

Table 3.7. *Trained ANNs Success Rates*

Type of Network	Number of Damaged Case Out of 21 Experiments	Success Rate
Type-A	2/21	10%
Type-B	3/21	14%
Type-C1 (type)	3/21	14%
Type-C2 (story)	10/21	48%
Type-C3 (plane)	2/21	10%
Type-D	2/21	10%

Type-C1, Type C2, and Type-C3 could not determine the damaged member for the same damage scenario. Therefore, these networks success rate cannot give not an opinion about the success of the Type-C. It cannot determine exactly which member has damaged. They define type, story and plane of the member separately.

The reasons of low success rate are thought to be because of the following:

1) Small changes in experimental measurements cannot be obtained with the same accuracy as in analytical simulation
2) Nonlinear joint connection properties and ambiguous support conditions (lifting, turning etc.) is thought to play a big role in the poor damage detection.
3) Slushing effect of the liquid mass in the storage tank affects the vibration characteristics of the lab experiment, while mass defined in the analytical model is stable.
4) Static load applied by pulling a rope cannot be perfectly aligned with the two horizontal axes. Variations in force alignment both in horizontal and vertical has an adverse effect on the test results being different than the analyses.
5) Although best effort was spent, small variations in the alignment of the LVDTs affected measurement results.
6) Nonlinear and viscoelastic behavior of the PVC pipes had adverse effects on the measurements making differences between the tests and analyses. The loading and unloading curves often had a hysteresis response and stiffness values were different.

7) The member connections were not fully rigid and bolted connections had slip and contact nonlinearity generating large damping and nonlinear static loading results. The differences between the actual and modelled connections had caused some differences to identify damage.
8) Figure 3.15 and Table 3.3 shows symmetry problems during static loading for out-of-plane bending and rotation. Undamaged condition showing these properties indicate some existing damage even for the undamaged case. Therefore, assumed undamaged case and relevant damage scenarios had intrinsic conceptual errors at the testing level.

In the light of the above discussions, it is thought that pure analytical simulations are successfully identified using trained ANNs; however, training data has to be obtained from actual laboratory or field structure for a successful experimental identification.

Generating thousands of damage scenarios using real structures is not feasible and most of the times not possible considering they will be submerged in water. Self-organizing Neural Networks are planned to be used as a future study to identify changes in structural properties in a heuristic learning pattern.

CHAPTER 4

VISUAL INSPECTION SUBMARINE DEVELOPMENT

4.1. Preliminary Model with Wireless Communication

Visual inspection of structural members under water is commonly carried out by trained divers, which is time consuming and costly. Hard to reach higher depths, caisson disease, shark attack are a few risks to list. A simple underwater camera and submarine system has been attempted to be developed within this study, in order to prevent restrictive situations such as diving, renting, training, limited time due to underwater air tube etc. Submarines that are ready in the market have been found to be very expensive or camera cannot be attached. Early model was planned to have a remote controlled motor driver and controller (Figure 4.2), which was purchased and placed in the waterproof container (Figure 4.1) and connection to two DC motors and propellers to trust and maneuver under water.

Figure 4.1. Underwater Observer Body and Drives.

Figure 4.2. Remote Control Device to Control the Underwater Monitoring Device

Underwater monitoring device can be seen in Figure 4.3 and Figure 4.4.

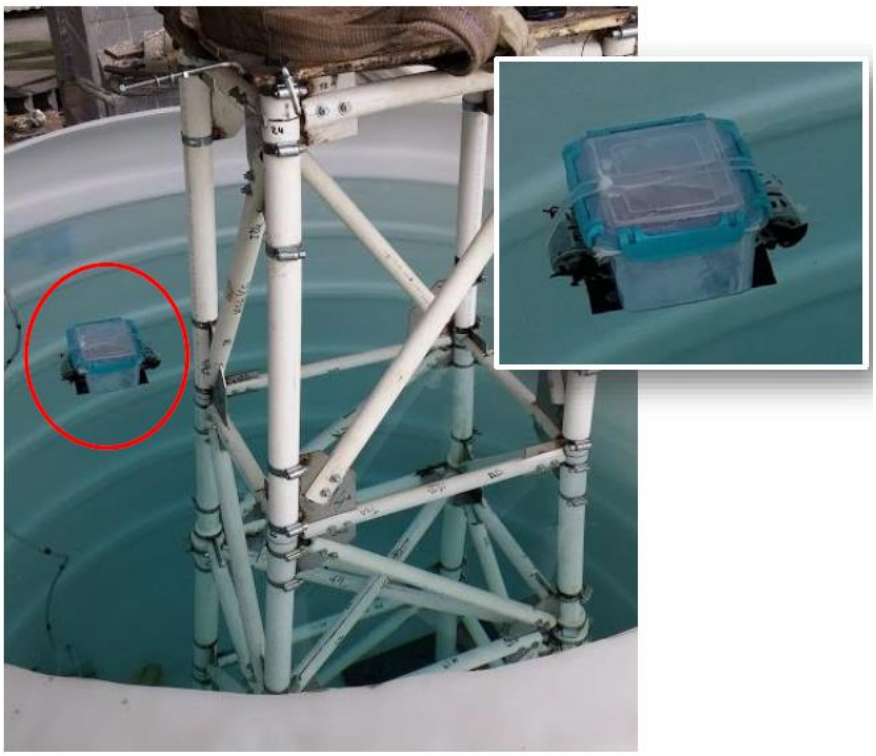

Figure 4.3. When Testing the Underwater Monitoring Device in the Pool

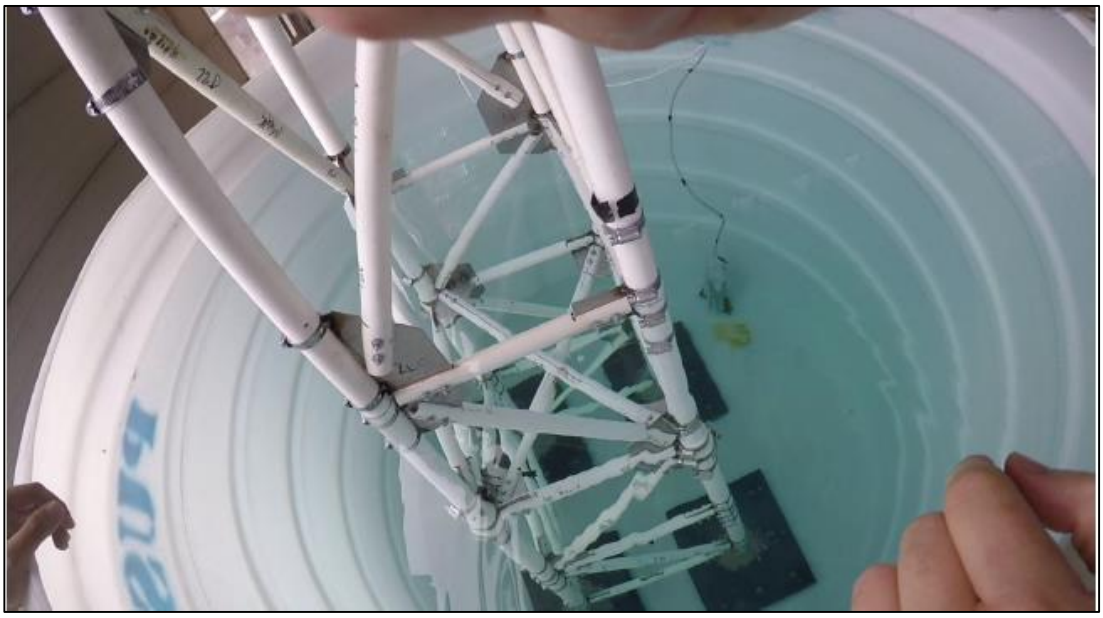

Figure 4.4. When the Underwater Monitoring Device Is Placed in the Pool (Own Camera)

The overall density of the box that contains battery, projector for light, camera, remote control to change voltage and rotation speed of two propellers was adjusted to match and be slightly larger than the density of water so that it would be suspended in water. A rope attached to the box is used to adjust the depth so that box would be free to investigate structural members at that depth. Changing the cable length and depth would allow investigation of all members and connections.

It was seen that the remote control does not work under water and larger depths and a power and signal cable is proposed to be replace the rope providing energy and remote control.

Using the in-water observation device, the upper joint region of the truss like structure (Figure 4.5), the observational control of the mid-level elements (Figure 4.6), and the joint control with the base plate (Figure 4.7) were performed.

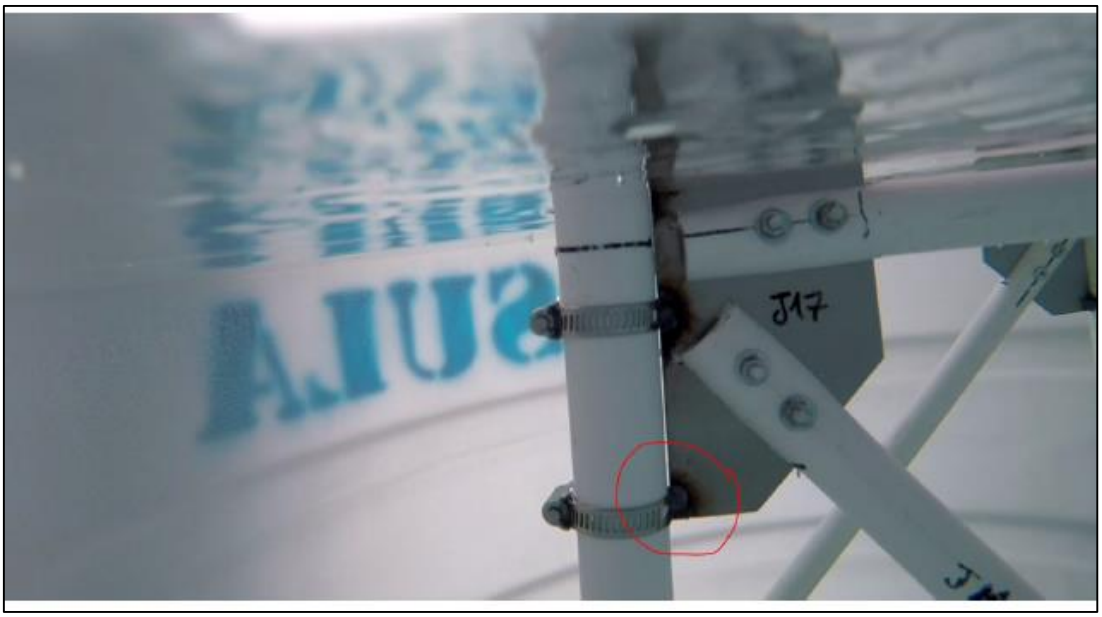

Figure 4.5. Connection Control with Underwater Monitoring Device

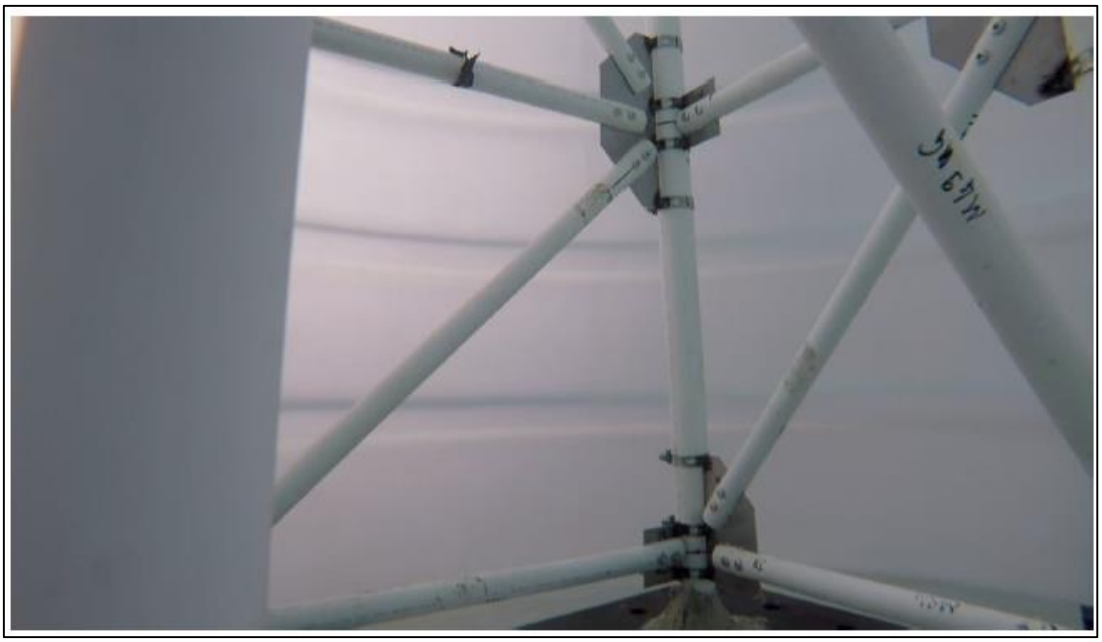

Figure 4.6. Overall View Control by Underwater Monitoring Device

Figure 4.7. Feet and Joint Control by Underwater Monitoring Device

4.2. Final Model with Cable Connection

Since it is seen that the coverage distance of radio frequencies in water may be limited to a few meters, the wired version of the model can be developed for monitoring of real examples. The wire would not only maintain the depth of the device at a certain depth but also provide large power demand, maneuver information for the propellers' controller, as well as live cable video feed back to the surface where Wi-Fi signals cannot reach.

4.3. Wave Measurement, Wave Load Calculation and Wave Property Measurement for Dynamic Excitation on Towers

The dynamic wave forces acting on the truss type tower structure in the water cause the structure to oscillate and vibrate. If information such as the direction, height, and

velocity of the incoming waves can be obtained, the vibrations of the structure can be normalized by dividing the forces that act on the structure. Thus, a quantitative approach for the response of the structure can be utilized to detect structural damage. The first of the studies on wavelength and period is aimed at obtaining the period of the wave. In order to obtain the information of the wave, a triaxial accelerometer was placed in a floating deck (Figure 4.8), which will be replaced by a water proof horizontal disk in the future. This may also be obtained by using two deep lids, in which the accelerometer is placed plates to be glued together. Charging problems may be overcome by using thin wires for power and data collection. A permanent disk with accelerometer in it will need to have a constant orientation to have x-axis in horizontal East, y-axis in horizontal North, and z-axis vertical directions. Thus, the angle of incidence of the wave can be determined with respect to the East and North directions.

Figure 4.8. Prototype Measuring Device (Triaxial Accelerometer) Developed to Measure Wave Characteristics in the Pool

Function of vertical movement of wave in motion can be simply defined as (assuming sensor rotations are negligibly small):

$$z=A\sin(wt)$$

Upward velocity of the same wave would be:

$$v=Awcos(wt)$$

and upward acceleration of the same wave would be:

$$a= - Aw^2sin(wt)$$

The frequency (f) of the incoming wave can be obtained by Fast Fourier Transform (FFT) of the recorded vertical acceleration data. In this case ($w = 2 * \pi * f$) and period (T) is equal to:

$$T = 2\pi / w = 1 / f$$

The period (T) and then the wave length can be calculated using Table 1.2 and as follow.

$$L = g\ T^2 / (2\pi)$$

Wave magnitude (A), the acceleration record obtained in the vertical (z) direction of the acceleration record

$$a= - Aw^2sin(wt) = Bsin(wt)$$

It is obtained by comparing with the size value seen in the formula. If the magnitude of the acceleration record is B, then wave height (A) is found as:

$$A = B / w^2$$

The velocity of the wave (C: Celerity) can also be calculated in terms of the wave period.

$$C = gT / (2\pi)$$

Thus, the obtained wave size (A), wave period (T), wavelength (L), and wave velocity (C) values can be obtained from a single acceleration record. The direction of the wave may also be obtained from the acceleration recordings in the x and y directions, which is called the angle of incidence of the wave.

Considering that accelerometer will generate a circular motion and tilting, the horizontal direction accelerometer may be assumed to have the following form ignoring rotation:

$$h=A\cos(wt)$$

The vectorial components of this movement in the x and y directions by considering α angle between x and in the first quadrant.

$$h_x=A\cos(wt)\cos(\alpha)$$

$$h_y=A\cos(wt)\sin(\alpha)$$

These two formulas are divided by each other

$$h_y/h_x=\tan(\alpha)$$

$$\alpha = \operatorname{atan}(h_y/h_x)$$

The angle (α) of the wave from east to north may be found by this formula. As a result, the magnitude of a wave (A), wave period (T), wavelength (L), wave velocity (C), and wave direction (α) can be obtained from three perpendicular acceleration recordings.

This approach was put to a simple test after a random transient wave was generated and measured in the pool (Figure 4.8). As an example, the recorded acceleration record for vertical direction has an amplitude (height/2) of 0.05 g = 0.5 m / s2 with a wave period of approximately 0.42 seconds for the ch3 record in the vertical direction. Frequency (f) = 2.38 Hz and ω = 15 rad/s are calculated. In this case, the wave amplitude is (height / 2) = 0.5 / 15 ^ 2 = 2.22 mm. The speed of the wave is 0.65 m/s with the formula gT / (2 π). The wave length is 0.27 m with the formula $L = gT^2 / (2\pi)$.

For the direction of the wave, the amplitude for ch2 channel is 0.0165 g and the amplitude of wave received from ch1 channel is 0.0475 g, so the angle of the wave with the x axis is calculated as 19.2 degrees.

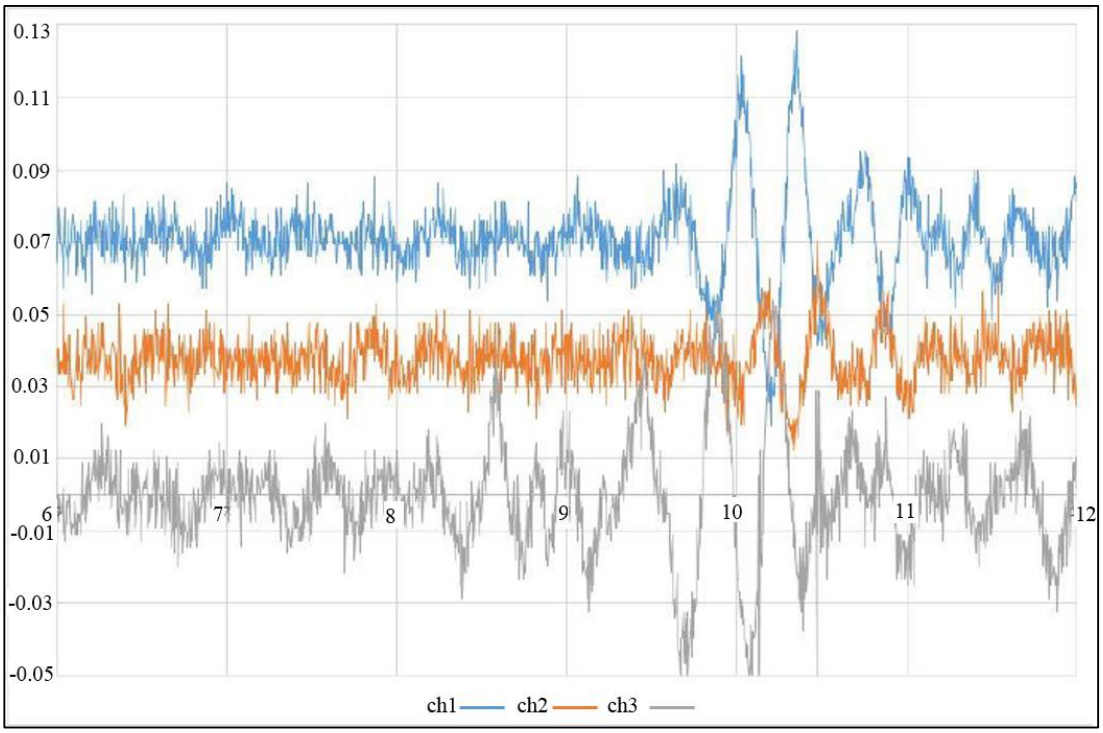

Figure 4.9. Test Data in the Pool to Obtain Wave Information (sec vs m/s^2)

CHAPTER 5

EARLY WARNING USER INTERFACE DEVELOPMENT

5.1. Design of User Interface for Early Warning of Damage

The ANN results will output between 0 and 1, which will determine which element has damaged. Zero means no damage and 1 means member has damaged. A Graphical User Interface (GUI) showing all of the members and alarm – warning condition buttons is designed (Figure 5.1). If multiple damage estimates are repeatedly received from the trained ANN for the same element, the element will be considered to be damaged and highlighted (Figure 5.2); subsequently, an alarm message will be sent to the relevant technical person by SMS. An audible warning can also be added.

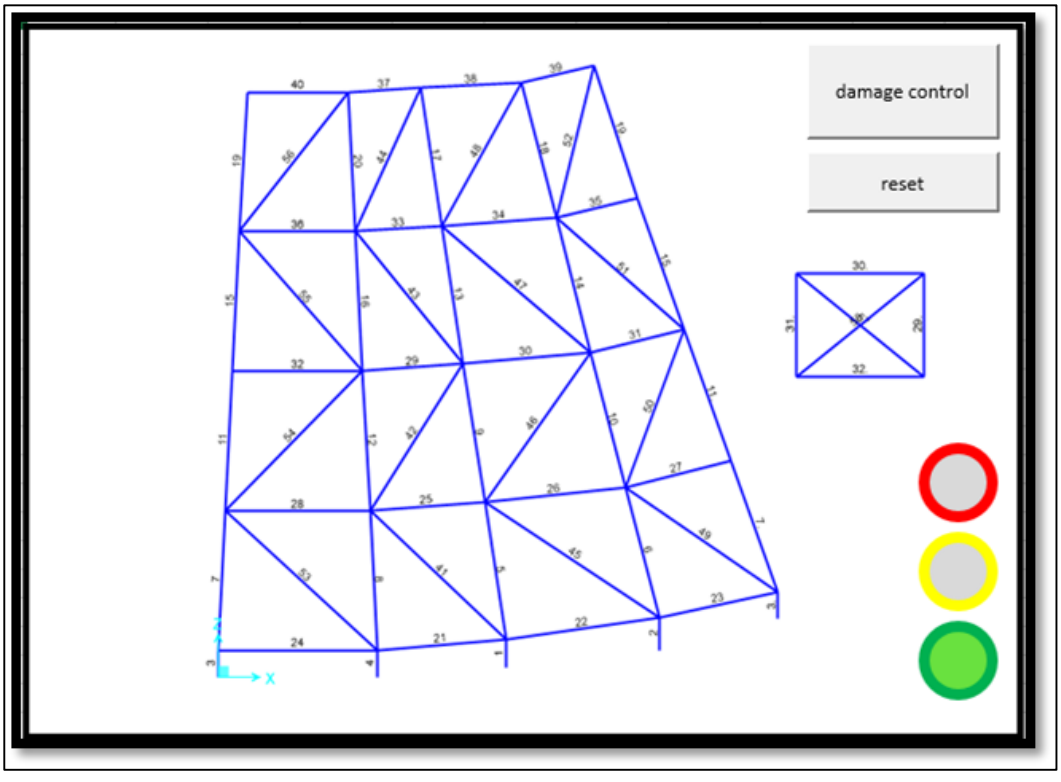

Figure 5.1. Graphical User Interface (GUI) View That Shows the Health Status of the Structure

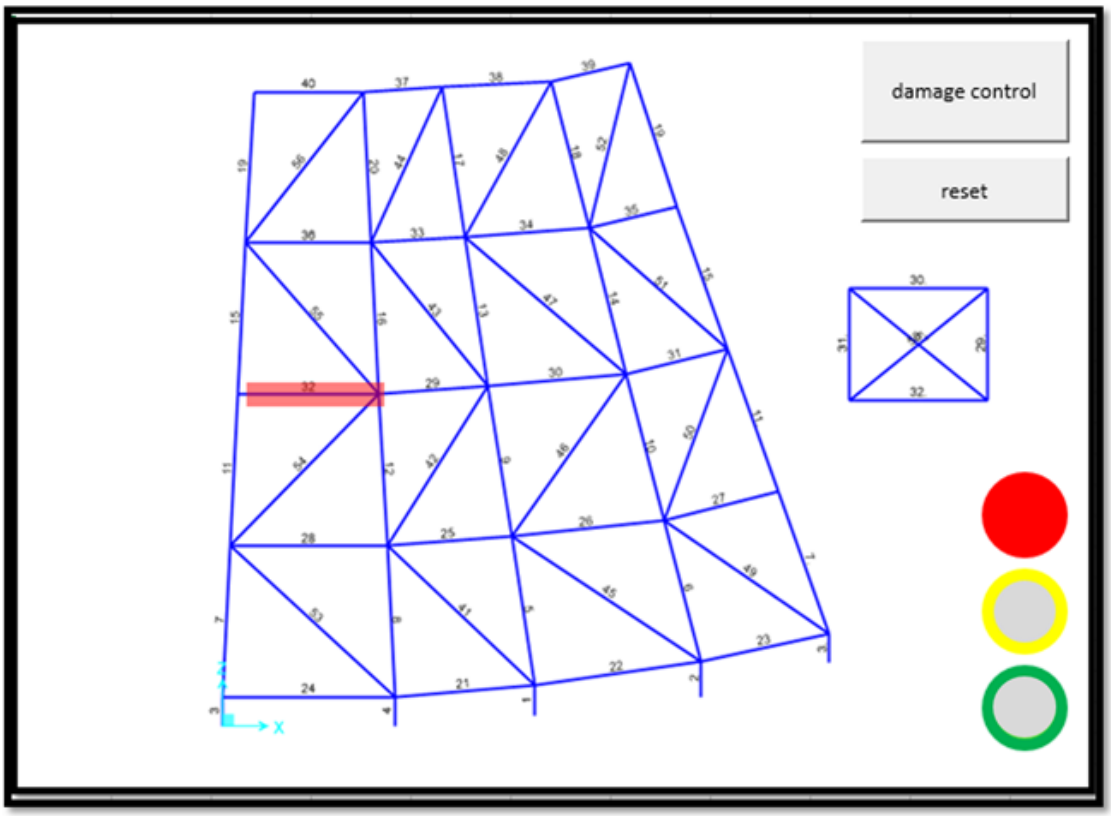

Figure 5.2. Damaged Member Alarm of the Structure (When Member is Selected and Red Light is On)

5.2. ANN Input Parameters and How to Obtain for a Full Size Tower

For full size in-water truss-like structures, the changes in the first three frequencies (1st bending in weak direction mode, 1st bending in strong direction mode and 1st torsion mode) can be obtained with accelerometers, GPS sensors would measure rough horizontal static movements and liquid level gauges placed in the tank determines the height and mass of stored liquid mass. These data are processed by using automatic FFT and peak finding algorithm and are entered as test input to trained ANN for damage detection.

In addition to these frequency changes, wave height, period, velocity etc. information and force values obtained by using Morison equations will be normalized with

displacement values obtained from GPS and entered into ANN. The displacements based on sinusoidal loading of waves may be indirectly obtained from dynamic data but a test boat may apply constant force to the platform pulling it in two orthogonal directions and repeating loading test every two months. This may be enough to track stiffness changes more accurately and obtain if any rotation deformation exists under lateral loading, which is an indication of a structural member loss on one side of the tower.

5.3. Recommendations and Future Work

Annual visual inspection by submarine, oyster, marine growth, mussel, etc. cleaning, strain gage, GPS based displacement measurement, ship pull on tower using load cell mounted cable for static load testing every 2 months to a year, different mass level dynamic measurement tests to obtain baseline frequencies, then continuous measurement of natural vibration frequencies normalized as a function of mass and comparison is recommended.

Self-learning adaptive neural networks are planned to conduct tests on actual test structures is planned for future study. Temperature effect on structural response will also be investigated and a temperature-humidity sensor will be incorporated as input channel.

CHAPTER 6

CONCLUSIONS

It is known that in-water structures perform under harsh and difficult conditions, stay in salty water which is very corrosive for steel members or reinforcement in concrete, structure is exposed to continuous and variable wave movements, high winds, wetting/drying cycles, and algae-mussels grow on it. Observation of structural elements is only possible with trained divers as it is in water and in hard-to-reach areas. Consequently, structural health monitoring (SHM) studies should be considered for in-water structures and should intelligently listen data combined with Artificial Neural Networks (ANN) that can warn authorities as soon as any structural differences are captured. Such a system would prevent occurrence of natural and economic disaster that may also be life threatening. The aim of this thesis is to use ANN to determine structural damage to members using data collected from accelerometers, liquid level sensors, load cells and displacement GPS sensors.

Analytical and experimental studies were performed following a comprehensive literature review was made, MATLAB code, ANN theory and toolboxes were investigated. Existing offshore oil platforms have been examined and generic plans were used to build a small-scale lab test structure. Representative analytical models were created, calibrated, and analyzed for different damage scenarios also comparing results with the actual lab model tests. Lab model tests included dynamic and static tests on undamaged and damaged conditions with and without additional liquid mass on the platform. Natural vibration frequencies and horizontal stiffness in orthogonal directions were obtained. PVC pipes were preferred to have relatively larger deflections and smaller vibration frequencies for modes. In this way, more accurate measurements were obtained.

Analytical studies conducted on the extent of damage causing detectable structural differences, it was found that cracks or localized section losses by rusting in the

elements will not generate detectable structural changes until total cross section is lost. Therefore, cracks and partial section losses that may occur at the connections or along the length are excluded from the simulation and only full member losses are considered. Crack formation generates very small axial member stiffness changes even close to full width cracks since the length of the cracked portion is too short to create any change to the axial stiffness of an element. It is also assumed that member loss – damage is limited to a single element only, because continuous monitoring ANN system will immediately sense and change and set alarm when the first element damage occurs before others can follow. It is assumed that losing more than one member at the same time is very unlikely. The structural parameters monitored by the ANN include the first three mode frequencies, normalized horizontal deflection, and also the amount of additional liquid mass held on the deck. Training, validation, and test data sets were prepared and numerous ANNs were tested. A total of 10 000 damage scenarios were randomly generated by means of an Excel VBA program and automatically generated to be analyzed by SAP2000 software. Large sets of analyses results were successfully learned by ANNs. The analyses were repeated by considering changing mass on deck and using calibrated analytical model based on non-destructive tests data obtained from lab model. Elasticity modulus, mass, natural frequencies, stiffness, etc. parameters were measured on lab model and PVC pipe materials and calibration studies were performed until analytical model to give similar results as the experiment. ANN training was completed using data for 10,200 damage and different mass scenarios reconstructed using the calibrated model. After that, 11 selected members were removed and non-destructive tests were repeated on the lab model. For some damage cases, the platform mass has been modified as well. Measurements made after each damage and mass change were entered into the final ANN which was trained by calibrated FEM. Success rate of the calibrated FEM based ANN using purely scenarios generated by analytical model was high in the order of 97%. (970 of the 1000 damaged and undamaged cases shown for the first time were known correctly). However, only 3 out of the 21 damage and mass change scenarios of experimental test results were correctly known by the ANN.

The reasons of low success rate of ANN are thought to be because of the following:

1) Small changes in experimental measurements cannot be obtained with the same accuracy as in analytical simulation.

2) Nonlinear joint connection properties and ambiguous support conditions (lifting, turning etc) is thought to play a big role in the poor damage detection.

3) Slushing effect of the liquid mass in the storage tank affects the vibration characteristics of the lab experiment, while mass defined in the analytical model is stable.

4) Static load applied by pulling a rope cannot be perfectly aligned with the two horizontal axes. Variations in force alignment both in horizontal and vertical has an adverse effect on the test results being different than the analyses.

5) Although best effort was spent, small variations in the alignment of the LVDTs affected measurement results.

6) Nonlinear and viscoelastic behavior of the PVC pipes had adverse effects on the measurements making differences between the tests and analyses. The loading and unloading curves often had a hysteresis response and stiffness values were different.

7) The member connections were not fully rigid and bolted connections had slip and contact nonlinearity generating large damping and nonlinear static loading results. The differences between the actual and modelled connections had caused some differences to identify damage.

8) Figure 3.14 and Table 3.5. Displacement and Rotation Values Obtained from FEM Analysis and Experiments for 500N Loading shows symmetry problems during static loading for out-of-plane bending and rotation. Undamaged condition showing these properties indicate some existing damage even for the undamaged case. Therefore, assumed undamaged case and relevant damage scenarios had intrinsic conceptual errors at the testing level.

In the light of the above discussions, it is thought that pure analytical simulations are successfully identified using trained ANNs; however, training data needs to be obtained from actual laboratory or field structure for a successful experimental identification. Generating thousands of damage scenarios using real structures is not feasible and most of the times not possible considering they will be submerged in water. Self-organizing Neural Networks are planned to be used as a future study to identify changes in structural properties in a heuristic learning pattern.

Further calibration of the analytical model including damaged condition test results was also considered, but it was abandoned because it may not be possible to damage members of an oil platform and take measurements in practice.

As a result, experimental and analytical modeling and simulation studies have been performed, although the results have been very successful analytically, the same success has not been achieved with the experimental data.

An underwater observation model has been manufactured and tested successfully for observing the underwater structures. Wireless communication has been a major problem for underwater and cabled power and communication may be the best for observation submarine.

Testing and monitoring actual in-water tower platforms might use wave generated dynamic forces on the structure and an attempt to obtain the magnitude of a wave (A), wave period (T), wavelength (L), wave velocity (C), and wave direction (α) has been demonstrated on a test data which was obtained using a single floating triaxial accelerometer.

REFERENCES

Abdo, M. A. -B., and Hori, M. 2002. "A numerical study of structural damage detection using changes in the rotation of mode shapes", *Journal of Sound and Vibration, 251*(2), 227-239.

American Petroleum Institute. (2000). Recommended practice for planning, designing and constructing fixed offshore platforms—working stress design (RP 2A-WSD).

Arangio, S., and Beck, J. L. 2012. "Bayesian neural networks for bridge integrity assessment", *Struct. Control Health Monit., 19,* 3-21.

Bakhary, N., Hao H. and Deeks, A. J. 2007. "Damage detection using artificial neural network with consideration of uncertainties", *Engineering Structures, 29,* 2806-2815.

Bakhary, N., Hao H. and Deeks, A. J. 2010. "Structure damage detection using neural network with multi-stage substructuring", *Advances in Structural Engineering, 13*(1).

Brincker, R. Kickergaard, P.H., Andersen, P., and Martinez, M. E. "Damage detection in an offshore structure"

Carden, E. P., and Fanning, P. 2004. "Vibration based condition monitoring: a review", *Structural Health Monitoring, 3*(4), 355-377.

Deo, M. C. 2010. "Artificial neural networks in coastal and ocean engineering", *Indian Journal of Geo-Marine Science, 39*(4), 589-596.

Dormehl, L. (2019). What is an artificial neural network? Here's everything you need to know. Retrieved 5 January 2019, from https://www.digitaltrends.com/cool-tech/what-is-an-artificial-neural-network/

Elshafey, A. A., Haddara, M. R., and Marzouk, H. 2009. "Dynamic response of offshore jacket structures under random loads", *Marine Structures, 22*, 504-521.

Elshafey, A. A., Haddara, M. R., and Marzouk, H. 2010. "Damage detection in offshore structures using neural networks", *Marine Structures, 23*, 131-145.

Elshafey, A. A., Haddara, M. R., and Marzouk, H. 2010. "Identification of excitation and reaction forces spectra for offshore platforms", *Can. J. Civ. Eng., 37,* 66-76.

Ergin, A. 2009. *Coastal Engineering*. Ankara:METU Press.

Friedmann, A., Mayer, D., Koch, M., and Siebel, T. "Monitoring and damage detection in structural parts of wind turbines", Fundamental and Advanced Topics in Wind Power.

Friswell, M. I., and Penny, J. E. T. 1997. "Is damage location using vibration measurements practical?", *EUROMECH 365 International Workshop: DAMAS 97, Structural Damage Assessment Using Advanced Signal Processing Procedures, Sheffield*, 351-362.

Gawronski, W., and Sawicki, J.T. 2000. "Structural damage detection using modal norms", *Journal of Sound and Vibration, 229*(1), 194-198.

Gökçe, K. T. and Keyder, E. 1991. "Offshore structure types and design principles", *Teknik Dergi, 2*, 103-106.

Hillis, A. J., and Courtney, C. R. P. 2011. "Structural health monitoring of fixed offshore structures using bicoherence function of ambient vibration measurements", *Journal of Sound and Vibration, 330*, 1141-1152.

Hu, S. J., Li, H., and Wang, S. 2007. "Cross-model cross-mode method for model updating", *Mechanical Systems and Signal Processing, 21,* 1690-1703.

Hu, S. J., Wang, S., and Li, H. 2006. “Cross-modal strain energy method for estimating damage severity”, *Journal of Engineering Mechanics, 132*(4), 429-433.

International Organization for Standardization. (2007). ISO 19902:2007 Petroleum and natural gas industries — Fixed steel offshore structures.

Jeary, A. P., “The identification of damage in large structures”

Kim, J. –T., and Stubbs, N. 1995. “Damage detection in offshore jacket structures from limited modal information”, *International Journal of Offshore and Polar Engineering, 5*(1).

Li, H., Wang, J., and Hu, S. J. 2008. “Using incomplete modal data for damage detection in offshore jacket structures”, *Ocean Engineering, 35,* 1793-1799.

Mangal, L., Idichandy, V. G., and Ganapathy, C. 2001. “Structural monitoring of offshore platforms using impulse and relaxation response”, *Ocean Engineering, 28,* 689-705.

Mei, Q., Gül, M., and Asce, A. M. 2014. “Novel sensor clustering-based approach for simultaneous detection of stiffness and mass changes using output-only data”, *Journal of Structural Engineering.*

Nallayarasu, S., “Offshore structures analysis and design”, Department of Ocean Engineering Indian Institute of Technology Madras, India.

Neves, A. C., González, I., Leander, J. and Karoumi, R. 2017. “Structural health monitoring of bridges: a model-free ANN-based approach to damage detection”, *Journal of Civil Structural Health Monitoring, 7*(5), 689-702.

Nichols, J. M. 2003. “Structural health monitoring of offshore structures using ambient excitation”, *Applied Ocean Engineering, 25*, 101-114.

Nicoreac, M.P., Pârv, B.R., Petrina, M. and Petrina, T. 2010. "Similitude theory and applications", *Acta Technica Napocensis: Civil Engineering & Architecture, 53*(1).

Priddy, K. L. and Keller, P. E. 2005, Artificial Neural Networks: An Introduction. doi: 10.1117/3.633187.ch1

Ruotolo, R., Surace, C., and Worden, K. "Application of two damage detection techniques to an offshore platform"

Salehi, M., Ziaei-Rad, S., Ghayour, M., and Vaziri-Zanjani, M. A. 2010. "A structural damage detection technique based on measured frequency response functions", *Contemporary Engineering Sciences, 3*(5), 215-226.

Selva, P., Cherrier, O., Pommier-Budinger, V., Lachaud, F. and Morlier, J. 2013. "Smart monitoring of aeronautical composites plates based on electromechanical impedance measurements", *Engineering Structures, 56,* 794-804.

Shehadeh, M., Shennawy, Y., and El-Gamal, H. 2015. "Similitude and scaling of large structural elements: case study", *Alexandria Engineering Journal, 54,* 147-154.

Shi, Z. Y., Law, S. S., and Zhang, L. M. 1998. "Structural damage localization from modal strain energy change", *Journal of Sound and Vibration, 218*(5), 825-844.

Sun, L., Li, H., Ren, L., and Jin, Q. 2007. "Dynamic response measurement of offshore platform model by FBG sensors", *Sensors and Actuators, 136,* 572-579.

Sundaram, B. A., Ravisankar, K., Senthil, R., and Parivallal, S. 2013. "Wireless sensors for structural health monitoring and damage detection techniques", *Current Science, 104*(11).

Vanik, M. W., Beck, J. L., and Au, S. K. 2000. "Bayesian probabilistic approach to structural health monitoring", *Journal of Engineering Mechanics, 126*(7), 738-745.

Viero, P. F., and Roitman, N. 1999. “Application of some damage identification methods in offshore platforms”, *Marine Structures, 12,* 107-126.

Wang, S. 2013. “Damage detection in offshore platform structures from limited modal data”, *Applied Ocean Research, 41*, 48-56.

Wang, S. 2013. “Iterative modal strain energy method for damage severity estimation using frequency measurements”, *Struct. Control Health Monit., 20,* 230-240.

Wang, S., Li, Y., and Li, H. 2015. “Structural model updating of an offshore platform using the cross model cross mode method: an experimental study”, *Ocean Engineering, 97,* 57-64.

Watkins, S. E., Akhavan, F., Dua, R., Chandrashekhara, K. and Wunsch, D. C. 2007. “Impact-induced damage characterization of composite plates using neural networks”, *Smart Materials and Structures, 1*6(2).

Yan, Y. J., Cheng, L., Wu, Z. Y., and Yam L. H. 2007. “Development in vibration-based structural damage detection technique”, *Mechanical Systems and Signal Processing, 21,* 2198-2211.

Yang, Q. W. 2009. “A numerical technique for structural damage detection”, *Applied Mathematics and Computation, 215,* 2775-2780.

Yang, Q. W., and Liu, J. K. 2007. “Structural damage identification based on residual force vector”, *Journal of Sound and Vibration, 305,* 298-307.

Yan, Y. J., Yam, L. H., Cheng, L., and Yu, L. 2006. “FEM modeling method of damage structures for structural damage detection”, *Composite Structures, 72,* 193-199.

Yoon, M. K., Heider, D., Gillespir, Jr. J. W., Ratcliffe, C. P., and Crane, R. M. 2005. “Local damage detection using the two-dimensional gapped smoothing method”, *Journal of Sound and Vibration, 279,* 119-139.

Yuen, K., and Katafygiotis, L. S. 2002. “Bayesian modal updating using complete input and incomplete response noisy measurements”, *Journal of Engineering Mechanics, 128*(3), 340-350.

APPENDICES

A. VBA Code for Analyses of 10,000+200 Scenarios

```
    Sub sap2000analysis()
'dimension variables
        Dim SapObject As SAP2000v15.SapObject
        Dim SapModel As cSapModel
        Dim FileName As String
        Dim ret As Long
        Dim Selected As Boolean
        Dim BuckModeStart As Long
        Dim BuckModeEnd As Long
Dim BuckModeAll As Boolean
        Dim NumberResults As Long
        Dim Obj() As String
        Dim Elm() As String
        Dim LoadCase() As String
        Dim StepType() As String
        Dim Period() As Double
        Dim Frequency() As Double
        Dim Circfreq() As Double
        Dim Eigenvalue() As Double
        Dim StepNum() As Double
```

```
        Dim U1() As Double
        Dim U2() As Double
        Dim U3() As Double
        Dim R1() As Double
        Dim R2() As Double
        Dim R3() As Double
        Dim ModalStiff() As Double
        Dim Ux() As Double
        Dim Uy() As Double
        Dim Uz() As Double
        Dim Rx() As Double
        Dim Ry() As Double
        Dim Rz() As Double
        Dim ModalMass() As Double
        Dim V() As Double
        Dim m() As Double
'create Sap2000 object
        Set SapObject = New SAP2000v15.SapObject
'start Sap2000 application
        SapObject.ApplicationStart
'create SapModel object
        Set SapModel = SapObject.SapModel
```

```
'initialize model
        ret = SapModel.InitializeNewModel
'open an existing file
        FileName = "C:\Users\serapkara\Desktop\model.sdb”
        ret = SapModel.File.OpenFile(FileName)
        Worksheets("Sheet1").Cells(1, 1).Value = "Damage Member"
        Worksheets("Sheet1").Cells(1, 2).Value = "area modifier"
        Worksheets("Sheet1").Cells(1, 3).Value = "inertia modifier"
        For ii = 4 To 9: Worksheets("Sheet1").Cells(1, ii).Value = "Mode " & (ii - 3)
        & " (cyc/sec)": Next
'HX
        Worksheets("Sheet1").Cells(1, 10).Value = "U1hx(102)"
        Worksheets("Sheet1").Cells(1, 11).Value = "U2hx(102)"
        Worksheets("Sheet1").Cells(1, 12).Value = "U1hx(103)"
        Worksheets("Sheet1").Cells(1, 13).Value = "U2hx(103)"
        Worksheets("Sheet1").Cells(1, 14).Value = "U1hx(104)"
        Worksheets("Sheet1").Cells(1, 15).Value = "U2hx(104)"
        Worksheets("Sheet1").Cells(1, 16).Value = "average_dXhx"
        Worksheets("Sheet1").Cells(1, 17).Value = "Rxhx"
        Worksheets("Sheet1").Cells(1, 18).Value = "Ryhx"
'HY
        Worksheets("Sheet1").Cells(1, 19).Value = "U1hy(102)"
```

```
        Worksheets("Sheet1").Cells(1, 20).Value = "U2hy(102)"
        Worksheets("Sheet1").Cells(1, 21).Value = "U1hy(103)"
        Worksheets("Sheet1").Cells(1, 22).Value = "U2hy(103)"
        Worksheets("Sheet1").Cells(1, 23).Value = "U1hy(104)"
        Worksheets("Sheet1").Cells(1, 24).Value = "U2hy(104)"
        Worksheets("Sheet1").Cells(1, 25).Value = "average_dYhy"
        Worksheets("Sheet1").Cells(1, 26).Value = "Ryhy"
        Worksheets("Sheet1").Cells(1, 27).Value = "Rxhy"
        Worksheets("Sheet1").Cells(1, 28).Value = "fullnessratio (%)"
        Worksheets("Sheet1").Cells(1, 29).Value = "m(0) - Ux" 'local joint masses
        Worksheets("Sheet1").Cells(1, 30).Value = "m(1) - Uy"
        Worksheets("Sheet1").Cells(1, 31).Value = "m(2) - Uz"
        Worksheets("Sheet1").Cells(1, 32).Value = "m(3) - Rx"
        Worksheets("Sheet1").Cells(1, 33).Value = "m(4) - Ry"
        Worksheets("Sheet1").Cells(1, 34).Value = "m(5) - Rz"
        Worksheets("Sheet1").Cells(1, 35).Value = "mass"
' "undamage case with different mass"
        fullmass = 10 'kg h=0.61 m
        a = 200
        For ii = 1 To a
        Worksheets("Sheet1").Cells(ii + 1, 1).Value = "Undamaged Case"
        Worksheets("Sheet1").Cells(ii + 1, 2).Value = "----"
```

```
        Worksheets("Sheet1").Cells(ii + 1, 3).Value = "----"
        h = Rnd() * 0.61
        mass = (0.0875 * 0.1875 * h) * 1000 'kg
        ReDim m(5)
        For I = 0 To 5
        m(I) = 0
        Next I
        For I = 0 To 2
        m(I) = mass / 21
        Next I
        ret = SapModel.PointObj.SetMass("massdeck", m, 1, True, True)
        ret = SapModel.Analyze.RunAnalysis
        ret = SapModel.Results.Setup.DeselectAllCasesAndCombosForOutput
        ret = SapModel.Results.Setup.SetCaseSelectedForOutput("HX")
        ret = SapModel.Results.JointDispl("ALL", GroupElm, NumberResults, Obj,
        Elm, LoadCase, StepType, StepNum, U1, U2, U3, R1, R2, R3)
'for displacement results:
'joint 102= 100
'joint 103= 101
'joint 104= 102
        Worksheets("Sheet1").Cells(ii + 1, 10).Value = U1(100)
        Worksheets("Sheet1").Cells(ii + 1, 11).Value = U2(100)
```

```
Worksheets("Sheet1").Cells(ii + 1, 12).Value = U1(101)

Worksheets("Sheet1").Cells(ii + 1, 13).Value = U2(101)

Worksheets("Sheet1").Cells(ii + 1, 14).Value = U1(102)

Worksheets("Sheet1").Cells(ii + 1, 15).Value = U2(102)

Worksheets("Sheet1").Cells(ii + 1, 16).Value = (U1(101) + U1(102)) / 2

Worksheets("Sheet1").Cells(ii + 1, 17).Value = (U1(102) - U1(101)) / 0.25

Worksheets("Sheet1").Cells(ii + 1, 18).Value = (U2(101) - U2(100)) / 0.35

ret = SapModel.Results.Setup.DeselectAllCasesAndCombosForOutput

ret = SapModel.Results.Setup.SetCaseSelectedForOutput("HY")

ret = SapModel.Results.JointDispl("ALL", GroupElm, NumberResults, Obj,
Elm, LoadCase, StepType, StepNum, U1, U2, U3, R1, R2, R3)

Worksheets("Sheet1").Cells(ii + 1, 19).Value = U1(100)

Worksheets("Sheet1").Cells(ii + 1, 20).Value = U2(100)

Worksheets("Sheet1").Cells(ii + 1, 21).Value = U1(101)

Worksheets("Sheet1").Cells(ii + 1, 22).Value = U2(101)

Worksheets("Sheet1").Cells(ii + 1, 23).Value = U1(102)

Worksheets("Sheet1").Cells(ii + 1, 24).Value = U2(102)

Worksheets("Sheet1").Cells(ii + 1, 25).Value = (U2(100) + U2(101)) / 2

Worksheets("Sheet1").Cells(ii + 1, 26).Value = (U2(101) - U2(100)) / 0.35

Worksheets("Sheet1").Cells(ii + 1, 27).Value = (U1(102) - U1(101)) / 0.25

ret = SapModel.Results.ModalPeriod(NumberResults, LoadCase, StepType,
StepNum, Period, Frequency, Circfreq, Eigenvalue)
```

```
For jj = 0 To 5: Worksheets("Sheet1").Cells(ii + 1, 4 + jj).Value = Frequency(jj): Next

ret = SapModel.SetModelIsLocked(False)

Next ii

For ii = 1 To 10000

he = Int(Rnd(1) * 58) + 1

mdfI = 0

mdfA = 0

mdfT = 0

ReDim V(7)

For I = 0 To 7

V(I) = 1

Next I

V(0) = mdfA

V(3) = mdfT

V(4) = mdfI

V(5) = mdfI

ret = SapModel.FrameObj.SetModifiers(he, V)

h = Rnd() * 0.61

mass = (0.0875 * 0.1875 * h) * 1000 'kg

ReDim m(5)

For I = 0 To 5
```

```
        m(I) = 0
        Next I
        For I = 0 To 2
        m(I) = mass / 21
        Next I
        ret = SapModel.PointObj.SetMass("massdeck", m, 1, True, True)
'get point mass
        ReDim m(5)
        For I = 0 To 5
        ret = SapModel.PointObj.GetMass(162, m)
        Worksheets("Sheet1").Cells(ii + a + 3, I + 29).Value = m(I)
        Worksheets("Sheet1").Cells(ii + a + 3, 28).Value = (mass / fullmass) * 100
        Worksheets("Sheet1").Cells(ii + a + 3, 35).Value = mass
        Next I
        ret = SapModel.Analyze.RunAnalysis
        ret = SapModel.Results.Setup.DeselectAllCasesAndCombosForOutput
        ret = SapModel.Results.Setup.SetCaseSelectedForOutput("HX")
        ret = SapModel.Results.JointDispl("ALL", GroupElm, NumberResults, Obj,
        Elm, LoadCase, StepType, StepNum, U1, U2, U3, R1, R2, R3)
'joint 102= 100
'joint 103= 101
'joint 104= 102
```

```
Worksheets("Sheet1").Cells(ii + a + 3, 10).Value = U1(100)
Worksheets("Sheet1").Cells(ii + a + 3, 11).Value = U2(100)
Worksheets("Sheet1").Cells(ii + a + 3, 12).Value = U1(101)
Worksheets("Sheet1").Cells(ii + a + 3, 13).Value = U2(101)
Worksheets("Sheet1").Cells(ii + a + 3, 14).Value = U1(102)
Worksheets("Sheet1").Cells(ii + a + 3, 15).Value = U2(102)
Worksheets("Sheet1").Cells(ii + a + 3, 16).Value = (U1(101) + U1(102)) / 2
Worksheets("Sheet1").Cells(ii + a + 3, 17).Value = (U1(102) - U1(101)) / 0.25
Worksheets("Sheet1").Cells(ii + a + 3, 18).Value = (U2(101) - U2(100)) / 0.35
ret = SapModel.Results.Setup.DeselectAllCasesAndCombosForOutput
ret = SapModel.Results.Setup.SetCaseSelectedForOutput("HY")
ret = SapModel.Results.JointDispl("ALL", GroupElm, NumberResults, Obj,
Elm, LoadCase, StepType, StepNum, U1, U2, U3, R1, R2, R3)
Worksheets("Sheet1").Cells(ii + a + 3, 19).Value = U1(100)
Worksheets("Sheet1").Cells(ii + a + 3, 20).Value = U2(100)
Worksheets("Sheet1").Cells(ii + a + 3, 21).Value = U1(101)
Worksheets("Sheet1").Cells(ii + a + 3, 22).Value = U2(101)
Worksheets("Sheet1").Cells(ii + a + 3, 23).Value = U1(102)
Worksheets("Sheet1").Cells(ii + a + 3, 24).Value = U2(102)
Worksheets("Sheet1").Cells(ii + a + 3, 25).Value = (U2(100) + U2(101)) / 2
Worksheets("Sheet1").Cells(ii + a + 3, 26).Value = (U2(101) - U2(100)) / 0.35
Worksheets("Sheet1").Cells(ii + a + 3, 27).Value = (U1(102) - U1(101)) / 0.25
```

```
        Worksheets("Sheet1").Cells(ii + a + 3, 1).Value = he
        Worksheets("Sheet1").Cells(ii + a + 3, 2).Value = mdfA
        Worksheets("Sheet1").Cells(ii + a + 3, 3).Value = mdfI
        ret = SapModel.Results.ModalPeriod(NumberResults, LoadCase, StepType,
        StepNum, Period, Frequency, Circfreq, Eigenvalue)
        For jj = 0 To 5: Worksheets("Sheet1").Cells(ii + a + 3, 4 + jj).Value =
        Frequency(jj): Next
        ret = SapModel.SetModelIsLocked(False)
        ReDim V(7)
        For I = 0 To 7
        V(I) = 1
        Worksheets("Sheet2").Cells(jj + 11, ii).Value = V(jj)
        Next I
        ret = SapModel.FrameObj.SetModifiers(he, V)
        ret = SapModel.File.Save("C:\Users\serapkara\Desktop\model.sdb")
        Next
'Close Sap2000
        SapObject.ApplicationExit False
        Set SapModel = Nothing
        Set SapObject = Nothing
        End Sub
```

B. VBA Code for Calibration

```
Sub sap2000analysis()
'dimension variables
Dim SapObject As SAP2000v15.SapObject
Dim SapModel As cSapModel
Dim FileName As String
Dim ret As Long
Dim Selected As Boolean
Dim BuckModeStart As Long
Dim BuckModeEnd As Long
Dim BuckModeAll As Boolean
Dim NumberResults As Long
Dim Obj() As String
Dim Elm() As String
Dim LoadCase() As String
Dim StepType() As String
Dim Period() As Double
Dim Frequency() As Double
Dim Circfreq() As Double
Dim Eigenvalue() As Double
Dim StepNum() As Double
Dim U1() As Double
```

```
        Dim U2() As Double
        Dim U3() As Double
        Dim R1() As Double
        Dim R2() As Double
        Dim R3() As Double
        Dim ModalStiff() As Double
        Dim Ux() As Double
        Dim Uy() As Double
        Dim Uz() As Double
        Dim Rx() As Double
        Dim Ry() As Double
        Dim Rz() As Double
        Dim ModalMass() As Double
        Dim V() As Double
        Dim m() As Double
        Dim old_value As String
        Dim new_value As String
        Dim k() As Double
'create Sap2000 object
        Set SapObject = New SAP2000v15.SapObject
'start Sap2000 application
        SapObject.ApplicationStart
```

```
'create SapModel object
        Set SapModel = SapObject.SapModel
'initialize model
        ret = SapModel.InitializeNewModel
'open an existing file
        FileName = "C:\Users\serapkara\Desktop\ model.sdb"
        ret = SapModel.File.OpenFile(FileName)
        Worksheets("Sheet1").Cells(1, 1).Value = "Damage Member"
        Worksheets("Sheet1").Cells(1, 2).Value = "mass"
        Worksheets("Sheet1").Cells(2, 3).Value = "average_dXhx"
        Worksheets("Sheet1").Cells(2, 4).Value = "Rxhx"
        Worksheets("Sheet1").Cells(2, 5).Value = "Ryhx"
        Worksheets("Sheet1").Cells(2, 6).Value = "average_dYhy"
        Worksheets("Sheet1").Cells(2, 7).Value = "Ryhy"
        Worksheets("Sheet1").Cells(2, 8).Value = "Rxhy"
'HX
        Worksheets("Sheet3").Cells(1, 3).Value = "U1hx(102)"
        Worksheets("Sheet3").Cells(1, 4).Value = "U2hx(102)"
        Worksheets("Sheet3").Cells(1, 5).Value = "U1hx(103)"
        Worksheets("Sheet3").Cells(1, 6).Value = "U2hx(103)"
        Worksheets("Sheet3").Cells(1, 7).Value = "U1hx(104)"
        Worksheets("Sheet3").Cells(1, 8).Value = "U2hx(104)"
```

```
        Worksheets("Sheet3").Cells(1, 9).Value = "U1hx(105)"
        Worksheets("Sheet3").Cells(1, 10).Value = "U2hx(105)"
'HY
        Worksheets("Sheet3").Cells(1, 11).Value = "U1hy(102)"
        Worksheets("Sheet3").Cells(1, 12).Value = "U2hy(102)"
        Worksheets("Sheet3").Cells(1, 13).Value = "U1hy(103)"
        Worksheets("Sheet3").Cells(1, 14).Value = "U2hy(103)"
        Worksheets("Sheet3").Cells(1, 15).Value = "U1hy(104)"
        Worksheets("Sheet3").Cells(1, 16).Value = "U2hy(104)"
        Worksheets("Sheet3").Cells(1, 17).Value = "U1hy(105)"
        Worksheets("Sheet3").Cells(1, 18).Value = "U2hy(105)"
        Worksheets("Sheet3").Cells(1, 19).Value = "fullnessratio (%)"
        Worksheets("Sheet3").Cells(1, 20).Value = "m(0) - Ux" 'local joint masses
        Worksheets("Sheet3").Cells(1, 21).Value = "m(1) - Uy"
        Worksheets("Sheet3").Cells(1, 22).Value = "m(2) - Uz"
        Worksheets("Sheet3").Cells(1, 23).Value = "m(3) - Rx"
        Worksheets("Sheet3").Cells(1, 24).Value = "m(4) - Ry"
        Worksheets("Sheet3").Cells(1, 25).Value = "m(5) - Rz"
        Worksheets("Sheet3").Cells(1, 26).Value = "mass"
' delta_k = -100000
        fullmass = 10
        unit_mass = 1100
```

```
        EE = 2800000000#
        kv = 5698238
        kh = 292980
        ums = 7850
        mm = 0.05
        Em = 0.05
        vm = -0.5
        hm = -0.5
        ms = 0.05
        umlow = 1100
        umhig = 1450
        Elow = 2400000000#
        Ehig = 4100000000#
        umslow = 7850
        umshig = 10000
        dntch = 1
        OF = 9999
111
        For kk = 1 To 5
        If kk = 1 Then unit_mass = (1 + mm) * unit_mass:
        If (unit_mass <= umlow) Then unit_mass = umlow: mm = -mm
        If (unit_mass > umhig) Then unit_mass = umhig: mm = -mm
```

```
        If kk = 2 Then EE = (1 + Em) * EE:
        If (EE < Elow) Then EE = Elow: Em = -Em
        If (EE > Ehig) Then EE = Ehig: Em = -Em
        If kk = 3 Then kh = (1 + hm) * kh:
        If kk = 4 Then kv = (1 + vm) * kv:
        If kk = 5 Then ums = (1 + ms) * ums:
        If (ums < umslow) Then ums = umslow: ms = -ms
        If (ums > umshig) Then ums = umshig: ms = -ms
        If dntch = 0 Then OF = Worksheets("Sheet1").Cells(45, 5).Value
        ReDim k(20)
        k(0) = kh
        k(2) = kh
        k(5) = kv
407     ret = SapModel.PointObj.SetSpringCoupled("spring", k, 1, False, True)
        ret = SapModel.PropMaterial.SetMPIsotropic("PVC", EE, 0.41, 0.000079)
        ret = SapModel.PropMaterial.SetMPIsotropic("PVC2", EE, 0.41, 0.000079)
        ret = SapModel.PropMaterial.SetWeightAndMass("PVC", 2, unit_mass)
        ret = SapModel.PropMaterial.SetWeightAndMass("PVC2", 2, unit_mass)
        ret = SapModel.PropMaterial.SetWeightAndMass("A992Fy50", 2, ums)
' ret = SapModel.PropMaterial.SetMPIsotropic("Steel", 29500, 0.25, 0.000006)
a = 22
For ii = 1 To a
```

```
he = Worksheets("Sheet1").Cells(ii + 2, 1).Value
If he = "nodamage" Then
Else
mdfI = 0
mdfA = 0
mdfT = 0
ReDim V(7)
For i = 0 To 7
V(i) = 1
Next i
V(0) = mdfA
V(3) = mdfT
V(4) = mdfI
V(5) = mdfI
ret = SapModel.FrameObj.SetModifiers(he, V)
End If
mass = Worksheets("Sheet1").Cells(ii + 2, 2).Value 'kg
ReDim m(5)
For i = 0 To 5
        m(i) = 0
        Next i
        For i = 0 To 2
```

```
        m(i) = mass / 21
        Next i
        ret = SapModel.PointObj.SetMass("massdeck", m, 1, True, True)
'get point mass
        ReDim m(5)
        For i = 0 To 5
        ret = SapModel.PointObj.GetMass(162, m)
        Worksheets("Sheet3").Cells(ii + 1, i + 20).Value = m(i)
        Worksheets("Sheet3").Cells(ii + 1, 19).Value = (mass / fullmass) * 100
        Worksheets("Sheet3").Cells(ii + 1, 26).Value = mass
        Next i
        ret = SapModel.Analyze.RunAnalysis
        ret = SapModel.Results.Setup.DeselectAllCasesAndCombosForOutput
        ret = SapModel.Results.Setup.SetCaseSelectedForOutput("HX")
        ret = SapModel.Results.JointDispl("ALL", GroupElm, NumberResults, Obj,
        Elm, LoadCase, StepType, StepNum, U1, U2, U3, R1, R2, R3)
'joint 102= 100
'joint 103= 101
'joint 104= 102
        Worksheets("Sheet3").Cells(ii + 1, 3).Value = U1(100)
        Worksheets("Sheet3").Cells(ii + 1, 4).Value = U2(100)
        Worksheets("Sheet3").Cells(ii + 1, 5).Value = U1(101)
```

```
Worksheets("Sheet3").Cells(ii + 1, 6).Value = U2(101)

Worksheets("Sheet3").Cells(ii + 1, 7).Value = U1(102)

Worksheets("Sheet3").Cells(ii + 1, 8).Value = U2(102)

Worksheets("Sheet3").Cells(ii + 1, 9).Value = U1(103)

Worksheets("Sheet3").Cells(ii + 1, 10).Value = U2(103)

Worksheets("Sheet1").Cells(ii + 2, 3).Value = ((U1(101) + U1(102)) / 2) *
1000

Worksheets("Sheet1").Cells(ii + 2, 4).Value = (U1(102) - U1(101)) / 0.25

Worksheets("Sheet1").Cells(ii + 2, 5).Value = (U2(101) - U2(100)) / 0.35

ret = SapModel.Results.Setup.DeselectAllCasesAndCombosForOutput

ret = SapModel.Results.Setup.SetCaseSelectedForOutput("HY")

ret = SapModel.Results.JointDispl("ALL", GroupElm, NumberResults, Obj,
Elm, LoadCase, StepType, StepNum, U1, U2, U3, R1, R2, R3)

Worksheets("Sheet3").Cells(ii + 1, 11).Value = U1(100)

Worksheets("Sheet3").Cells(ii + 1, 12).Value = U2(100)

Worksheets("Sheet3").Cells(ii + 1, 13).Value = U1(101)

Worksheets("Sheet3").Cells(ii + 1, 14).Value = U2(101)

Worksheets("Sheet3").Cells(ii + 1, 15).Value = U1(102)

Worksheets("Sheet3").Cells(ii + 1, 16).Value = U2(102)

Worksheets("Sheet3").Cells(ii + 1, 17).Value = U1(103)

Worksheets("Sheet3").Cells(ii + 1, 18).Value = U2(103)

Worksheets("Sheet1").Cells(ii + 2, 6).Value = ((U2(100) + U2(101)) / 2) *
```

```
1000
Worksheets("Sheet1").Cells(ii + 2, 7).Value = (U2(101) - U2(100)) / 0.35
Worksheets("Sheet1").Cells(ii + 2, 8).Value = (U1(102) - U1(101)) / 0.25
ret = SapModel.Results.ModalPeriod(NumberResults, LoadCase, StepType, StepNum, Period, Frequency, Circfreq, Eigenvalue)
For jj = 0 To 2: Worksheets("Sheet2").Cells(ii + 2, 3 + jj).Value = Frequency(jj): Next
ret = SapModel.SetModelIsLocked(False)
If he = "nodamage" Then
Else
ReDim V(7)
For i = 0 To 7
V(i) = 1
Next i
ret = SapModel.FrameObj.SetModifiers(he, V)
End If
222
Next ii
'~~~~~~~~~~~~~~~~~~~~~~~~~~~~~~~~~~~~~~~~~~~~~~~~
        Worksheets(1).Calculate
        OF2 = Worksheets("Sheet1").Cells(45, 5).Value
        dntch = 0
```

```
If OF2 > OF Then
If kk = 1 Then unit_mass = unit_mass / (1 + mm): mm = -mm * 0.8
If kk = 2 Then EE = EE / (1 + Em): Em = -Em * 0.8
If kk = 3 Then kh = kh / (1 + hm): hm = -hm * 0.8
If kk = 4 Then kv = kv / (1 + vm): vm = -vm * 0.8
If kk = 5 Then ms = ms / (1 + ms): ms = -ms * 0.8
dntch = 1
End If
If OF2 < 0.5 Then
ret = SapModel.File.Save("C:\Users\serapkara\Desktop\model.sdb”)
GoTo 302
End If
Next kk
GoTo 111
302 End Sub
```